ABSTRACT

Title of Dissertation:	INVESTIGATION OF CYCLIC DINUCLEOTIDE HOMEOSTASIS AND THE HYDROLYSIS OF THEIR LINEAR INTERMEDIATES IN BACTERIA
	Cordelia Anne Weiss, Doctor of Philosophy, 2019
Dissertation directed by:	Professor Wade C. Winkler, Department of Cell Biology and Molecular Genetics

The synthesis of cyclic dinucleotides as signals is one strategy bacteria use to sense and adjust to environmental changes. Cyclases synthesize the cyclic dinucleotide, while phosphodiesterases cleave it to yield a linear diribonucleotide, which is recycled into monoribonucleotides by other enzymes. For many bacteria, cyclic di-GMP (c-di-GMP) regulates the transition from a unicellular motile state to a multicellular sessile community. However, c-di-GMP signaling has been less intensively studied in Gram-positive organisms. *Bacillus subtilis* is a model for the study of bacterial differentiation, yet how c-di-GMP functions in this organism is not fully understood. This work began with construction of a fluorescent reporter to measure c-di-GMP abundance in *B. subtilis,* which showed that c-di-GMP levels are strikingly different among differentiated subpopulations. These data highlight how single-cell approaches can be used to analyze metabolic trends within bacterial populations and demonstrate that for

some bacteria, c-di-GMP levels are adjusted heterogeneously across bulk populations. The enzymes Orn, NrnA, NrnB, and NrnC have been proposed to act as general 3'-5' exoribonucleases that preferentially process 'short' oligoribonucleotides. Intriguingly, Orn also performs a crucial role in c-di-GMP homeostasis by processing the pGpG generated from c-di-GMP production. To discover the molecular basis for Orn's ability to 'select' short RNAs, and to elucidate the relationship between Orn and the diribonucleotide pGpG, we combined structural, biochemical, and *in vivo* analyses of RNA cleavage. These data reveal that Orn is not a general exoribonuclease of short RNA oligoribonucleotides, as previously believed, but instead acts as a dedicated 'diribonucleotidase'. Our studies indicate RNA degradation as a step-wise process with a dedicated enzyme for the clearance of diribonucleotides, which affect cellular physiology and viability. Examination of the roles of NrnA and NrnB is underway. We conducted an initial study to determine if NrnA and NrnB are redundant proteins, as has been proposed, and if they might also act as 'diribonucleotidases'. These data show that they exhibit different substrate preferences and that they may have unique cellular functions. Therefore this work changes the perception of the role(s) Orn plays and that a re-evaluation of 'short' RNases is needed.

INVESTIGATION OF CYCLIC DINUCLEOTIDE HOMEOSTASIS AND THE HYDROLYSIS OF THEIR LINEAR INTERMEDIATES IN BACTERIA

by

Cordelia Anne Weiss

Dissertation submitted to the Faculty of the Graduate School of the
University of Maryland, College Park, in partial fulfillment
of the requirements for the degree of
Doctor of Philosophy
2019

Advisory Committee:
Professor Wade C. Winkler, Chair
Professor Vincent T. Lee
Professor Kevin S. McIver
Professor Antony M. Jose
Professor Leslie Pick

Dedication

"The function of education is to teach one to think intensively and to think critically. Intelligence plus character—that is the goal of true education."

-- Martin Luther King Jr.

I dedicate this dissertation to my parents, Drs. Frank D. Weiss and Mary E. Crowther, who have spent their lives teaching others. This dissertation could not have been completed without them.

Table of Contents

List of Tables

List of Figures

List of Abbreviations

AMP: adenosine monophosphate

ATP: adenosine triphosphate

cAMP: cyclic 3'-5' adenosine phosphate

c-di-AMP: bis-(3′,5′)-cyclic diadenosine monophosphate

c-di-GMP: bis-(3'-5')-cyclic dimeric guanosine monophosphate

cGAMP: cyclic GMP-AMP

cD-NTases: cGAS/DncV-like nucleotidyltransferases

DFHBI: 3,5-difluoro-4-hydroxybenzylidine imidazolinone

DGC: diguanylate cyclase

DHHA1: DHH-associated domain

DNA: deoxyribonucleic acid

GMP: guanosine monophosphate

GTP: guanosine triphosphate

HPLC: high performance liquid chromatography

K_d: dissociation constant

LB: lysogeny broth

LC-MS/MS: liquid chromatography-tandem mass spectrometry

MBP: maltose binding protein

MSgg: minimal salts glycerol glutamate

OD_{600}: optical density at 600 nm

ORFeome: open reading frame library

PAGE: polyacrylamide gel electrophoresis

pAp: 3’-phosphoadenosine 5’-phosphate

PCR: polymerase chain reaction

PDE-A: phosphodiesterase A

PDE-B: phosphodiesterase B

pGpG: 5’ phosphoguanylyl (3’-5’)-guanosine

PMSF: phenylmethane sulfonyl fluoride or phenylmethylsulfonyl fluoride

PNAG: poly-N-acetylglucosamine

(p)ppGpp: guanosine-(penta)tetraphosphate

PNAG: poly-N-acetylglucosamine

RNA: ribonucleic acid

rNTP: ribonucleotide triphosphate

SD: standard deviation

SDS: sodium dodecyl sulfate

STING: stimulator of IFN genes

TLC: thin layer chromatography

Chapter 1: Introduction

1.1 Copyright notice

Portions of the Introduction were originally published as: Weiss CA and Winkler WC. (2019). Cyclic di-GMP Signaling in Bacillus subtilis. In: Chou S-H, Guiliani N, Lee V, Römling, U (Eds.) Microbial Cyclic Di-Nucleotide Signaling. Switzerland: Springer Nature. In Press

1.2 Bacterial nucleotide second messenger signaling

Bacteria occupy diverse niches, both within the surrounding environment as well as part of other multicellular organisms. As such, bacteria use diverse strategies to sense alterations in their environment and rapidly adjust to those changes. Several signal transduction strategies have evolved the use of different modular protein domains to integrate a sensory input with a corresponding regulated response (1). These strategies have allowed for a complex systemwide network of bacterial signaling, and include the use of chemoreceptors, one and two-component systems, and phosphorelay systems, among others (2). Additionally, a number of nucleotide derivatives have been shown to serve as signaling molecules to coordinate bacterial behavior (3–7). These 'second messengers' are synthesized and hydrolyzed by proteins with conserved domains. Following synthesis, the second messenger can then go on to bind various receptors, also known as effectors, to target changes in bacterial physiology, behavior, or metabolism (Figure 1A). The first signaling nucleotide to be

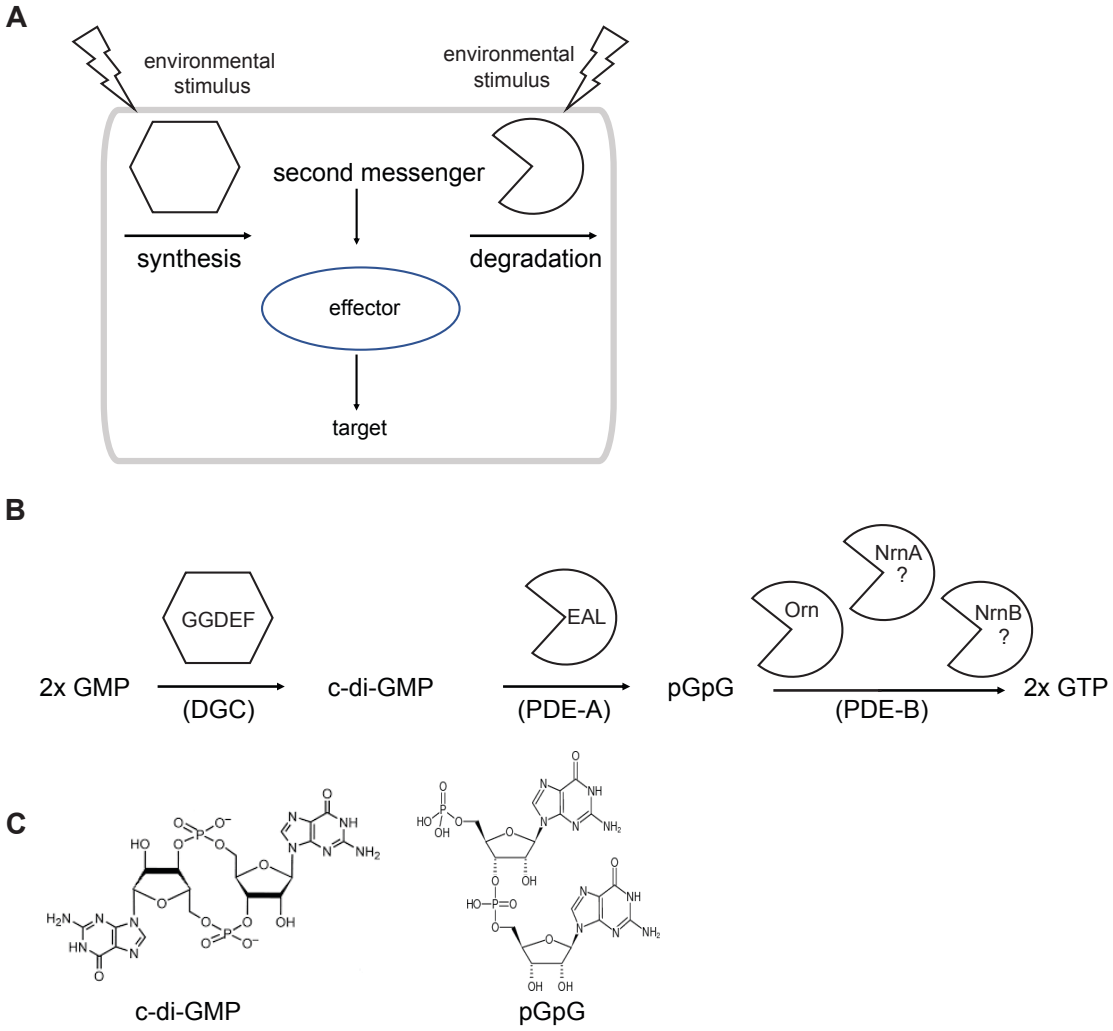

Figure 1. Schematic diagram of second messenger and c-di-GMP signaling. (A) Second messenger signaling systems. (B) C-di-GMP is synthesized from 2 GTP molecules by diguanylate cyclases (DGCs) with GGDEF domains. Phosphodiesterases (PDE-As) hydrolyze c-di-GMP to pGpG, which is in turn hydrolyzed to 2 GMP molecules PDE-Bs. These include Orn and possibly RNases NrnA and NrnB. (C) Structural schematic of the c-di-GMP and pGpG molecules.

discovered in bacteria was cyclic 3'-5' adenosine phosphate (cAMP) (8). cAMP signaling was found to regulate catabolite repression in *Escherichia coli,* thereby allowing the organism to preferentially utilize glucose before other sugars (9). Simultaneously, guanosine-(penta)tetraphosphate ((p)ppGpp) was shown to accumulate as growth rate decreased in *E. coli* and it is now a widely appreciated alarmone found in many bacteria critical for bacterial stress responses (10–13). Nearly twenty years later, the first cyclic dinucleotide, bis-(3′,5′)-cyclic diguanosine monophosphate (c-di-GMP), was discovered. Moshe Benziman and his colleagues first described c-di-GMP as an activator of bacterial cellulose biosynthesis (14). Since then, an ever-increasing number of studies have shown that c-di-GMP is a key regulator of lifestyle choice in bacteria. C-di-GMP has been shown to promote adhesion and biofilm formation, while simultaneously preventing motility (15). C-di-GMP has also been shown to regulate a number of other phenotypes, such as cell cycle control and virulence (16, 17). The discovery of c-di-GMP prompted investigators to wonder if other cyclic nucleotide derivatives existed in bacteria. Indeed, the next second messenger to be identified was bis-(3′,5′)-cyclic diadenosine monophosphate (c-di-AMP) (18). C-di-AMP has been shown to regulate very different processes, particularly in Gram-positive bacteria (19, 20). Cell wall homeostasis, ion transport, osmolyte uptake, DNA integrity, and biofilm formation have all been linked to c-di-AMP regulation (21–28). Sporulation-related processes may also be affected by c-di-AMP dynamics (29–31). Interestingly, unlike c-di-GMP, c-di-AMP signaling is essential under standard lab conditions in a number of bacteria including the model organism *Bacillus subtilis,* and pathogens such as *Listeria monocytogenes, Streptococcus*

pneumoniae, Staphylococcus aureus, and *Mycoplasma pneumoniae* (32–35). Moreover, accumulation of c-di-AMP leads to cell death, suggesting that intracellular c-di-AMP levels are tightly regulated to control central processes.

Cyclic dinucleotides are also recognized by the innate immune system (36). Recent studies of c-di-AMP regulation of the intracellular pathogen *L. monocytogenes* revealed that c-di-AMP is secreted into the cytosol of host cells, which consequently elicits a type I interferon (IFN) response (37, 38). Yet two more cyclic dinucleotides based on cyclic GMP-AMP (cGAMP) exist and have also been implicated in host immunity. 3′,3′-cGAMP, synthesized from the enzyme DncV, was identified as a bacterial second messenger that regulates chemotaxis and intestinal colonization in the bacterial pathogen *V. cholerae* (39). In mammalian cells, the enzyme cGAS synthesizes 2′,3′-cGAMP, which has been shown to induce innate immune signaling and antiviral response cells via the receptor STING (stimulator of IFN genes) (40–42). STING was also shown to target c-di-GMP and c-di-AMP (43, 44). In addition to STING, DDX41 was, until recently, the only other host receptor shown to induce a type I IFN response upon cyclic dinucleotide binding (45–47). However, a new receptor, the host oxidoreductase RECON, was shown to exhibit high affinity towards c-di-AMP and bacterial 3′,3′-cGAMP, but not mammalian 2′,3′-GAMP (48, 49). Investigations of nucleotide second messengers are continuing to reveal how second messenger signaling systems intersect, as observed during host immune responses.

Until recently, the only nucleotide signaling molecules discovered were purine derivatives. However, a new family of enzymes, cGAS/DncV-like nucleotidyltransferases (CD-NTases) have been reported to use both purine and

pyrimidine nucleotides to synthesize a diverse range of cyclic dinucleotides (50). For example, CdnE was found to be one member of this family that synthesizes cyclic AMP-UMP, a hybrid purine-pyrimidine cyclic dinucleotide. Additionally, several CD-NTases were shown to synthesize cyclic trinucleotides. The functional role of CD-NTases, as well as the physiological outcomes of the cyclic di- and trinucleotides that they produce in bacteria and/or their host remain unexplored.

Bacteria oftentimes encode numerous enzymes and receptors for an individual signaling system (15). Furthermore, multiple second messenger signaling systems can be used. This suggests that the cell might experience a regulatory nightmare in establishing target specificity within each regulatory pathway; yet bacteria do not. This puzzle has been most extensively studied in the context of c-di-GMP signaling. One important mechanism that allows specificity of individual c-di-GMP metabolizing enzymes is through their regulation by sensory domains in response to specific environmental signals (51). The differential transcriptional regulation of some DGCs and PDE-As is also critical for establishing specificity of c-di-GMP signaling. While many DGCs and PDE-As are expressed under general laboratory conditions, several have been shown to be regulated during stress or particular growth phases in some bacteria, thereby allowing temporal regulation of c-di-GMP signaling (52–54). Additional studies have lent evidence to the idea of 'local' pools of c-di-GMP production, which are thought to allow spatial regulation of c-di-GMP signaling. In support of this, individual DGCs and PDE-As have been shown to regulate specific bacterial processes. For example, in a *Salmonella enterica* serovar Typhimurium strain where all GGDEF domain-encoding genes were deleted, only three were found to

stimulate cellulose biosynthesis (55). Additionally, the DGC DgcC in *E. coli* was recently shown to directly interact with proteins that make up the machinery for synthesis, secretion, and modification of cellulose biosynthesis (56, 57). A further example was also observed in *B. subtilis,* where a fluorescent fusion of the DGC DgcK colocalized with the effector YdaK, which in turn colocalized with proteins that synthesize a specialized polysaccharide (54, 58). Localization and binding studies of other pairs of DGCs and PDE-As, and c-di-GMP receptors in other organisms will continue to reveal the full extent of spatial regulation of c-di-GMP signaling.

The different binding affinities that receptors show for c-di-GMP is yet another way in which c-di-GMP can target specific bacterial processes. In support of this model, one recent study showed that in *S. enterica* serovar Typhimurium, deletion of PDE-A YhjH led to an increase in intracellular c-di-GMP that was sufficient to inhibit motility through the c-di-GMP receptor YcgR, but insufficient to stimulate cellulose synthesis through the receptor BcsA (59). The study further demonstrated that the two c-di-GMP receptors exhibited over a 40-fold difference in binding affinities for c-di-GMP. Therefore, the range at which different receptors can bind c-di-GMP may allow for specific activation of certain receptors and subsequent biological targets.

How different second messenger systems interact with each other remains largely unknown. Yet, several studies have revealed connections among c-di-GMP, c-di-AMP, (p)ppGpp, and cAMP signaling networks. For example, transcriptomic analysis recently showed that in *V. cholerae,* cAMP-binding transcription factor CRP regulates the expression of genes encoding c-di-GMP DGCs and PDE-As (60). Moreover, in *E. coli,* both c-di-GMP and (p)ppGpp were shown to inversely regulate

the polysaccharide adhesin poly-GlcNac that induces biofilm formation (61). This suggests a model in which *E. coli* simultaneously monitors ribosome stress using (p)ppGpp signaling, while modulating c-di-GMP-regulated biofilm formation. Cross-talk between (p)ppGpp and c-di-AMP was also recently observed. C-di-AMP accumulation was shown to induce the stringent response and stimulate (p)ppGpp synthesis in *S. aureus*, although the mechanism remains to be elucidated (62). Furthermore, (p)ppGpp was shown to be a strong competitive inhibitor of one class of c-di-AMP phosphodiesterases, GdpP (63). Other examples of cross-talk among other signaling systems and their effect on bacterial physiology undoubtedly await discovery.

1.3 C-di-GMP synthesis and degradation

In response to environmental cues, c-di-GMP is synthesized from 2 GTP molecules by GGDEF domain-containing diguanylate cyclases (DGCs) (Figure 1B) (14, 64–68). The GGDEF motif represents the highly conserved active site (A-site), whereby 2 GTP molecules become linked via 2 3'-5' phosphodiester bonds in a cyclic configuration. Following synthesis of c-di-GMP, the molecule can then bind several distinct classes of receptors that go on to mediate diverse phenotypes (69). C-di-GMP signaling is terminated by classes of phosphodiesterases (PDE-As) that contain conserved EAL or HD-GYP domains, which linearize c-di-GMP to the dinucleotide 5′-phosphoguanylyl-(3′-5′)-guanosine (pGpG) (Figure 1B) (70–74). GGDEF, EAL, and HD-GYP domains can be the only domains associated with DGCs and PDE-As or can also be found as part of multi-domain signaling proteins that include sensory domains such as PAS, GAF, REC, and BLUF (75–79). These sensory domains allow for post-

translational regulation of DGC or PDE-A activity through activation by an extracellular signal. Furthermore, DGCs and PDE-As can also contain tandem arrangements of GGDEF and EAL domains, in which only one domain retains enzymatic activity (70, 80, 81).

1.4 C-di-GMP receptors

While GGDEF or EAL/HD-GYP domain proteins alone are responsible for the synthesis and hydrolysis of c-di-GMP, there is a greater diversity of c-di-GMP receptors, including both RNA and protein factors. The first c-di-GMP receptor to be identified was the PilZ domain (82). Bioinformatic and phylogenetic analyses identified two motifs, RxxxR—D/NxSxxG, critical for c-di-GMP binding (83, 84). First identified as part of the BcsA subunit of the cellulose synthase complex in the Alphaproteobacteria *Komagataeibacter xylinus* (formerly *Gluconacetobacter xylinus* or *Acetobacter xylinum*), the PilZ domain is found within many other proteins and acts as an effector protein to allow c-di-GMP to target diverse processes (15, 82). For example, many Proteobacteria often use PilZ domain proteins, such as YcgR and DgrA, to inhibit flagellum-based motility in the presence of increased intracellular c-di-GMP (81, 85, 86). Conversely, c-di-GMP binding to the PilZ domain-containing protein BcsA activates cellulose synthesis to promote biofilm formation in a number of bacteria, including *E. coli* and *S. enterica* serovar Typhimurium (55, 87).

In addition to the PilZ domain, enzymatically inactive DGCs and PDEs with respective nonconsensus GGDEF- and EAL-domain active site sequences have also been shown to serve as c-di-GMP receptors (88–92). Some DGCs were shown to be

enzymatically inactive due to a degenerate catalytic A-site motif and have therefore lost the ability to synthesize c-di-GMP, but have retained the ability to bind c-di-GMP. Structural studies of GGDEF domain-containing proteins complexed with c-di-GMP revealed that many DGCs also have an additional c-di-GMP binding site, distinct from the A-site (93, 94). The residues that make up this allosteric inhibitory site (I-site), RxxD, are highly conserved in a number of active and inactive DGCs (95). For active DGCs, the I-site prevents overproduction of c-di-GMP by the DGC once a certain threshold has been reached. However, for enzymatically inactive proteins, the I-site allows these proteins to function as one class of c-di-GMP receptors.

Not all c-di-GMP receptors can be easily predicted, as exemplified by the discoveries that c-di-GMP binds to certain transcription factors (96–101) and to the protein MshE (102). This last receptor is a member of a family of ATPases that are associated with type IV pili and type II secretion systems. Simply put, it is difficult to accurately predict regulatory proteins that might bind c-di-GMP through bioinformatic approaches alone. The c-di-GMP binding proteins that have been identified have been found to exhibit significant differences in sequence and structure and individually required experimental analysis of c-di-GMP binding. Given the extensive regulation by c-di-GMP in bacteria, it is reasonable to suspect that other classes of receptors have yet to be identified.

Another large class of c-di-GMP receptors is comprised of noncoding RNA elements called riboswitches. Riboswitches are cis-acting regulatory RNAs that modulate downstream gene expression in response to changing intracellular metabolite concentrations (103). The sensor domain (aptamer), folds into a complex three-

dimensional shape that binds target metabolites with high affinity and selectivity, while the expression platform couples the ligand-induced conformational changes to control of downstream gene expression. To date, two distinct structural classes of c-di-GMP riboswitches, each characterized by a GEMM (Genes for the Environment, Membranes, and Motility) motif, have been discovered (104, 105). Over 500 examples of c-di-GMP riboswitches have been identified among diverse bacterial species (106). For example, c-di-GMP riboswitches are dispersed among Gram-positive Firmicutes such as Bacilli and Clostridia, as well as many Gram-negative Proteobacteria. Sequences have been identified in Bacillales such as *B. cereus, B. thuringiensis*, *B. anthracis,* and *B. licheniformis,* although none have been found in *B. subtilis*. Some bacterial species appear to be more replete in c-di-GMP riboswitches than others. For example, there are 16 different c-di-GMP riboswitches located across the *Clostridioides difficile* genome (107). Astoundingly, the Deltaproteobacterium *Geobacter uraniireducens* carries at least 30 c-di-GMP riboswitch elements. It should be noted that in some closely related species, *Geobacter metallireducens* and *Geobacter sulfurreducens,* a majority of the encoded GEMM-I riboswitches were shown to be selective for cGAMP (108). This is in part due to a nucleotide change in the GEMM-I motif that can be found in about 20% of all predicted GEMM-I sequences. Therefore, it is possible that a subset of the GEMM riboswitches found in a given bacterium may also sense cGAMP and not c-di-GMP. In general, riboswitches are almost always found in the 5' untranslated regions (UTRs) of mRNAs, and typically regulate gene expression by controlling formation of transcription termination sites or by affecting the efficiency of translation initiation (109). Interestingly, a novel form of

gene regulation by a c-di-GMP riboswitch was recently elucidated (110). One of *V. cholerae's* two c-di-GMP riboswitches, Vc2, is encoded in the 5' UTR of the *tfoY* gene (111). Further inspection, however, revealed that Vc2 resides within the 3' end of a putative sRNA (P_1-Vc2). Binding of Vc2 to c-di-GMP did not appear to regulate transcriptional termination, but rather, stabilized the presence of the putative sRNA, which lead to accumulation of the sRNA when intracellular c-di-GMP levels were high. When overexpressed, the sRNA was shown to enhance motility of *V. cholerae* 2.4 fold. C-di-GMP riboswitches are predicted to regulate expression of a broad array of functional gene categories, including but not limited to genes encoding GGDEF/EAL/HD-GYP proteins, flagella and pili, other motility factors, transcription factors, and membrane transporters (112). This diversity allows for the control of a complicated network of c-di-GMP-responsive changes in gene expression. Many associated genes, such as the ones in *G. uraniireducens,* code for proteins of unknown function, and therefore there is still far more to learn about the processes regulated by c-di-GMP. Furthermore, as more c-di-GMP riboswitches are discovered in other organisms, they will undoubtedly reveal new regulatory connections.

1.5 Degradation of dinucleotide intermediates in bacteria

C-di-GMP signaling is terminated when c-di-GMP is hydrolyzed by a two-step process to the dinucleotide pGpG, followed by cleavage into nucleoside monophosphates (14). While pGpG was known to be hydrolyzed into two GMP molecules, the phosphodiesterase (PDE-B) that performed this terminal step remained elusive for many years. A screen was recently performed to identify other proteins that

could function as PDE-Bs and hydrolyze the diribonucleotide pGpG. A Differential Radial Capillary Action of Ligand Assay (DRaCALA) was used to screen an ORF library of *Vibrio cholerae* El Tor N16961 for proteins that bind pGpG (113). This screen identified Oligoribonuclease (Orn) as a protein that bound pGpG and not c-di-GMP. Originally discovered in the 1960's, Orn was described as a 3'-5' exoribonuclease responsible for processing short oligoribonucleotides 2 to 7 nucleotides in length (114–117). Subsequent investigations also found that: (1) Orn rapidly degraded pGpG *in vitro,* (2) lysates of *Pseudomonas aeruginosa orn* mutants were defective in PDE-B activity, and (3) loss of *orn* resulted in increased intracellular pGpG and c-di-GMP (113, 118). The accumulation of c-di-GMP due to loss of Orn results in several c-di-GMP-regulated phenotypes, due to feedback inhibition of PDE-As by accumulation of pGpG. In summary, in addition to its perceived role as an oligoribonuclease, Orn was found to be the primary PDE-B responsible for pGpG hydrolysis to GMP, and therefore the terminal member in c-di-GMP signaling in bacteria.

Yet, Orn is not found in all bacteria. Accordingly, there has been interest in identifying if other proteins perform the same function as Orn. Orn is essential in a number of organisms, including *E. coli* (119). To bypass this essentiality, several types of conditional *orn* mutants were created to assess the genetic function of *orn* (119). In *E. coli*, expression of a conditional *orn* mutant resulted in pin-point sized colonies that stopped growing (120, 121). The ability to rescue this growth defect through complementation of gene candidates was used to identify functional analogs of Orn. As *B. subtilis* is a Firmicute and a model for the study of endospore forming Gram-

positive organisms, preliminary studies focused on RNases encoded by *B. subtilis* that could heterologously complement the *orn* growth defect in *E. coli.* Two previous genes of unknown function were identified in *B. subtilis*—NanoRNase A (NrnA) and NanoRNase B (NrnB) (120, 121). Biochemical and functional characterization of NrnA and NrnB will be discussed further in Chapter 4. Evaluation of genomes in the Alphaproteobacteria, Chlamydiae, and Cyanobacteria phyla revealed that no Orn, NrnA, or NrnB homologs existed. Consequently, a genomic library of the obligate intracellular pathogen *Bartonella birtlesii* was screened for genes that can complement the *E. coli* conditional *orn* mutant (122). This led to the identification of NanoRNase C (NrnC), formerly BA0969. Subsequent biochemical characterization showed that NrnC readily degraded 5'Cy5-labeled 5mer RNAs. Unlike deletion of *nrnA* or *nrnB* in *B. subtilis,* knockdown of *nrnC* in *Bartonella henselae* did result in a growth defect.

Several bacterial phyla such as Firmicutes and Alphaproteobacteria were found to (1) not encode *orn*, (2) still utilize c-di-GMP signaling, and (3) encode functional Orn analogs. Therefore, researchers wanted to know if these functional Orn analogs also had the ability to cleave pGpG to terminate c-di-GMP signaling. To answer this, a similar *orn* complementation strategy was implemented in *P. aeruginosa* to determine which RNases could specifically hydrolyze pGpG (123). The deletion of *orn* in *P. aeruginosa* results in viable cells with several c-di-GMP dependent phenotypes such as enhanced biofilm formation and aggregation. Of the genes tested, only *orn*, *B. subtilis nrnA* and *nrnB*, and *Caulobacter crescentus nrnC* could reduce aggregation of the *P. aeruginosa* Δ*orn* strain. Biochemical data showed that these enzymes specifically cleaved pGpG, and expression of the genes encoding these enzymes

restored levels of intracellular pGpG and c-di-GMP to wild-type levels in a Δ*orn* strain as measured by mass spectrometry. In summary, a subset of RNases—namely Orn, NrnA, NrnB, and NrnC—serve as PDE-Bs and cleave pGpG.

In turn, c-di-AMP signaling is terminated in a similar fashion to c-di-GMP, where several classes of conserved phosphodiesterases hydrolyze c-di-AMP to pApA, before pApA is hydrolyzed into two AMP molecules (124). However, termination of c-di-AMP seems to be more diverse, as four different classes of c-di-AMP PDEs have been characterized and have different but overlapping enzymatic activities. Two classes, GdpP-type and PgpH-type PDEs are only able to convert c-di-AMP to pApA. For a time, it was unclear as to what other enzymes cleaved pApA to AMP. One class of c-di-AMP phosphodiesterases, DhhP-type however, combine the two step process and cleave cy-di-AMP to pApA and then hydrolyze pApA to AMP. Lastly, CdnP from the human pathogen *Streptococcus agalactiae* acts with a second nucleotidase NudP to degrade extracellular c-di-AMP to adenosine (45, 46). While no cGAMP-specific phosphodiesterases have been identified to date, it is likely that all cyclic dinucleotide signaling is terminated in a similar fashion, where a linear dinucleotide intermediate is formed prior to being recycled into nucleoside pools. Roles for Orn, NrnA, NrnB, and NrnC in c-di-AMP and cGAMP signaling systems, however, require further investigation.

1.6 *B. subtilis* lifestyles

The ubiquitous soil species *B. subtilis* is the central model bacterium for the study of Gram-positive endospore-forming microorganisms. Originally identified more

than 150 years ago, the intensive study of this microorganism as well as its genetic malleability have led to many fundamental discoveries, greatly improving the basic knowledge of bacterial biology. As early as 1877, Ferdinand Cohn had already described one of *B. subtilis'* most enduring features: *B. subtilis* incorporates concepts of multicellularity into its bacterial communities (125, 126). Indeed, any culture of *B. subtilis* is likely to feature multiple, mutually exclusive subpopulations. The first cell type to be described by Cohn was sporulation, a process where vegetatively growing cells differentiate into metabolically inactive endospores. The genetic malleability of *B. subtilis* has allowed researchers to uncover many of the key molecular strategies that underlie this alternative life-style choice—for cells that will be encouraged into endospore formation, nutrient limitation stimulates a phosphorelay that results in phosphorylation of the master regulator Spo0A, which triggers the onset of sporulation (127, 128). Yet, endospore formation is not the only cellular differentiation pathway for this bacterium. For example, during exponential growth only a subset of cells is motile. These cells express the sigma factor SigD*,* which is required for activation of flagellar genes and motility (129). *B. subtilis* uses peritrichous flagella for two forms of motility: swimming and swarming. Swimming takes place autonomously through liquid, while swarming is a highly coordinated, social form of solid surface migration, only observed by undomesticated strains of *B. subtilis* (130, 131). Another distinct small proportion of the population corresponds to competent cells, which can proficiently import extracellular DNA, when activated by the transcription factor ComK (132, 133). Other cells within the population are triggered by regulatory proteins (*e.g.,* SinR/SinI, SlrR, and DegU) to differentiate into sessile chains and produce key

extracellular components that assist assembly of an extracellular matrix to promote biofilm formation (134, 135). Therefore, the *B. subtilis* community presents a population of genetically identical yet phenotypically distinct cells that presumably benefits from an efficient "division of labor," by performing different tasks that optimize population survival (136–138).

The collective behavior of *B. subtilis* cell types is particularly evident during biofilm formation, in which these multicellular communities can be highly resilient to environmental stresses, due in part to the extracellular matrix that encases these cells (139, 140). In the lab, biofilms can form as colonies at the agar-air interface, or as floating communities at the liquid-air interface (pellicles). In both instances, these biofilms form architecturally complex morphologies. Biofilm formation begins when a subset of cells become activated for expression of genes required for extracellular matrix production. A major component synthesized by the subpopulation of matrix-producing cells is exopolysaccharide (EPS) (141). In *B. subtilis,* the EPS is poly-N-acetylglucosamine (PNAG), which is produced from proteins encoded by genes within the *epsA-O* operon, a long 15-gene cluster that is 16 kb in length (142). Matrix producers simultaneously produce TasA and BslA, which serve as structural protein components of the biofilm. TasA is a secreted protein that assembled into long fibers that are akin to amyloid fibers (143, 144). BslA has been shown to form a hydrophobic layer on the biofilm surface (145, 146). Indeed, both TasA and BslA are required for proper assembly of colony and pellicle biofilms (147). Many other extracellular components are produced during biofilm formation; other cells in the population produce the antimicrobial lipopeptide surfactin, which has been shown to act as a

signaling molecule to trigger a number of adaptive processes (148–150). Exoprotease production is also associated with an additional subpopulation and is believed to promote the acquisition of nutrients for the biofilm (151, 152). In addition to matrix-producing cell types, a subset of the bacteria remains motile, and are thought to use flagellar motility to disperse from the biofilm to seed new environments (153, 154). Furthermore, spores are spatially organized within aerial structures toward the top of the maturing biofilm (140, 155). In summary, all of these different cellular subpopulations are likely to be critical for proper biofilm formation, and their formation is therefore tightly regulated at multiple levels (156–159).

C-di-GMP has been shown in many bacteria to regulate the transition from a unicellular motile state to a multicellular sessile community (15, 160). C-di-GMP signaling networks are encoded in almost every phylum in the bacterial domain, making this molecule a near-universal second messenger, although it has still been incompletely examined in several model microbes. The genetic malleability and wealth of knowledge regarding *B. subtilis* development make it an excellent experimental model in which to interrogate the contribution of c-di-GMP regulation to cell differentiation in Firmicutes.

1.7 C-di-GMP signaling in *B. subtilis*

1.7.1 C-di-GMP Metabolizing Enzymes in *B. subtilis*

Bioinformatic analysis has revealed that *B. subtilis* encodes three GGDEF-domain proteins (YdaK, DgcK and DgcP), two EAL-domain proteins (PdeH and YkuI), and one dual GGDEF-EAL protein DgcW. No HD-GYP domains have been

identified (Table 1). Three c-di-GMP protein receptors have been identified in *B. subtilis* to date: the PilZ domain-containing protein MotI, the degenerate GGDEF domain-containing protein YdaK, and the degenerate EAL domain-containing protein YkuI. Characterization of the enzymes and receptors involved in c-di-GMP signaling has been performed both biochemically and genetically. Diguanylate cyclase activity was confirmed biochemically for the purified GGDEF-domain fragments of DgcK and DgcP, as well as the dual GGDEF-EAL protein DgcW, which were all able to synthesize c-di-GMP in the presence of GTP (161). Diguanylate cyclase activities of DgcP and DgcW were enhanced when the respective GAF and PAS sensory domains were expressed and purified with the GGDEF domains. In contrast to DgcP and DgcW, DgcK does not appear to have an additional sensory domain. While DgcK, DgcP, and DgcW were catalytically active in *vitro*, YdaK was not (161). Further confirmation of these enzyme activities was acquired using mass spectrometry assays, where c-di-GMP levels were directly quantified from within appropriate cell extracts. For example, cell lysates from *B. subtilis* strains that overexpressed DgcK, DgcP, or DgcW exhibited elevated c-di-GMP relative to the wild-type strain. A number of experiments have shown that in *B. subtilis,* elevated c-di-GMP levels also leads to suppression of flagellar motility (161, 162). To assess the contribution of each individual DGC in *B. subtilis,* single deletions of GGDEF domain proteins (DgcK, DgcP, DgcW, and YdaK) were made. However, these mutants did not exert a strong effect on motility, likely due to some level of functional redundancy for the DGCs. A quadruple GGDEF mutant devoid of these proteins was also constructed. While this mutant showed no difference

Table 1. Genes involved in *B. subtilis* c-di-GMP signaling

Gene	Prior Gene Names	Domain	Activity	Biological Function
dgcK	*yhcK*	GGDEF	DGC	Synthesizes c-di-GMP
dgcW	*ytrP*	GGDEF	DGC	Synthesizes c-di-GMP
dgcW	*ykoW*	GGDEF-EAL	DGC	Synthesizes c-di-GMP
ydaK		GGDEF	c-di-GMP binding	Stimulates synthesis of an unknown EPS
*gdpP**	*yybT*	GGDEF	ATPase	c-di-AMP phosphodiesterase
pdeH	*yuxH*	EAL	PDE	Hydrolyzes c-di-GMP
ykuI		EAL	c-di-GMP binding	Zinc homeostasis
motI	*ypfA/dgrA*	PilZ	c-di-GMP binding	Inhibits motility

*Initially thought to be a nonconsensus GGDEF domain-containing protein involved in c-di-GMP signaling, GdpP does not synthesize c-di-GMP. Rather, GdpP is involved in c-di-AMP signaling.

in swarming compared to wild-type, individual overexpression of the active DGCs DgcP, DgcK, and DgcW$^{\Delta EAL}$ in this mutant background led to a reduction in swarming.The two EAL domain containing proteins PdeH and YkuI were also tested for phosphodiesterase activity in *vitro* (161, 163). C-di-GMP was hydrolyzed to the linear product pGpG only in the presence of purified PdeH, suggesting it is the only active PDE. Lysates from a Δ*pdeH* strain also exhibited higher levels of c-di-GMP, as measured by mass spectrometry. The role of PdeH as an active PDE-A was also demonstrated through its effect on motility. Specifically, deletion of *pdeH* caused a severe defect in swarming (161, 162). Together, these studies reveal that *B. subtilis* expresses the necessary enzymes for c-di-GMP signaling—namely, three diguanylate cyclases DgcK, DgcP, DgcW, and one phosphodiesterase PdeH (Figure 2A).

1.7.2 C-di-GMP Regulation by MotI of *B. subtilis* Motility

C-di-GMP has been shown in a number of bacteria to inhibit flagellar rotation at the post-translational level (164, 165). In enteric bacteria such as *E. coli* and *S. enterica* serovar Typhimurium, one such mechanism has been investigated in great detail. Briefly, elevated c-di-GMP levels inhibit flagellar rotation through the PilZ domain-containing c-di-GMP receptor YcgR. Upon binding of c-di-GMP, YcgR undergoes a drastic conformational change that subsequently allows YcgR to directly interact with components of the flagella to slow down rotation (84, 166, 167). MotI (previously named YpfA and DgrA), exhibits an intact RxxxR—D/NxSxxG motif, consistent with the notion that MotI is a PilZ domain-containing c-di-GMP receptor (82). Additionally, MotI is a YcgR homolog. As such, MotI is thought to perform a

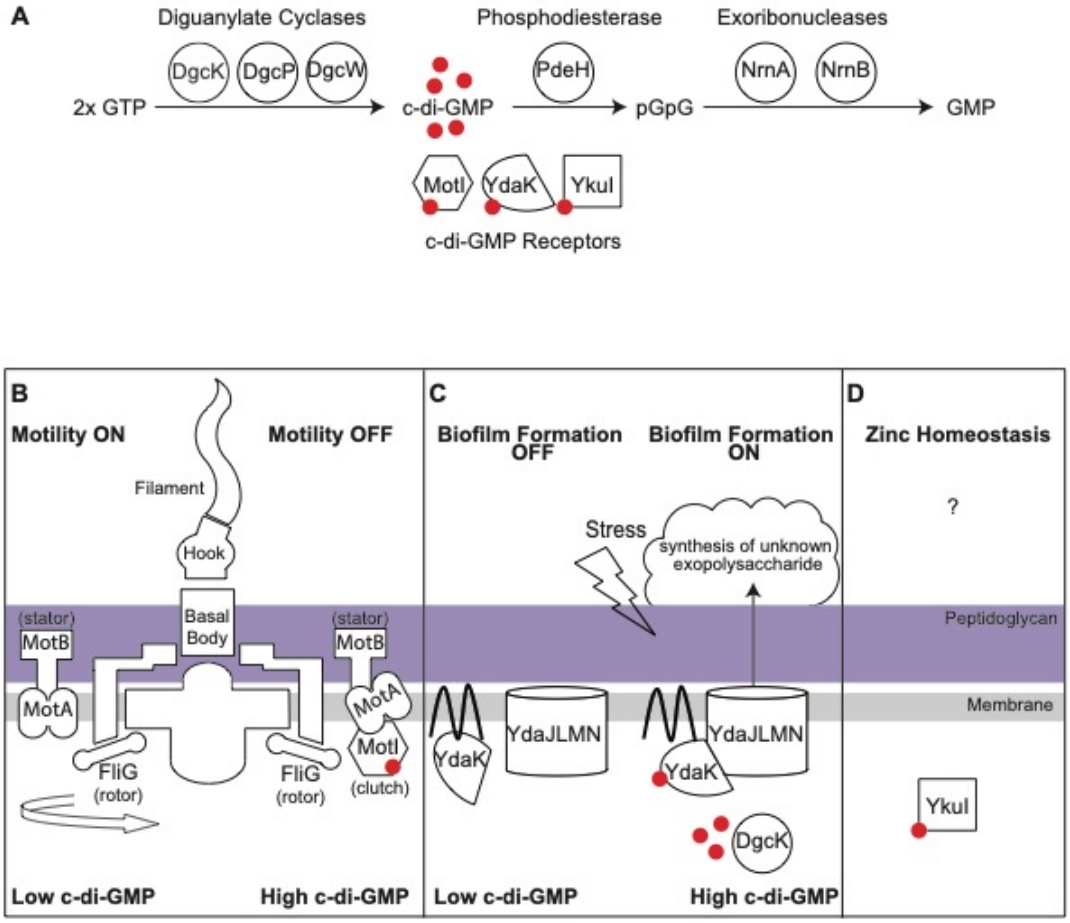

Figure 2. Schematic diagram of c-di-GMP regulation in *B. subtilis*. (A) Diguanylate cyclases (DgcK, DgcP, DgcW) synthesize c-di-GMP from 2 GTP molecules. Phosphodiesterases (PdeH) hydrolyze c-di-GMP to pGpG, which is in turn hydrolyzed to 2 GMP molecules by RNases NrnA and NrnB. C-di-GMP binds effectors (MotI, YdaK, YkuI). Putative functions and interactions of c-di-GMP effectors (B) MotI during motility, (C) YdaK during biofilm formation, and (D) YkuI in zinc homeostasis.

similar function as YcgR in regulating the flagellar apparatus. Biochemical experiments supported a direct interaction between MotI and c-di-GMP: a combination of size exclusion chromatography and isothermal titration calorimetry revealed that MotI bound c-di-GMP with high affinity—with an equilibrium dissociation constant of 11 nM (161). Furthermore, recent high-resolution structural studies revealed the molecular basis of c-di-GMP binding to MotI (168). The observed protein-ligand complex was similar to other PilZ domain-containing proteins such as PP4397 and Alg44 from *Pseudomonas putida* and *Pseudomonas aeruginosa*, respectively, in which two molecules of c-di-GMP bound between the N- and C-terminal domains of MotI (83, 169, 170). Overexpression of MotI resulted in a severe defect in swarming motility as compared to wild-type (161, 162). Swarming was completely abolished when MotI was simultaneously overexpressed in a Δ*pdeH* background, providing further evidence that the combination of MotI and elevated c-di-GMP levels negatively regulate motility. Conversely, this phenotype could be alleviated by deletion of MotI in a Δ*pdeH* background, suggesting that c-di-GMP regulation of flagellar motility in *B. subtilis* is primarily through MotI (162). Inhibition of swarming was also rescued similar to that of wild-type by site-directed mutagenesis of conserved binding site residues, thereby showing that the MotI c-di-GMP binding site is functionally relevant. In contrast, site-directed mutations of residues outside of the c-di-GMP binding site did not alter MotI's ability to inhibit swarming motility. In total, these results suggest that MotI represses *B. subtilis* motility when bound to c-di-GMP (Figure 2B). To identify MotI targets, bacterial two-hybrid assays showed that MotI interacts directly with the flagellar stator protein MotA (162, 171). This interaction was supported by additional localization

studies and suppressor analyses (168). Furthermore, mutations in the PilZ domain of MotI abolished its ability to interact with MotA. In *B. subtilis,* MotA is part of the MotA/B stator complex, which exploits the proton motive gradient to impart torque on the rotor, FliG. The torque on FliG subsequently generates force to the flagellum, allowing rotation. Therefore, MotI is thought to behave as a molecular clutch by disengaging the stator MotA's contact with the rotor FliG (Figure 2B).

Unlike MotI, overexpression of the putative receptors YdaK or YkuI in a Δ*pdeH* background did not impact motility, suggesting that YdaK and YkuI may target other pathways in *B. subtilis.*

1.7.3 C-di-GMP Regulation by YdaK of *B. subtilis* Biofilm Formation

Inhibition of motility due to elevated c-di-GMP levels also generally coincides with biofilm formation (15). Specifically, regulation of PNAG and other exopolysaccharides by c-di-GMP has emerged as a frequent theme among bacteria (172, 173). After all, the discovery of c-di-GMP by Moshe Benziman and his colleagues arose from their investigation of the regulation of cellulose synthesis in *Komagataeibacter xylinus* (formerly *Gluconacetobacter xylinus* or *Acetobacter xylinum*) (14). In the Gram-positive organism *Listeria monocytogenes,* exopolysaccharide biosynthesis was also shown to be increased in response to elevated c-di-GMP levels (174, 175). Yet it is not fully resolved whether c-di-GMP regulates exopolysaccharides for *B. subtilis.* While *epsA-O* gene expression is controlled by multiple transcription factors and signaling pathways, c-di-GMP does not appear to affect *epsA-O* gene expression (141). These results suggest that c-di-GMP is not

important for control of PNAG. Furthermore, no apparent change to *B. subtilis* biofilm colonies or pellicles has been observed upon mutation of the DGCs or PDE-As (161, 162). While deletion of *pdeH* results in a swarming motility defect, it does not result in any obvious changes to biofilm colonies or pellicles. Overexpression of the DGCs did not appear to affect biofilms either, initially suggesting c-di-GMP is not important for control of biofilm formation in this organism. Recent data suggests that the degenerate DGC YdaK is a c-di-GMP receptor that is likely to participate in biofilms.

Inspection of the YdaK sequence revealed a nonconsensus GGDEF active site (A-site) motif. The presence of an intact I-site, but not an A-site, in YdaK suggests that it is an enzymatically inactive DGC that instead functions as a receptor. Consistent with this prediction, the purified nonconsensus GGDEF domain from YdaK bound c-di-GMP with a Kd of 1.1 μM, but was unable to synthesize c-di-GMP (161). Furthermore, overexpression of YdaK *in vivo* did not result in detectable elevation of c-di-GMP, as compared to a wild-type strain. Future studies of YdaK complexed with c-di-GMP will resolve whether c-di-GMP binds to the inactive A-site, the RxxD I-site, or both locations. Recent data suggest that YdaK targets production of an as yet unidentified polysaccharide during biofilm formation.

The first clue that YdaK participates in biofilm formation arose from its genomic location within the *ydaJKLMN* operon (54, 58). Bioinformatics approaches proposed that members of some of the genes in the *ydaJKLMN* operon encode for exopolysaccharide synthesis machinery. Because manipulation of *ydaK* alone had no effect on biofilm formation or motility, the entire operon was overexpressed and biofilm formation was assessed by standard colony morphology and Congo Red (CR)

staining. CR stains amyloid fibrils and some polysaccharides and it has therefore been employed previously as a reporter for measuring matrix production in biofilms and for indirectly measuring elevated c-di-GMP levels (143, 176, 177). Overexpression of *ydaJKLMN* resulted in enhanced CR-binding and a visible increase in colony rugosity, implying a change in extracellular matrix composition. Analysis of each gene encoded by the operon suggested that YdaLMN are involved in the synthesis of a new, but still unknown, polysaccharide product, which is likely to be modified by YdaJ (54). Furthermore, YdaK is required for the synthesis of the unknown polysaccharide by YdaLMN, suggesting that YdaK somehow activates production of the unknown EPS (Figure 2C). But is YdaLMN YdaK's target? A fluorescent YdaK-YFP fusion appeared to co-localize with YdaM and YdaN at the cell poles and septa. This observation is somewhat reminiscent of the subcellular localization pattern of the large biosynthesis complex that produces the polyketide bacillaene (178). Also, deletion of one of the DGCs, *dgcK*, inhibited synthesis of the putative EPS machinery encoded by the *yda* operon, suggesting that the *yda* EPS is *dgcK*-dependent (58). Fluorescent DgcK fusions localized similarly to YdaK at the poles and septa, suggesting spatial proximity between the putative DGC-effector pair (Figure 2C). Intriguingly, the fluorescent YdaK reporter was observed in only a small subset of the population (~18.5%), suggesting that the *yda* operon is expressed in only a subpopulation of *B. subtilis* cultures (54). Furthermore, the *yda* operon is regulated by SigB, an alternate sigma factor induced in response to general cellular stresses (179). Together, these observations might suggest that the unknown *yda* EPS is stimulated during conditions of stress that remain to be elucidated.

1.7.4 C-di-GMP Regulation by YkuI of Other *B. subtilis* Pathways

To assess YkuI function (as a receptor or PDE), a *ykuI* mutant was tested for swarming motility (162). Compared to a *pdeH* mutant, deletion of *ykuI* only mildly impaired swarming. A mutant lacking both *ykuI* and *pdeH* resulted in inhibition of swarming motility to an extent that resembled the single *pdeH* mutation. Therefore, under the tested conditions, YkuI does not contribute significantly to inhibition of swarming. Recently, a transposon mutagenesis screen of wild-type *B. subtilis* cells revealed that insertion of transposons into *ykuI* conferred resistance to inhibitory (millimolar) concentrations of zinc (180). Yet, unlike other zinc resistance mutants, a *ykuI* mutant did not accumulate intracellular zinc, suggesting that inactivation of *ykuI* affects the metal indirectly. It is possible that deletion of *ykuI* somehow restricts access to zinc, although a mechanistic model for this phenotype has not yet been identified (Figure 2D).

Biochemical analysis of both the full-length and truncated EAL domain variants of *B. subtilis* YkuI failed to demonstrate PDE-A activity (163). The presence of an EAL domain, but lack of PDE-A activity in *vitro* allows it to potentially function as another c-di-GMP receptor. While many inactive PDE-As have degenerate active site sequences, intriguingly, YkuI has a perfectly intact active site sequence. Furthermore, high-resolution structural analyses of full-length YkuI confirmed binding of c-di-GMP to the EAL domain. Unlike other active PDE-As, however, the structure of YkuI revealed an alternate arrangement for D152, a residue involved in the coordination of a divalent cation for other PDEs. The lack of one metal ion might render the protein catalytically inactive. It should be noted, however, that YkuI has a C-terminal domain

(PF10388) with a PAS-like fold. This PAS-like domain is found immediately adjacent to the EAL domain and is highly conserved in *Bacillus* species. Given that PAS domains frequently function as sensors, it remains possible that YkuI could still be activated for PDE-A activity with the appropriate PAS-like ligand.

Interestingly, *B. subtilis* YkuI has an ortholog in *B. cereus* group bacteria named CdgJ, which does have a degenerate EAL domain. Gene expression patterns of *B. thuringiensis cdgJ* showed an increase in expression during the transition from planktonic growth to biofilm (181). Subsequent overexpression of *cdgJ* resulted in increased biofilm formation and earlier entry into sporulation. Conversely, no sporulation was observed in a *B. thuringiensis cdgJ* mutant. Given the 55% identity in protein sequences between *B. subtilis* YkuI and *B. thuringiensis* CdgJ, it is therefore possible that YkuI might also exhibit a similar role in *B. subtilis*, although this has yet to be explored.

1.8 Outlook

For many bacteria, c-di-GMP acts as an important intracellular signal to control lifestyle choice. In general, increased levels of c-di-GMP favors sessility and biofilm formation; correspondingly, decreased cellular levels of c-di-GMP promotes flagellar formation and motility (160, 182). While this theme has been established for Gram-negative bacteria and is largely maintained in Gram-positive organisms, additional developmental lifestyles such as sporulation and competence offer new and exciting avenues to explore c-di-GMP signaling in Gram-positive bacteria. Given the

importance of *B. subtilis* as a model system for Firmicutes, there is a clear need to thoroughly examine the regulation by c-di-GMP signaling in this organism. Yet the methods used to examine whether c-di-GMP affects biofilm formation have thus far incompletely considered that *B. subtilis* biofilms are heterogeneously composed of several sub-populations. This study began with the creation of a fluorescent c-di-GMP sensor with which to assess intracellular c-di-GMP dynamics in single cells of differentiated sub-populations of *B. subtilis,* as described in Chapter 2.

Accordingly, the c-di-GMP intermediate, pGpG, has been shown in several organisms to be cleaved by Orn. In bacteria that do not encode Orn, other enzymes such as NrnA, NrnB, and NrnC are thought to perform this function in a redundant manner instead (123). However, Orn, NrnA, and NrnB have been described as general 3'-5' exonucleases of short ribonucleotides. Therefore, how these enzymes target short RNAs and participate in cyclic dinucleotide signaling remains an open area of investigation. We aim to understand mechanistically how RNases such as Orn, NrnA, and NrnB are able to selectively target pGpG, other linear dinucleotides, and/or longer RNA polymers. The mechanistic details of how Orn senses pGpG will be described in Chapter 3. Chapter 4 investigates if NrnA and NrnB are functionally redundant and are mechanistically similar to Orn. Elucidating the function of the RNases that have dinucleotidase activity will represent a significant advancement in cyclic dinucleotide regulation as well as RNA recycling mechanisms in bacteria.

Chapter 2: Single-cell microscopy reveals that levels of c-di-GMP vary among *B. subtilis* subpopulations

2.1 Copyright notice

Chapter 2 was originally published by the Journal of Bacteriology as: Weiss CA, Hoberg JA, Liu K, Tu BP, Winkler WC. (2019). Single-cell microscopy reveals that levels of cyclic di-GMP vary among *Bacillus subtilis* subpopulations. *J Bacteriol.* 201: e00247-19.

Author contributions: Weiss, Hoberg, and Liu performed the research. Weiss, Liu, Tu, and Winkler analyzed the data. Weiss and Winkler wrote the paper.

2.2 Introduction

In many bacteria, c-di-GMP regulates the transition from a unicellular motile state to a multicellular sessile state (15, 160). However, c-di-GMP signaling has been less intensively studied in Gram-positive organisms as compared to their Gram-negative counterparts. To visualize the relative abundance of c-di-GMP for single cells of the Gram-positive model organism *B. subtilis*, we sought to construct a genetic reporter of c-di-GMP levels based on a c-di-GMP-responsive riboswitch. The interaction between the riboswitch aptamer domain and its cognate ligand induces a conformational change in the structure of the transcript, or expression platform, that modulates downstream gene expression (183). The changes in gene expression that are

triggered by riboswitches most commonly arise from regulation of transcription attenuation or translation initiation. However, other mechanisms have been observed, such as regulation of mRNA stability and protein sequestration (103, 110, 184, 185). These "molecular switches" bind their ligand with exquisite affinity and specificity, thereby discriminating against closely-related ligand variants. Therefore, riboswitches may be attractive tools for imaging metabolic changes within individual bacterial cells. Several types of highly selective fluorescent c-di-GMP biosensors have been developed in recent years and have largely focused on interrogation of c-di-GMP dynamics in Gram-negative bacteria. Riboswitch aptamers have been used as allosteric regulators of the conditionally fluorescent Spinach RNA aptamer (186, 187). Spinach and Spinach2 aptamer RNAs fluoresce upon binding of 3,5-difluoro-4-hydroxybenzylidene imidazolinone (DFHBI) (188, 189). Spinach variants can be carefully fused to riboswitch aptamer domains such that the Spinach domain fluoresces only in response to binding of the riboswitch ligand (186, 190). Yet, while they exhibit ideal performance characteristics *in vitro*, they require further optimization for routine usage in bacterial cells. For example, Spinach-based biosensors exhibit lower fluorescence than common fluorescent proteins. Some researchers have circumvented this limitation by tagging targeted RNAs with up to 64 spinach aptamers in tandem, thereby increasing the brightness of tagged RNA molecules (191); yet, this approach is not ideal for biosensor purposes. Prior expression studies in *Escherichia coli* have required the addition of a $tRNA^{Lys}$ scaffold sequence to aid in mRNA stability (192). Additionally, significant amounts of DFHBI have to be added to cells and allowed to incubate for prolonged interims, in order to allow for sufficient quantities of the chromophore to

passage through the cell membrane. A protein-based biosensor for c-di-GMP was also previously developed. The *Salmonella typhimurium* c-di-GMP binding protein YcgR was used to couple binding of c-di-GMP to Förster Resonance Energy Transfer (FRET) (193, 194). This genetically encoded biosensor protein was previously used for FRET-based microscopy of Gram-negative organisms such as *C. crescentus* and *P. aeruginosa* (193, 195). However, FRET-based biosensors also exhibit lower fluorescence intensities compared to individual fluorescent proteins, which can result in an overall narrowing of their dynamic range. Furthermore, many c-di-GMP protein receptors remain to be discovered in Gram-positive organisms for use in FRET microscopy. Based on all of these considerations, we chose to pursue development of a riboswitch-*yfp* reporter fusion that could provide useful information on *B. subtilis* c-di-GMP abundance. The fluorescent proteins used in this study have also been used in multiple studies regarding *B. subtilis* cell differentiation (196, 197). They have been shown to exhibit a shortened half-life and therefore can be expected to report relative differences in gene expression; however, it remains to be determined whether these reporters are sufficient to measure rapid dynamics.

A bioinformatics-based search (Rfam) for c-di-GMP-responsive riboswitches in Bacillales revealed a particularly interesting candidate in the untranslated leader region of the *Bacillus licheniformis lch* gene cluster. This nearly 27 kb operon (*lchA*) encodes the subunits of the nonribosomal peptide synthetase that makes lichenysin. Lichenysin is an antimicrobial cyclic lipopeptide that is virtually identical to surfactin, an important specialized metabolite produced by *B. subtilis* (198–200). The location of

this riboswitch is particularly interesting given that riboswitches have not been previously analyzed as being important for genetic regulation of secondary metabolites.

Herein, we confirmed the function of the putative class-I *lchAA* c-di-GMP riboswitch in regulating downstream gene expression via transcription attenuation. Construction of the fluorescent riboswitch reporter and quantification of its expression *in vivo* revealed that c-di-GMP levels are markedly different among *B. subtilis* cellular subpopulations. To elucidate c-di-GMP dynamics in each subpopulation, the riboswitch reporter was coupled with fluorescent reporters that demarcate the primary classes of *B. subtilis* cell types. These reporters revealed that cells that have made the decision to become matrix producers maintain higher intracellular c-di-GMP concentrations as compared to motile cells. Similarly, we find that c-di-GMP levels are raised in sporulating cells and reduced in competent cell types. These results suggest that biochemical measurements of c-di-GMP abundance are likely to be inaccurate for a bulk ensemble of *B. subtilis* cells, as such measurements will average c-di-GMP levels across the population. This study therefore emphasizes the importance of using single-cell approaches for analyzing metabolic trends within ensemble bacterial populations. These data also demonstrate that for some bacteria, c-di-GMP levels are adjusted heterogeneously across bulk populations.

2.3 Results

2.3.1 C-di-GMP attenuates transcription of the *lchAA* riboswitch in *vitro*

Many riboswitches couple detection of their target signal to transcription attenuation (103). In the unbound state, these riboswitches will oftentimes adopt a conformation in which an "anti-terminator" helix is created from the left half of the terminator and an upstream sequence. Then, when bound to its cognate ligand, the riboswitch will adopt an alternate conformation that allows for formation of an intrinsic terminator, causing disassociation of the transcription elongation complex. Manual inspection of the *lchAA* putative riboswitch revealed that its sequence included a candidate terminator site (Figure 3A). Therefore, to determine if c-di-GMP modulates downstream gene expression of the putative *B. licheniformis* riboswitch, a transcription termination assay was performed *in vitro* (Figure 3B). A DNA template of the *lchAA* untranslated element that included 50 nucleotides beyond the putative terminator ("run-off") was generated by PCR (Appendix) and mixed with RNA polymerase holoenzyme in the presence of varying amounts of c-di-GMP. Under the conditions that we used, a concentration of 10 μM c-di-GMP began to promote transcription termination at the terminus of the riboswitch, and ligand-responsive termination continued to increase up to the maximum concentration tested, 1 mM c-di-GMP.

To directly measure binding of c-di-GMP to the *lchAA* riboswitch, the *lchAA* aptamer domain was identified via manual inspection and fused to the P2 stem loop of the Spinach2 aptamer (Appendix). We hypothesized this would create an allosteric version of Spinach2, thereby creating an RNA with two distinct binding sites, for which binding of the *lchAA* aptamer to its cognate ligand would then trigger binding of

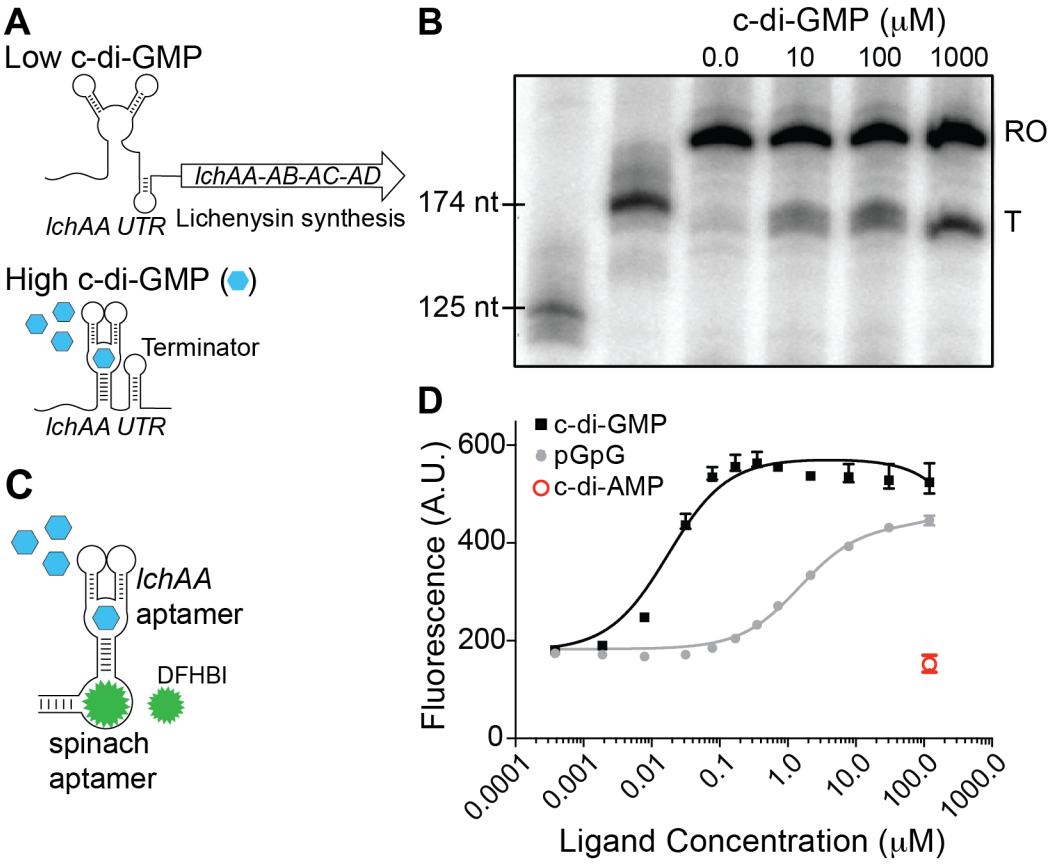

Figure 3. The *lchAA* riboswitch terminates in response to c-di-GMP. (A) Schematic of the mechanism of regulation by the *B. licheniformis lchAA* riboswitch in response to high and low levels of c-di-GMP. (B) A transcription termination assay of the *lchAA* UTR RNA with increasing concentrations of c-di-GMP (0 to 1000 μM) shows premature termination of run-off (RO) within the leader sequence, as compared to a terminated (T) transcript. (C) Schematic of the Spinach2 RNA allosterically regulated by the *lchAA* riboswitch aptamer in response to c-di-GMP. (D) *In vitro* fluorescence assay of the riboswitch-Spinach2 RNA (100 nM) in the presence of saturating DFHBI (10 μM) and increasing concentrations of c-di-GMP or pGpG. Binding affinity measurements are representative of two independent replicates.

DFHBI to Spinach2 (Figure 3C). To test if the molecule behaved as predicted, Spinach2 fluorescence was measured in the presence of saturating concentrations of DFHBI and with increasing concentrations of c-di-GMP (Figure 3D). This revealed that fluorescence of the *lchAA* aptamer-Spinach2 RNA was dependent on an appropriate amount of c-di-GMP, confirming that the *lchAA* aptamer acts as a sensor of c-di-GMP. In contrast, we did not detect Spinach2 fluorescence in the presence of 100 μM c-di-AMP. The *lchAA* aptamer, as part of a Spinach2 biosensor construct, bound c-di-GMP with an apparent K_d of 17 nM (Figure 3D). While this apparent Kd is much lower than the concentration of c-di-GMP required to promote transcription termination *in vitro* on purified DNA templates, there is a potential explanation for this difference. It has been previously observed that many riboswitches are not driven by equilibrium ligand interactions. Instead, they are driven by coordination of the kinetics of ligand association and RNA polymerization speed (201, 202). Therefore, one must be cautious in overinterpreting differences in equilibrium binding affinities for transcription attenuation-based riboswitches. If the *lchAA* riboswitch is kinetically driven, as we anticipate, a higher concentration of c-di-GMP would be required to promote a conformational change of the expression platform *in vitro*, as was suggested by our transcription termination data. Fluorescence of the *lchAA*-Spinach2 aptamer was also measured when the RNA was incubated in the presence of pGpG, the linear dinucleotide and c-di-GMP degradation product; however, the apparent K_d for this molecule was two orders of magnitude higher than that for c-di-GMP (Figure 3D). This roughly agrees with previous results on a different c-di-GMP riboswitch, which showed that pGpG binds the riboswitch with much poorer affinity than c-di-GMP (203). We

conclude from these aggregate data that c-di-GMP specifically interacts with the *lchAA* riboswitch to promote transcription attenuation of the *lchAA* operon.

2.3.2 *B. subtilis* heterogenously expresses a *lchAA* riboswitch-*yfp* reporter

We next wanted to assess c-di-GMP levels in single cells of *B. subtilis in vivo.* The entire leader sequence of *B. licheniformis lchAA* was inserted between the constitutively active promoter sequence and *yfp* (Appendix). Unlike the constitutive *yfp* reporter, a strain containing the riboswitch-*yfp* reporter exhibited two prominently distinct levels of fluorescence within the population. Nearly 70% of the cells were moderately fluorescent as compared to the constitutive *yfp* strain, while the remaining cells exhibited significantly diminished fluorescence (Figure 4A, B). Therefore, unlike the unimodal distribution of fluorescence exhibited by the constitutive *yfp* reporter, the riboswitch-*yfp* reporter strain appeared to show a bimodal distribution of fluorescence. To determine whether this distribution was due to riboswitch regulation of YFP, the riboswitch element was mutated, so that 65 nucleotides from the 5' end of the *lchAA* leader, which includes part of the c-di-GMP-binding aptamer, was removed. When examined for cellular fluorescence, this population of cells uniformly expressed YFP at levels similar to the constitutive *yfp* reporter construct (Figure 4A, C). These findings together suggest that the c-di-GMP riboswitch-*yfp* reporter is bimodally expressed within a population of *B. subtilis.*

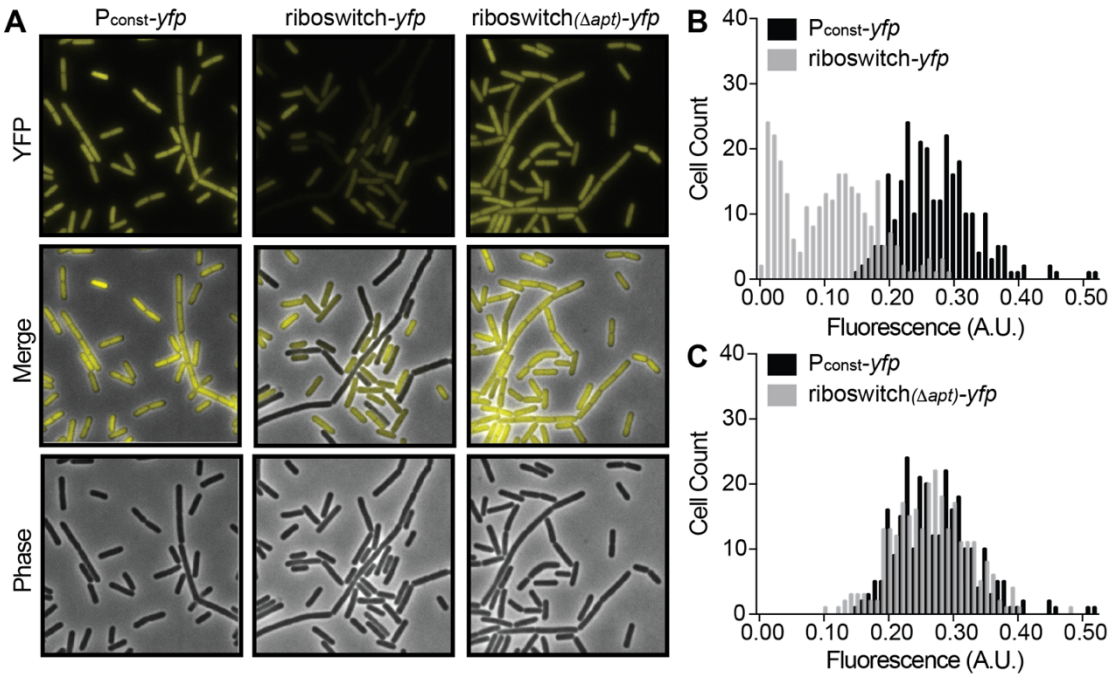

Figure 4. Expression of a *lchAA* riboswitch-*yfp* reporter *in vivo* results in bimodal distribution of fluorescence. (A) Representative microscopy images of wild-type *B. subtilis* PY79 expressing a constitutive P_{const}-*yfp* reporter, a riboswitch reporter construct P_{const}-riboswitch-*yfp,* or a riboswitch reporter construct comprising a deletion corresponding to the riboswitch aptamer (P_{const}-riboswitch$^{\Delta apt}$-*yfp*). (B) Histograms of the quantification of fluorescence intensity per cell of wild-type *B. subtilis* PY79 expressing P_{const}-*yfp* compared to P_{const}-riboswitch-*yfp* or (C) P_{const}-*yfp* compared to P_{const}- riboswitch $^{\Delta apt}$-*yfp* (n~300).

2.3.3 The riboswitch reduces gene expression due to elevated c-di-GMP

To confirm that the bimodal distribution of fluorescence observed in single cells of *B. subtilis* was solely due to differences in intracellular c-di-GMP levels, we integrated the constitutive *yfp* and riboswitch-*yfp* reporter fusions into a Δ*pdeH* knockout strain. Loss of the PdeH phosphodiesterase should inhibit hydrolysis of c-di-GMP and consequently elevate intracellular levels. We predicted that this should promote premature transcription termination in the riboswitch-*yfp* reporter fusion, thereby reducing YFP signal. Indeed, the riboswitch-*yfp* reporter resulted in significantly decreased *yfp* expression in the Δ*pdeH* background, suggesting intracellular c-di-GMP was elevated in all cells at late-log phase (OD_{600}=1.0) (Figure 5B, D). Conversely, constitutive *yfp* expression was unaffected by the Δ*pdeH* mutation, confirming the specificity of the riboswitch-*yfp* reporter for c-di-GMP (Figure 5A, C). Liquid chromatography-tandem mass spectrometry (LC-MS/MS) was also employed to detect c-di-GMP levels in both PY79 wild-type and Δ*pdeH*, grown to late-log phase (OD_{600}=1.0). A roughly 3-fold increase in c-di-GMP was observed by LC-MS/MS for the bulk population of Δ*pdeH* cells (Figure 6).

2.3.4 Expression of the riboswitch reporter correlates with specific cell types

We next sought to correlate c-di-GMP levels with subpopulations of *B. subtilis*. The gene encoding for *yfp* was replaced with another gene encoding for a red fluorescent protein, mCherry. This new riboswitch reporter was introduced in strains that already harbored transcriptional *gfp* or *yfp* reporters that demarcate the most

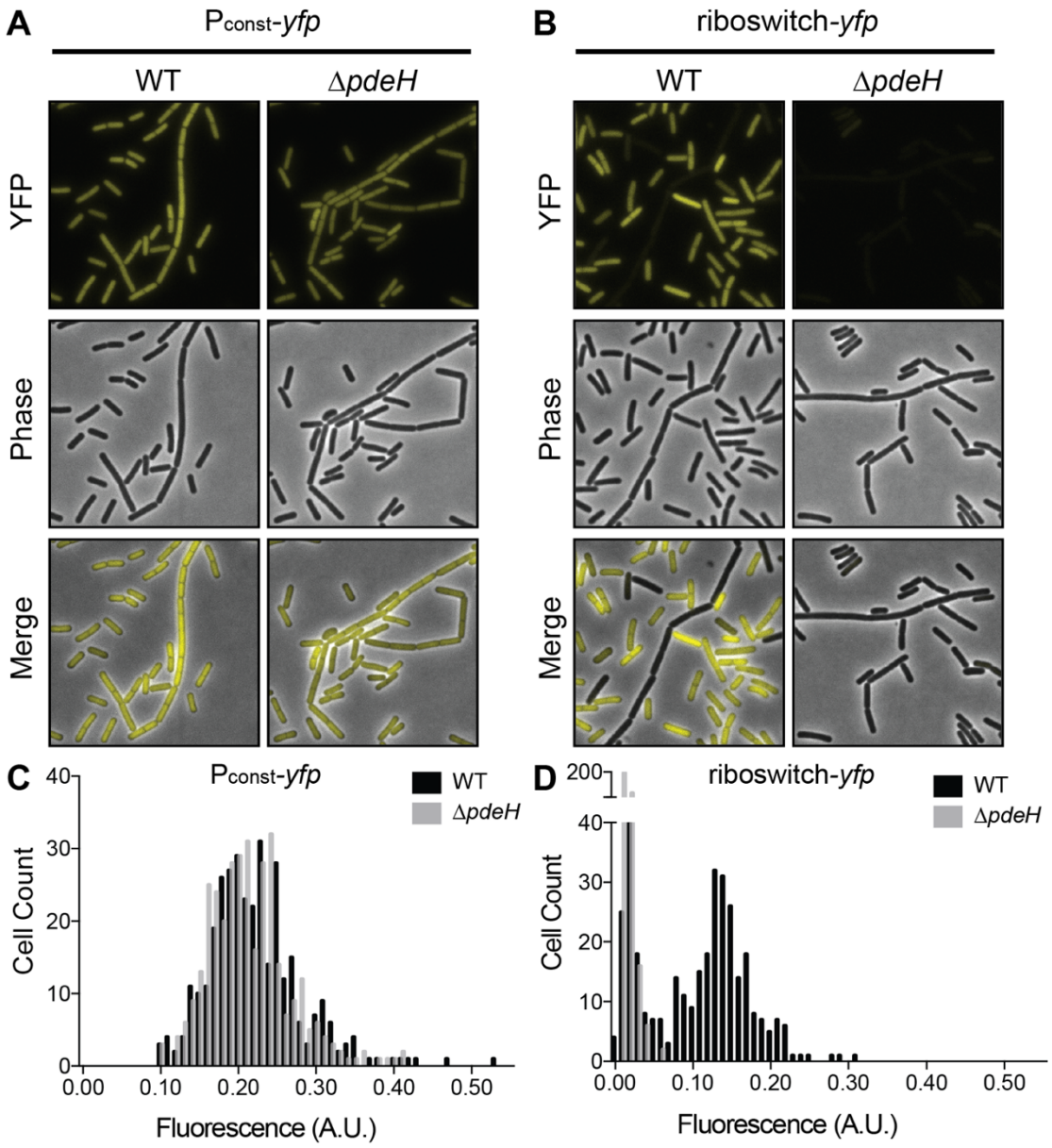

Figure 5. Deletion of *pdeH* results in increased c-di-GMP. (A) Representative microscopy images of *B. subtilis* PY79 wild-type (WT) or Δ*pdeH* expressing the constitutive P_{const}-*yfp* reporter, or (B) the riboswitch reporter construct P_{const}- riboswitch-*yfp*. (C-D) Histograms of the quantification of fluorescence intensity per cell comparing *B. subtilis* PY79 WT or Δ*pdeH* expressing P_{const}-*yfp* or P_{const}-riboswitch-*yfp* (n~300).

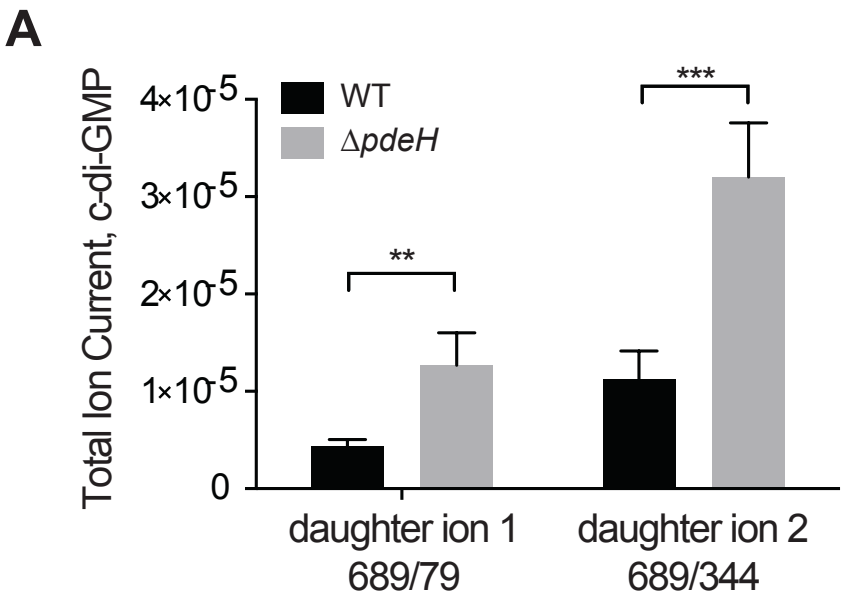

Figure 6. LC-MS/MS detects increased c-di-GMP in *B. subtilis* Δ*pdeH*. Quantification by LC-MS/MS of intracellular c-di-GMP levels in *B. subtilis* PY79 wild-type (WT) or Δ*pdeH* in late-log phase (OD_{600}=1.0). Results were obtained for two daughter ions. A roughly 3-fold increase in c-di-GMP was observed in Δ*pdeH* for daughter ion 1 (**P=0.0026) and daughter ion 2 (***P=0.0006) Error bars represent mean ± SD (n=3). Statistical significance determined by unpaired two-tailed Student's *t*-test.

common *B. subtilis* cell types including: motile, matrix-producing, or competent. When analyzed by fluorescence microscopy at late-log phase (OD_{600}=1.0), a majority of cells exhibited high expression of a P_{hag}-*gfp* reporter (denoting motility) and high expression of the riboswitch-*mCherry* reporter (signifying low c-di-GMP). Of the cells that were transcriptionally active for motility gene expression, 89.8% also exhibited fluorescence from the riboswitch reporter. This suggests that c-di-GMP abundance is uniformly low in motile cells (Figure 7A, D), and that a positive correlation exists between the genetic reporters. Low c-di-GMP levels were also observed in competent cells. While roughly 20% of cells in the population were competent, as indicated by a P_{comG}-*yfp* reporter, 79.7% of these cells exhibited high fluorescence from the c-di-GMP riboswitch-*mCherry* reporter (Figure 7C, F). However, when we analyzed the riboswitch-*mCherry* reporter in the context of matrix-producing cells, as identified by a P_{tapA}-*yfp* reporter, we observed an anti-correlation between both reporters. Cells activated for producing extracellular matrix (as denoted by *tapA* gene expression) were observed mainly as long chains. Of these activated cells, 81.0% exhibited diminished fluorescence from the riboswitch-*mCherry* reporter *(*Figure 7B, E). This suggests that c-di-GMP levels are high in matrix-producing cells. Conversely, cells that showed high fluorescence for the riboswitch-*mCherry* reporter were almost never activated for *tapA* expression. Additionally, a small population of cells that had c-di-GMP levels sufficiently high enough to shut off the riboswitch reporter, but that had not activated the transcriptional reporter for biofilm formation (P_{tapA}-*yfp*), was observed. It is possible that these cells had not been activated yet for extracellular matrix production, which might suggest that c-di-GMP levels change prior to activation of matrix production. The riboswitch-*yfp*

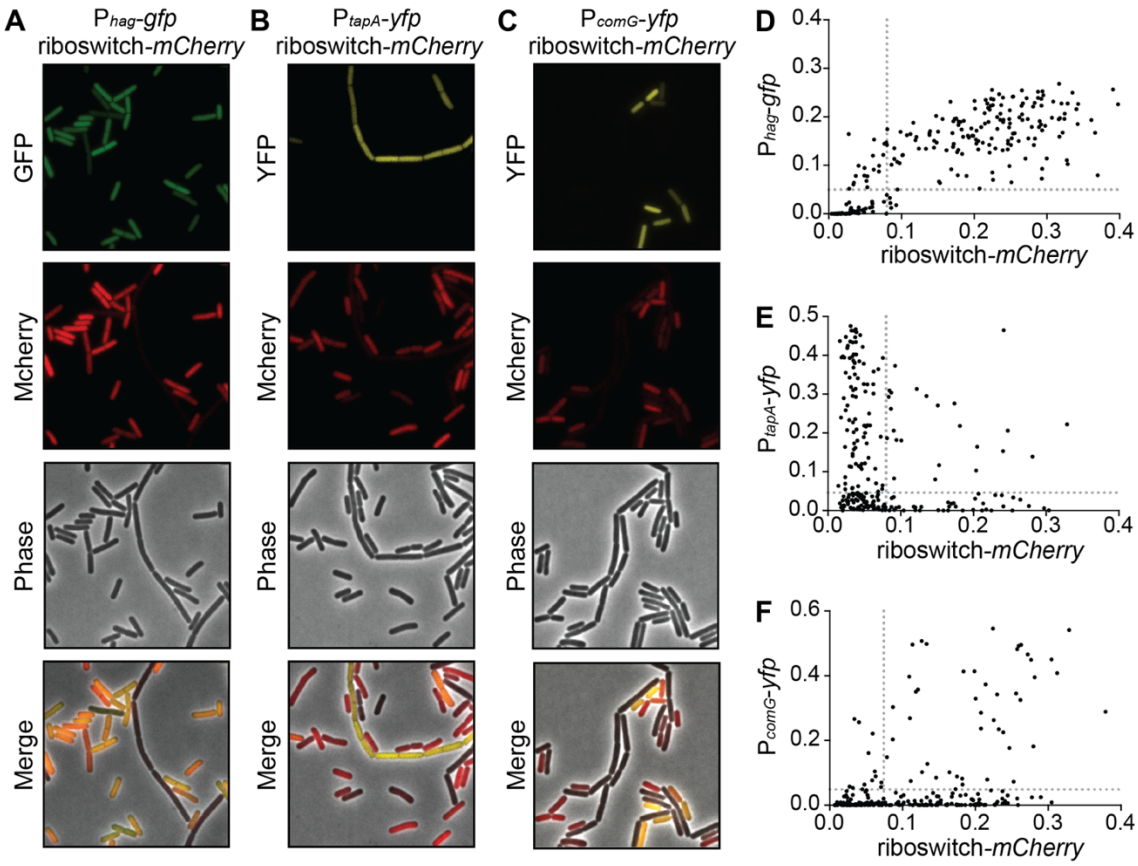

Figure 7. Expression of the riboswitch reporter varies nonrandomly among *B. subtilis* cell types. (A) Representative microscopy images of wild-type *B. subtilis* PY79 expressing the riboswitch reporter construct P_{const}- riboswitch-*mCherry* and the motility reporter P_{hag}-*gfp*. Statistical analyses show these reporters are significantly correlated (*****P*<0.0001). (B) Expression of P_{const}- riboswitch-*mCherry* and the biofilm reporter P_{tapA}-*yfp* are anti-correlated (***P*=0.0039). (C) Expression of P_{const}- riboswitch-*mCherry* and the competence reporter P_{comG}-*yfp* are correlated (*****P*<0.0001). (D-F) Quantification of the fluorescence intensity per cell of P_{const}- riboswitch-*mCherry* compared to each cell type reporter in each construct (n~300). Dotted lines represent the cut-off that divides fluorescent cells from non-fluorescent cells. Statistical significance determined by chi-square analysis.

reporter was also introduced in a strain that harbored a P_{const}-*mCherry* reporter, so that c-di-GMP levels could be assessed in cells that were activated for sporulation. Cells that progressed through spore development maintained expression of *mCherry,* but were uniformly low in riboswitch-*yfp* expression, suggesting that c-di-GMP levels are high overall during endospore formation (Figure 8).

2.3.5 An increase in c-di-GMP does not appear to change cell identity

To see if the manipulation of intracellular c-di-GMP levels could influence the proportion of cells that became matrix producers (as well as motile or competent), we used the "high c-di-GMP" strain, Δ*pdeH,* and integrated both transcriptional reporters for c-di-GMP levels and cell type in this background. When cells were analyzed by fluorescence microscopy, uniformly low mCherry levels of fluorescence were observed, thereby confirming the elevated levels of c-di-GMP in the Δ*pdeH* strain (Figure 9 A-F). Additionally, no obvious consequence on cell fate at the transcriptional level was observed. In many instances, however, c-di-GMP regulates phenotypic outputs at the post-translational level (164, 166, 167). This is exemplified in *B. subtilis* motile cells*,* where the binding of MotI to c-di-GMP directs MotI to directly disengage MotA from the rotor of the flagellar apparatus (168). It is possible that c-di-GMP post-translationally regulates YdaK as well, and this interaction activates production of the unknown EPS. So, while the proportion of cells in each sub-type was consistent between the wild-type and Δ*pdeH* mutant, and the level of activation for motility (Figure 9A, D) and matrix (Figure 9B, E) gene expression as measured by the reporters was the same, it remains possible that c-di-GMP could be a regulator of *B. subtilis'*

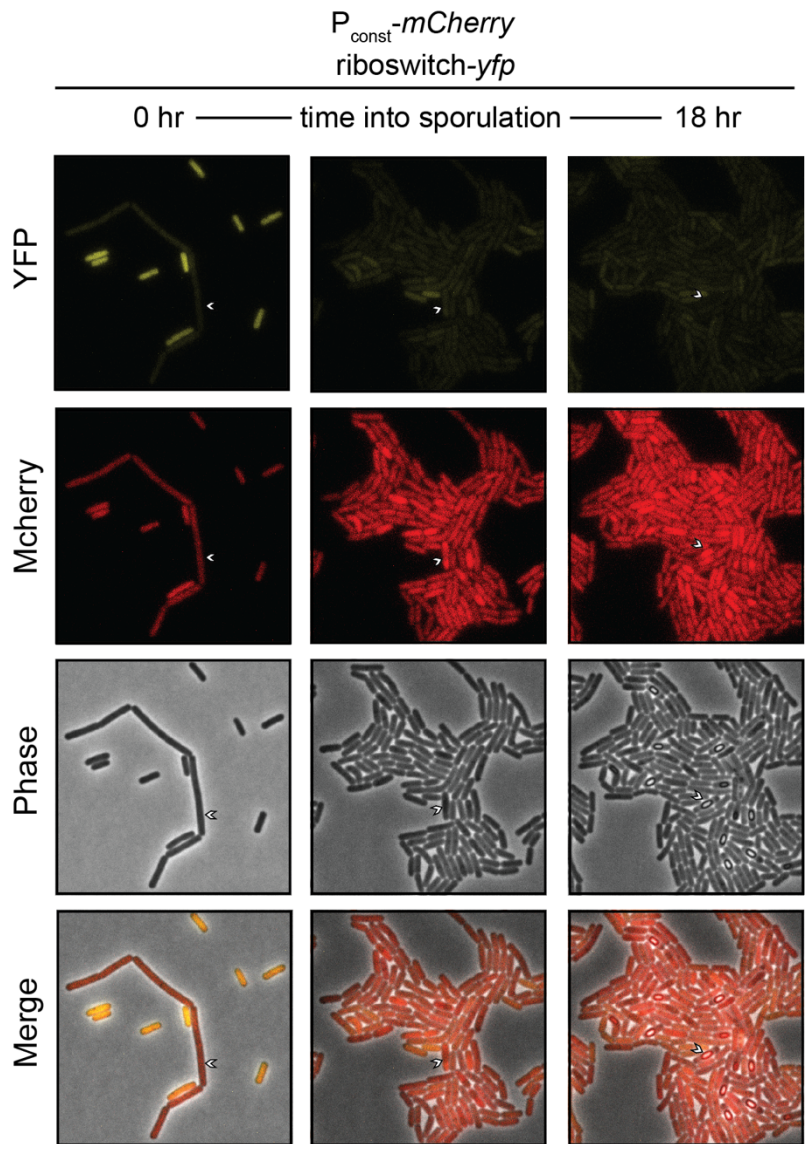

Figure 8. High c-di-GMP levels correlate with sporulation. Representative microscopy images of a time course through sporulation of the wild-type *B. subtilis* PY79 expressing the riboswitch reporter construct P_{const}- riboswitch-*yfp* and a constitutive reporter P_{const}-*mCherry*.

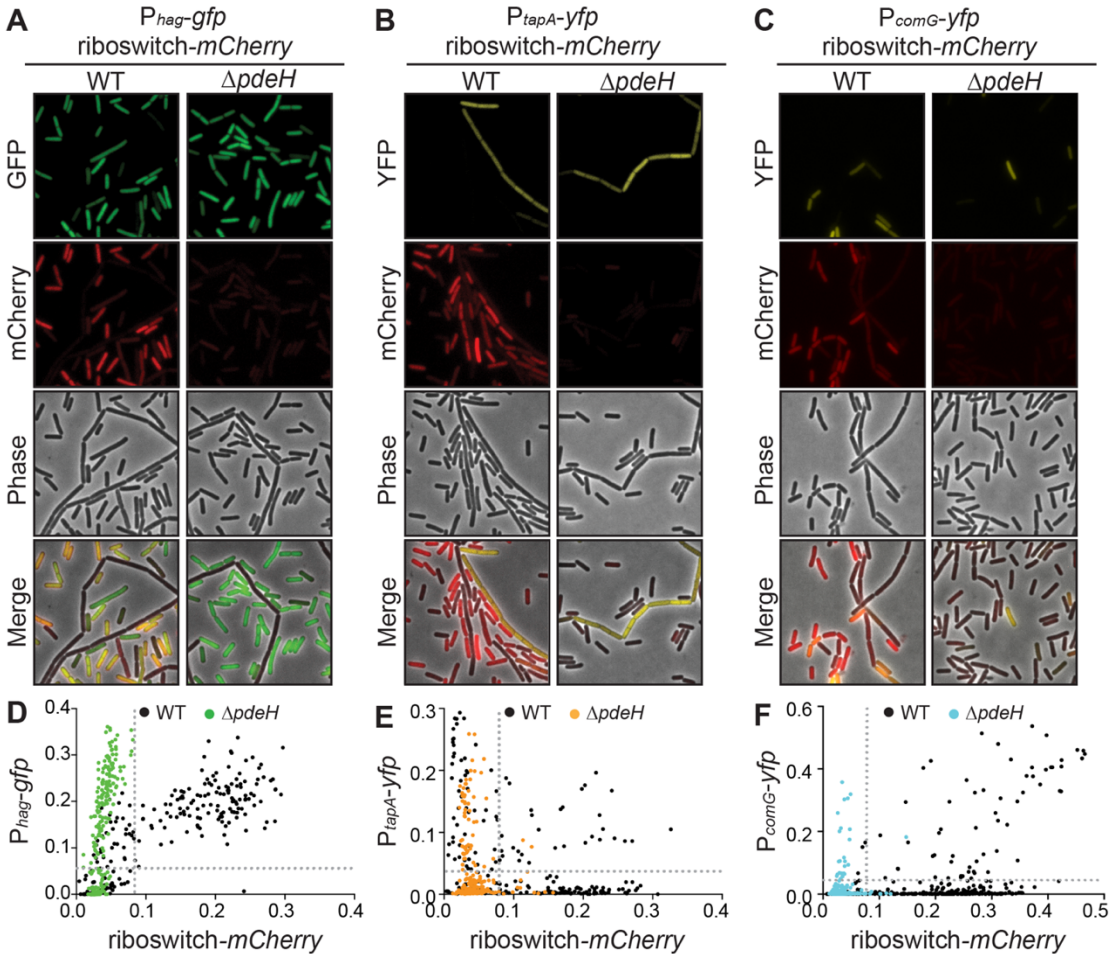

Figure 9. Deletion of *pdeH* does not change expression of each cell type reporter. (A) Representative microscopy images of *B. subtilis* PY79 wild-type (WT) or Δ*pdeH* expressing the riboswitch reporter construct P_{const}- riboswitch-*mCherry* and the motility reporter P_{hag}-*gfp*, or (B) P_{const}- riboswitch-*mCherry* and the biofilm reporter P_{tapA}-*yfp,* or (C) P_{const}- riboswitch-*mCherry* and the competence reporter P_{comG}-*yfp*. (D-F) Quantification of the fluorescence intensity per cell of P_{const}- riboswitch-*mCherry* compared to each cell type reporter, expressed in *B. subtilis* PY79 WT or Δ*pdeH* (n~300).

differentiation at the post-translational level. Interestingly, mild repression of the competence transcriptional reporter was observed in the Δ*pdeH* strain as compared to wild-type (Figure 9C, F).

2.3.6 *pdeH* expression is regulated transcriptionally

In addition to the catalytic EAL domain that provides phosphodiesterase activity, some PDEs also contain sensory domains (e.g. PAS) that allow for post-translational regulation of phosphodiesterase activity through activation by an extracellular signal. No such domain has been identified in *B. subtilis* PdeH. However, *pdeH* transcription was previously suggested to be repressed by Spo0A (162, 204), indicating that *pdeH* might be regulated transcriptionally. We therefore sought to ascertain if heterogeneous expression of the riboswitch reporter was due to heterogeneous expression of *pdeH* in each cellular sub-type. A transcriptional fusion of the *pdeH* promoter to a reporter gene encoding Superfolder GFP ('P_{pdeH}-*sf gfp'*) was created and ectopically integrated into wild-type and Δ*spo0A* background strains. Mean fluorescence for the Δ*spo0A* background (0.162, 95% CI 0.158-0.167) increased by roughly 2-fold as compared to wild-type (0.086, 95% CI 0.082-0.090) (Figure 10A). This agrees with prior data showing Spo0A inhibition of *pdeH* expression (162). Furthermore, quantification of the P_{pdeH}-*sf gfp* reporter revealed a single peak, implying a normal distribution of *pdeH* expression across the population. While a Δ*sigD* mutation had little effect on mean fluorescence (0.075, 95% CI 0.071-0.080) (Figure 10C), a Δ*sinR* mutation (0.050, 95% CI 0.046-0.054) led to a roughly 2-fold decrease in

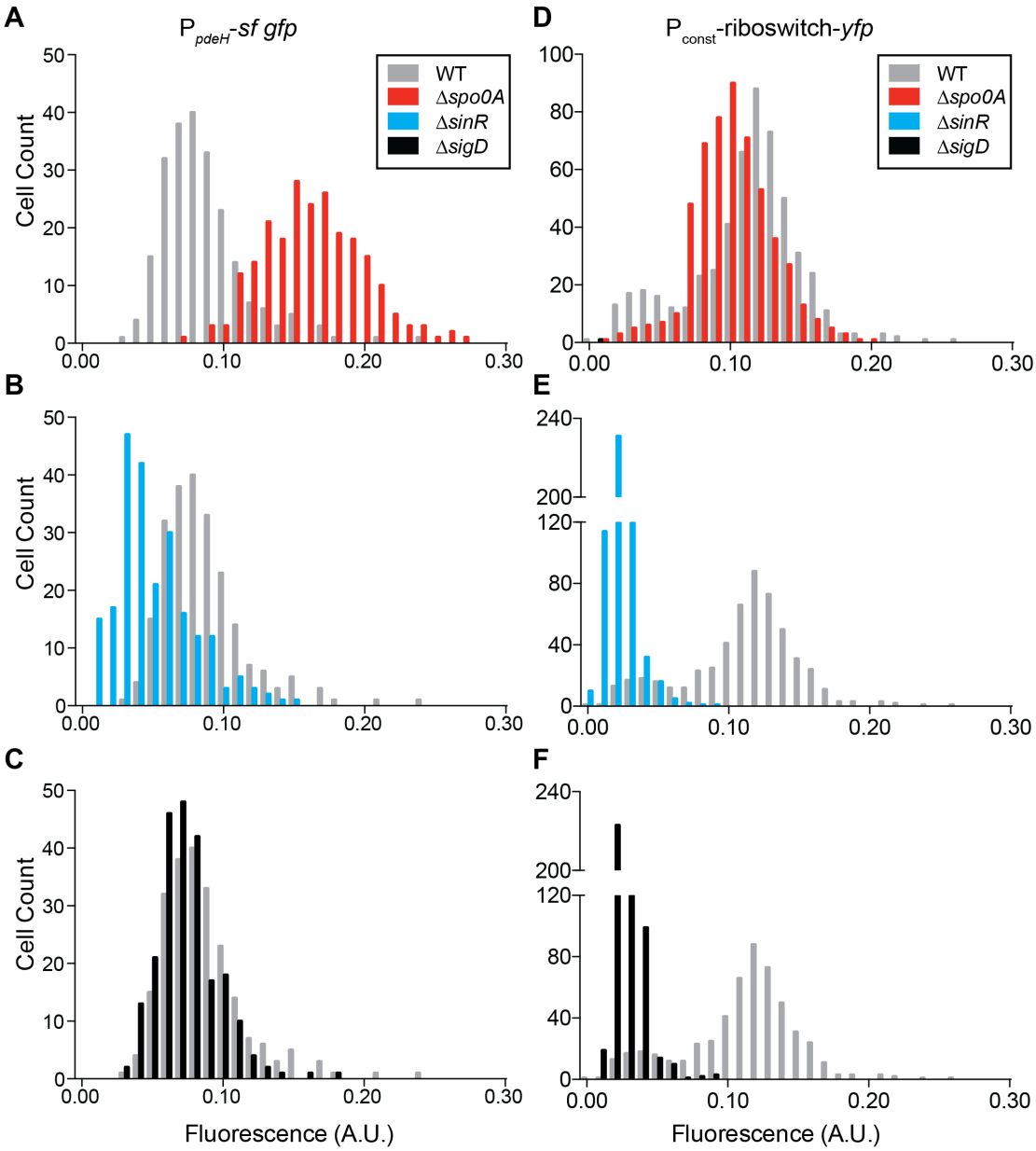

Figure 10. Deletion of global regulators affects *pdeH* expression and c-di-GMP levels. Quantification of the fluorescence intensity per cell of P_{pdeH}-*sf-gfp* in *B. subtilis* PY79 wild-type (WT), and (A) Δ*spo0A*, (B) Δ*sinR,* or (C) Δ*sigD* genetic backgrounds (n~300). Quantification and comparison of the fluorescence intensity per cell of P_{const}- riboswitch-*mCherry* in *B. subtilis* PY79 wild-type (WT), and (D) Δ*spo0A*, (E) Δ*sinR,* or (F) Δ*sigD* genetic backgrounds (n~500).

mean fluorescence (Figure 10B). From this, we speculate that removal of SinR might lead to physiological changes that enhance activation of Spo0A, thereby maximizing the Spo0A-mediated inhibition of *pdeH* transcription. Alternatively, it is possible that SinR might activate expression of *pdeH,* directly or indirectly, through an unknown mechanism. We also quantified fluorescence from the riboswitch reporter in these genetic backgrounds to correlate c-di-GMP levels with activity from *pdeH.* Our data predicts that de-repression of *pdeH* due to Δ*spo0A* should lead to lower intracellular c-di-GMP, exhibited by uniformly high fluorescence from the riboswitch reporter. Conversely, repression of *pdeH* due to Δ*sinR* should result in higher intracellular c-di-GMP and result in uniformly lower fluorescence from the riboswitch reporter. As predicted, the riboswitch reporter followed the hypothesized trends. A Δ*spo0A* mutation led to loss of a bimodal distribution of fluorescence, and the population exhibited similar fluorescence to the "low c-di-GMP" population of wild-type (Figure 10D). Mean fluorescence in a Δ*sinR* mutant was uniformly low (0.023, 95% CI 0.022-0.023), indicating high intracellular c-di-GMP (Figure 10E). Unexpectedly, however, we observed uniformly low fluorescence from the riboswitch reporter in a Δ*sigD* background (0.029, 95% CI 0.028-0.030). This suggests Δ*sigD* cells have an increase in intracellular c-di-GMP that cannot be explained by *pdeH* activity alone (Figure 10C, F).

2.4 Discussion

Given the importance of *B. subtilis* as a model system for the study of bacterial development, it is essential that its c-di-GMP regulatory mechanisms be further elucidated. In order to study c-di-GMP abundance for single cells of *B. subtilis*, we employed a constitutively expressed c-di-GMP riboswitch fused to *yfp* as our biosensor. Coupled with cell type-specific transcriptional reporters, our single cell microscopy shows definitively that intracellular c-di-GMP differs among *B. subtilis* cell types within a single population. Cells that have made the decision to become matrix producers maintain higher intracellular c-di-GMP as compared to motile cells. This study also shows that the transition into endospore formation correlates with high c-di-GMP levels, while competent cells correlate with lower c-di-GMP levels. This trend has not been previously examined in other studies.

One of the most common assays to measure the impact of mutations on biofilm formation, such as those affecting c-di-GMP homeostasis, is to visually assess the complexity of colony topology. While this can be qualitatively useful, it may not be representative of changes that occur at the cellular level. We take this to be due to the inherently heterogeneous composition of cell types within biofilm communities. Instead, the recent development of cell type-specific fluorescent reporters, as well as our c-di-GMP riboswitch reporter, allows investigators to examine features of *B. subtilis* subpopulations and their relationship to c-di-GMP effector proteins, DGCs, and PDEs. (51–53).

Physiological roles have been determined for several of *B. subtilis'* c-di-GMP enzymes and receptors. For example, MotI has been shown to inhibit motility (161,

162, 168). While the exact role of the *yda* operon has yet to be determined, the operon may be involved in the synthesis of an unknown exopolysaccharide, which may bolster the resistance of the biofilm during conditions of stress (54, 58). Our own analyses confirmed that *pdeH* is inhibited by the master regulator Spo0A, further establishing a connection between PdeH and c-di-GMP dynamics in specialized cell types during biofilm formation and/or sporulation. The roles of other enzymes and receptors, such as DgcK, DgcP, DgcW, and YkuI, remain to be elucidated. Single cell analyses are likely to be an important first step towards identifying the physiological conditions that activate c-di-GMP dynamics in a heterogeneous population of *B. subtilis*. For example, transcriptional data sets suggest that *dgcW* is regulated by sigma factor D, suggesting it may have a specialized role in motility. Future analyses of *dgcW*, in conjunction with visualization of our c-di-GMP riboswitch and cell type reporters, may help validate *dgcW's* function. The *yda* EPS is thought to be dependent on DgcK (54, 58). If YdaK is paired with DgcK activity, is *dgcK* also induced by stress? Furthermore, what are the exact physiological conditions under which c-di-GMP and YdaK regulate *YdaJLMN*? Also, our riboswitch reporter could also potentially be used to help reveal if YkuI is indeed involved in the regulation of sporulation or zinc homeostasis. Assessment of c-di-GMP abundance following deletion of *ykuI* could help determine whether YkuI acts as a c-di-GMP PDE or receptor. From these results, c-di-GMP riboswitch-*yfp* reporters could be used in other bacteria—Bacillales in particular—for single cell analyses of c-di-GMP abundance. These riboswitch-reporters may prove to be useful tools in elucidating the increasingly diverse c-di-GMP regulatory mechanisms used by Gram-positive bacteria.

The study herein also shows that a c-di-GMP riboswitch is likely to control expression of a *B. licheniformis* lichenysin biosynthesis gene cluster. This observation suggests that in some bacteria antibiotic synthesis is under the purview of c-di-GMP signaling. By extension, these data suggest that surfactin biosynthesis could also be subjected to c-di-GMP regulation in other *Bacillus* species. Interestingly, a peptide essential for competence (ComS) is encoded within the surfactin operon *srfAA-AD* in *B. subtilis* (205). *srfAA-AD* is also regulated by the transcription factor ComA, which is ultimately activated by the quorum sensing molecule ComX (206–208). This regulatory arrangement allows *B. subtilis* to integrate a single signaling pathway into multiple adaptive processes. Prior studies have shown that surfactin-producing cells coexist with, but are phenotypically distinct from, cells that produce the extracellular matrix components (150). Therefore, our observation that c-di-GMP is low in competent cells implies that c-di-GMP should also be low for surfactin-producing cells. Indeed, the presence of the c-di-GMP riboswitch upstream of *B. licheniformis lchAA* operon indicates that lichenysin is only produced when c-di-GMP levels are low. ComA has been shown to also recognize the *B. licheniformis lchAA* promoter, further supporting a relationship between lichenysin and competence gene expression (209, 210). While a c-di-GMP-responsive riboswitch does not seem to be located in the leader of *B. subtilis srfAA*, it is possible that c-di-GMP could regulate this gene cluster by an as yet undiscovered mechanism, which may foreshadow a role for c-di-GMP signaling during competence development in *B. subtilis*.

While our data demonstrate that c-di-GMP levels vary significantly between different cell types, we provide evidence that a general increase in c-di-GMP

abundance is not likely to change the proportion of each cell type at the transcriptional level. Our data suggests that c-di-GMP metabolic enzymes act downstream of the master regulators that drive genetic regulation of cellular differentiation such as Spo0A and SinR (Fig 7A, B), and that in *B. subtilis*, changes in c-di-GMP abundance occur as a result of cellular decision-making. However, the molecular details of how c-di-GMP levels affect cellular differentiation require further exploration. Furthermore, it is possible that effector targets for c-di-GMP-binding proteins have yet to be identified, as might be suggested by the recently discovered link to the *yda* exopolysaccharide pathway. The regulatory mechanisms that dictate these pathways, as well as new candidates for c-di-GMP receptors, undoubtedly still await discovery.

2.5 Materials and Methods

2.5.1 Transcription termination assay

PCR amplification was performed on the *B. licheniformis lchAA* leader sequence using primers that place it downstream of a constitutive promoter P_{const} and that ended 216 nts downstream of the transcription start site (Supp Fig 2). Transcription reactions were performed on the PCR-generated DNA template, resulting in a terminated (T) transcript of approximately 174-nt, or a 217-nt run-off (RO) transcript. These reactions comprised 5 µM template, 250 uM NTPs, 1X *E. coli* RNA Polymerase Reaction Buffer (NEB- 40 mM Tris-HCl pH 7.5, 150 mM KCl, 10 mM $MgCl_2$, 1 mM DTT, 0.01% Triton X-100), 20 µCi α-^{32}P-UTP, and 0.5 units of *E. coli* RNA Polymerase, Holoenzyme (NEB). C-di-GMP was added to the run-off transcription

reactions to a final concentration of 10 µM, 100 µM, and 1 mM. A 125-nt size marker was also transcribed. All reactions were incubated at 37˚C for 2 hours. Reactions were resolved by 6% urea-denaturing polyacrylamide gel electrophoresis (PAGE).

2.5.2 Spinach activation assay

PCR was performed to amplify two aptamers: a $tRNA^{Lys}$-lchAA-Spinach2 template, and a $tRNA^{Lys}$-Spinach 2 control template. A forward annealing primer was used to introduce the T7 promoter sequence, resulting in a 230-bp and 168-bp DNA template, respectively. Transcription reactions were performed, purified, and quantified as previously described (211). The *in vitro* Spinach2 fluorescence activation assay was modified from methods described previously (186). Briefly, the two RNA aptamers were each diluted to 2 µM and added to an equal volume of 2X renaturation buffer (80 mM HEPES pH 7.5, 250 mM KCl, 6 mM $MgCl_2$), heated to 70˚C for 3 minutes, and cooled at room temperature for 5 minutes. To test binding affinity of c-di-GMP for the *lchAA* aptamer, binding reactions were prepared for each RNA aptamer (40 mM HEPES pH 7.5, 125 mM KCl, 3 mM $MgCl_2$, 100 nM RNA, 10 µM DFHBI) and incubated in the dark at room temperature for 30 minutes. Stocks of c-di-GMP or pGpG were prepared and added to the binding reaction every 30 minutes to achieve the final concentrations that are graphed. Ligands were added until saturation of fluorescence was reached. A Quantus™ Fluorometer (Promega) was used to excite the reaction at 495 nm every 30 minutes after incubation with increasing amounts of c-di-GMP and pGpG. Binding to c-di-AMP was also assessed. The experiment was

replicated twice, and the background fluorescence of DFHBI alone was subtracted from all data points.

2.5.3 Bacterial strains, plasmids, and growth conditions

All *B. subtilis* strains in this study are derived from PY79 (unless otherwise noted). Strains were grown at 37˚C on Lysogeny Broth (LB) plates supplemented with 1.5% Bacto Agar and when appropriate, with final concentrations of the following antibiotics: 5 μg/mL chloramphenicol, and 1 μg/mL erythromycin added alongside 25 μg/mL lincomycin (mls). Integration at the *amyE* locus was performed with plasmids derived from pJG019 (GenBank: KX499653.1), or pVMZ006, both derivatives of pDG1662 (BGSC). To construct pRSL_F4, the *lchAA* leader sequence was synthesized (GenScript) and subcloned into the HindIII restriction site of pJG019. For construction of the P_{pdeH}-*sf gfp* reporter, the constitutive promoter of pVMZ006 was replaced with the *pdeH* promoter sequence that has been described previously (162). The sequence of *sf- gfp* was amplified from pJ204:102624 (DNA2.0, Inc.) and was used to replace the *yfp* sequence of pVMZ006 via Gibson assembly (212). The fluorescent transcriptional cell-type reporters P_{hag}-*gfp*, P_{tapA}-*yfp*, and P_{comG}-*yfp* that were used in this study have been described previously (135, 140, 213, 214). To construct the plasmids harboring these reporters, promoter sequences of *tapA* and *comG* were amplified from *B. subtilis* and used to replace the constitutive promoter upstream of *yfp* in pVMZ006 by Gibson assembly. The *amyE*::P_{hag}-*gfp* fusion from DS4432 (provided by D. Kearns, Indiana University) was introduced into the PY79 chromosome through double homologous recombination of competent cells. Plasmids derived from

pDG1664 (BGSC) were used for integration at the *thrC* locus. To make markerless deletions of Δ*pdeH*, Δ*spo0A,* Δ*sinR,* and Δ*sigD,* strains harboring an erythromycin-resistance cassette inserted in loci BSU31740 (*pdeH*), BSU24220 (*spo0A*), BSU24610 (*sinR*), and BSU16470 (*sigD*) were obtained from the BKE collection (BGSC). Markerless deletions were created through transformation with pDR244 (BGSC), as previously described (215). Removal of the erythromycin-resistance cassette was verified by Sanger sequencing. Transformation of PY79 was performed using a previously described protocol (216).

2.5.4 Fluorescence microscopy and quantification

Single colonies were used to inoculate liquid MSgg medium (155) and grown at 37˚C shaking overnight. The following morning, cultures of each strain were inoculated 1:50 in fresh medium and grown at 37˚C shaking until reaching an optical density at 600 nm (OD_{600}) of 1.0. Aliquots of these cultures were placed on 1.5% low-melting agarose MSgg pads and allowed to dry for 10 minutes. Agarose pads were inverted onto a glass bottom dish (Willco Wells). Cells were imaged at room temperature using a Zeiss Axio-Observer Z1 inverted fluorescence microscope, equipped with a Rolera EM-C_2 electron-multiplying charge-coupled (EMCC) camera, enclosed within a temperature-controlled environmental chamber. Fluorescence intensity per cell was quantified using Oufti analysis software (217). Images were analyzed and adjusted with FIJI software (218).

2.5.5 Metabolite extraction of c-di-GMP in *B. subtilis*

Three independent replicates of *B. subtilis* PY79 WT and Δ*pdeH::mls* were grown overnight in liquid MSgg medium (155) shaking at 37˚C. The following day cultures of each strain were inoculated (1:50) into fresh MSgg and agitated at 37˚C until reaching an optical density at 600 nm (OD_{600}) of 1.0. Metabolite extraction was performed as described previously (219). 5 mLs of each culture were passed through 0.2 μm nylon filters (EMD Millipore). Metabolites were extracted by inverting the filters into petri dishes that contained 1.5 mL pre-chilled extraction solvent composed of 40:40:20 acetonitrile/methanol/water. Dishes were placed on dry ice for 15 minutes before the wash was collected and spun at max speed for 5 minutes at 4˚C. The supernatant was then placed in a vacuum centrifuge until metabolite extracts were dry.

2.5.6 Detection and quantification of c-di-GMP by LC-MS/MS

Detection of c-di-GMP by LC-MS/MS was previously described (220). Briefly, bacterial extract was resuspended in Solvent A (10 mM tributylamine in water, pH 5.0) and centrifuged twice to remove insoluble particles. Metabolites were then separated on a Synergi Fusion-RP column (4 μm particle size, 80 Å pore size, 150 mm x 2 mm, Phenomenex) using a Shimadzu high performance liquid chromatography machine and simultaneously analyzed by a triple quadrupole mass spectrometer (3200 QTRAP, ABSCIEX). The total run time was 20 min at a binary flow rate of 0.5 ml min^{-1}, with 10 mM tributylamine in water (pH 5.0) as Solvent A and 100% methanol as Solvent B. The following gradient was performed: 0.01 min, 0% B, 4 min, 0% B, 11 min, 50% B, 13 min, 100% B, 15 min, 100% B, 16 min, 0% B, 20 min, 0% B. C-di-GMP was

detected by multiple reaction monitoring (MRM) under negative mode using the ion pairs 689/79 and 689/344 (c-di-GMP). C-di-GMP was quantified using the Analyst® software (version 1.6.2) by calculating the total peak area and normalized by total ion current (TIC). Authentic c-di-GMP standards were injected and analyzed alongside samples.

Chapter 3: A dedicated diribonucleotidase resolves a key bottleneck for the terminal step of RNA degradation

3.1 Copyright Notice

Author Contributions: Kim[#], Lormand[#], and Weiss[#] equally contributed to this work and performed the research. Additionally, Eger K, Turdiev H, and Turdiev A helped with research as well as formal analysis. Kim[#], Lormand[#], Weiss[#], Winkler, Sondermann, and Lee conceptualized, formally analyzed the research, and wrote the paper.

3.2 Introduction

C-di-GMP is widely used among bacterial phyla. Synthesized from 2 GTP molecules by diguanylate cyclases (DGCs) with conserved GGDEF domains, c-di-GMP binds a diverse array of receptors that control numerous physiological outcomes (15). Hydrolysis of c-di-GMP to two GMP molecules occurs in a two-step process, with the linear diribonucleotide pGpG as an intermediate. The hydrolysis of c-di-GMP to pGpG is performed by conserved phosphodiesterases (PDE-As), that contain a canonical EAL or HD-GYP domain (70, 73). While pGpG was known to be hydrolyzed

into two GMP molecules, the phosphodiesterase (PDE-B) that performed this terminal step remained elusive for many years. It was previously proposed that HD-GYP domain-containing PDE-As might also perform this PDE-B function. Despite the genetic and biochemical evidence that heterologously expressed HD-GYP proteins from different organisms complement the function of EAL proteins in c-di-GMP hydrolysis, several biochemical experiments indicated the main product of c-di-GMP hydrolysis to be GMP, not pGpG (221). Furthermore, the HD-GYP protein PA4718 was shown to have a 5-fold higher affinity for pGpG than c-di-GMP. The observation that not all bacteria that utilize c-di-GMP signaling encode HD-GYP domain-containing proteins suggested that other enzymes could be responsible for the terminal step of c-di-GMP signaling. Consequently, a DRaCALA screen for pGpG-binding proteins was performed, which identified Oligoribonuclease (Orn) as the primary protein responsible for binding pGpG and cleaving pGpG to GMP (113). Subsequent studies showed that *P. aeruginosa* lysates corresponding to transposon mutants of two HD-GYP still retained the ability to cleave pGpG similar to wild-type. This suggested that HD-GYP PDE-As do not contribute to pGpG turnover *in vivo.*

Interestingly, several publications characterizing the role of Orn already existed (114–116). Orn was discovered in the 1960s, during some of the earliest investigations of RNA polymerization, decades before the discovery of c-di-GMP by Moshe Benziman and his colleagues. Shortly after the discovery of RNA Polymerase, great efforts were made to understand the properties and mechanisms of RNA Polymerase during transcription initiation. Although transcription initiation in all cells is dependent on ribonucleotide triphosphates (rNTPs), the observation that short

oligoribonucleotides could serve as templates for transcription by RNA Polymerase *in vitro* was well established (222, 223). While testing different oligoribonucleotides for priming activity with RNA Polymerase, Niyogi and Stevens observed that priming could only take place in the presence of purified RNA Polymerase. If crude extracts from *E. coli* were used, no priming activity was observed. This result suggested that there was something in the crude extract that interfered with the ability of oligoribonucleotides to stimulate RNA synthesis. Soon after, an enzyme fraction was isolated from *E. coli* and shown to hydrolyze adenine oligoribonucleotides to 5'-adenosine monophosphate (5'-AMP) as the major product (114). Subsequent purification of the enzyme led to the characterization of Orn's function. Since then, all available literature has assumed that Orn is a 3'-5' exoribonuclease that is responsible for processing of short oligoribonucleotides 2 to 7 nucleotides in length (114–117). The ability of Orn to degrade the linear diribonucleotide pGpG therefore falls within the confines of Orn's presumed function as an oligoribonuclease. Interestingly, Orn is essential for viability in a number of γ-proteobacteria such as *E. coli* (119). This essentiality makes Orn unique among all other known 3'-5' exoribonucleases, which have been shown in some instances to be functionally redundant.

The molecular basis of Orn's unique cellular functions in γ-proteobacteria that distinguishes it from all other exoribonucleases remained unexplained. Furthermore, it was not clear how Orn might selectively target 'short' RNAs, rather than simply binding to the penultimate sequence at the 3' termini of single-stranded RNA of any length. The Winkler (University of Maryland), Lee (University of Maryland) and Sondermann (Cornell University) labs sought to rectify this through a combination of

biochemical, genetic, and structural approaches. To that end, we incubated Orn with 5' ^{32}P end-labeled RNAs of varying lengths and analyzed the products of that reaction over time. Our data show that Orn exhibits a surprisingly narrow substrate preference for diribonucleotides. We sought to understand this remarkable substrate selectivity of Orn by determining the crystal structure of Orn in complex with pGpG, which allowed us to identify key residues for recognizing diribonucleotides. Furthermore, we took advantage of the fact that *P. aeruginosa orn* mutants are still viable and found that Orn is the only diribonucleotidase in *P. aeruginosa*. The aggregate data shows that Orn exhibits such a striking preference for diribonucleotide substrates that the function of Orn as a general exoribonuclease should be reconsidered.

3.3 Results

3.3.1 Selection of a method to assess biochemical activity of Orn

Orn is presumed to function as a 3'-5' exonuclease specific for small oligoribonucleotides. Prior studies employed chromatographic techniques, to be able to analyze the product composition of these reactions over time (115–117). Generally, ^{14}C-labeled (pA)n oligonucleotides 2-5 in length were incubated with purified Orn, other enzymes, or lysates. After the reaction was stopped, the reaction products were separated by paper chromatography and quantified by scintillation counting. Later studies relied on gel electrophoresis techniques. RNA substrates used in these studies were tagged at the 5' terminus with fluorophores such as Cy5 (118, 120–122, 224). The products of this reaction were resolved by denaturing polyacrylamide gels, thereby allowing for detection of products with one or more nucleotides removed from the 3'

end. To understand Orn's substrate preferences, Orn would have to be purified and incubated with RNAs of varying lengths. Unlike fluorophore-labeled RNA used in prior studies, which contain a large planar chemical moiety at their 5' terminus, we wanted to use substrates that resembled native ligands as closely as possible. To this end, native oligomers 2-7 ribonucleotides in length were synthesized, and the 5' phosphate of each RNA was radiolabeled with ^{32}P-γ-ATP, to ensure that the substrate structure was unperturbed. The diribonucleotide substrate in our subsequent studies was pGpG (GG), whereas the longer oligoribonucleotides included an increasing number of adenine nucleotides at the 5' end. This arrangement ensured that the same GG sequence was maintained at the 3' end while also avoiding stable G quadruplex formation that may be observed with RNAs containing stretches of poly-G (225).

The ability to analyze the product composition of these reactions over time would subsequently require chromatographic techniques to accurately resolve single nucleotide differences in RNA products from cleavage by Orn for quantitative analysis. Three assays that can perform this function were considered: thin layer chromatography (TLC), high performance liquid chromatography (HPLC), and gel electrophoresis. While TLC is the fastest method for separation, this method also offers the least sensitivity for accurately quantifying the relative accumulation of each product during Orn cleavage. Under the conditions we tested, we were not able to accurately discriminate among single nucleotide differences (Figure 11). In contrast, HPLC is likely to be a superior method in the separation of products, as it is sensitive and can be automated. It can be performed in a relatively short amount of time, accurately resolves products, and can be controlled with the aid of a computerized system.

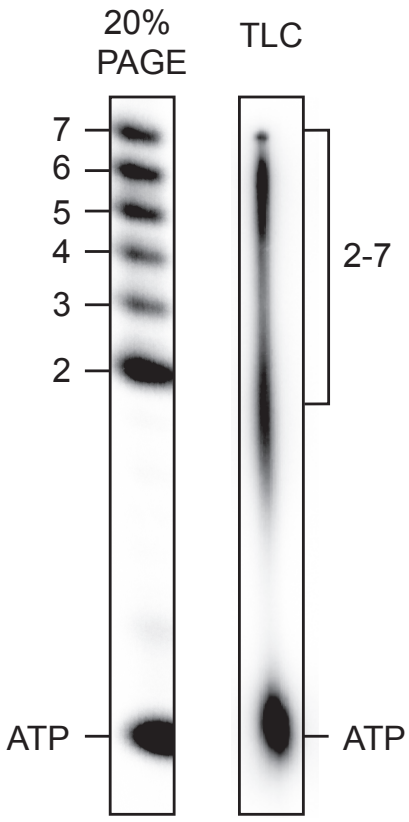

Figure 11. Resolution of single ribonucleotide species by PAGE or TLC. 5' ^{32}P-radiolabeled RNAs 2-7 nucleotides in length were generated and combined in a single mixture. RNAs were resolved either by 20% urea-denaturing PAGE or TLC.

However, HPLC requires larger amounts of starting material and was not immediately available to us. These considerations led us to find gel electrophoresis conditions that would separate RNA products with single nucleotide resolution. Prior studies used constituents that included 20% polyacrylamide and SDS as a denaturant. We chose to also use 20% polyacrylamide but chose to provide denaturing conditions from urea. Under these electrophoresis conditions, the mononucleotides and oligonucleotides that were tested (between 2 and 7 nucleotides in length) could be resolved (Figure 11).

3.3.2 Orn functions as a diribonucleotidase *in vitro*

To understand the length preference of Orn, recombinant affinity-tagged *Vibrio cholerae* Orn (Orn_{Vc}) was purified and then tested biochemically. Orn_{Vc} was incubated with 5'-^{32}P-radiolabeled oligoribonucleotides of varying lengths in the presence of magnesium, to support catalysis. Assays were also performed at near-physiological ionic strength, in contrast to prior studies that often utilized buffer lacking salt (NaCl/KCl). The products of these reactions were resolved by urea-denaturing 20% PAGE. At substrate concentrations that far exceed enzyme concentration (200:1), the diribonucleotide substrate was already fully processed to nucleoside monophosphates by 30 minutes (Figure 12A, B), which agrees with prior observations (113). In contrast, longer substrates (i.e. from 3-mers to 7-mers) were not processed at their 3' end, even at 30 minutes (Figure 12A, B). These results suggest that Orn prefers dinucleotides. This strong substrate preference stands in stark contrast to previous studies arguing Orn acts as a general exoribonuclease that cleaves oligoribonucleotides with two to seven residues in length.

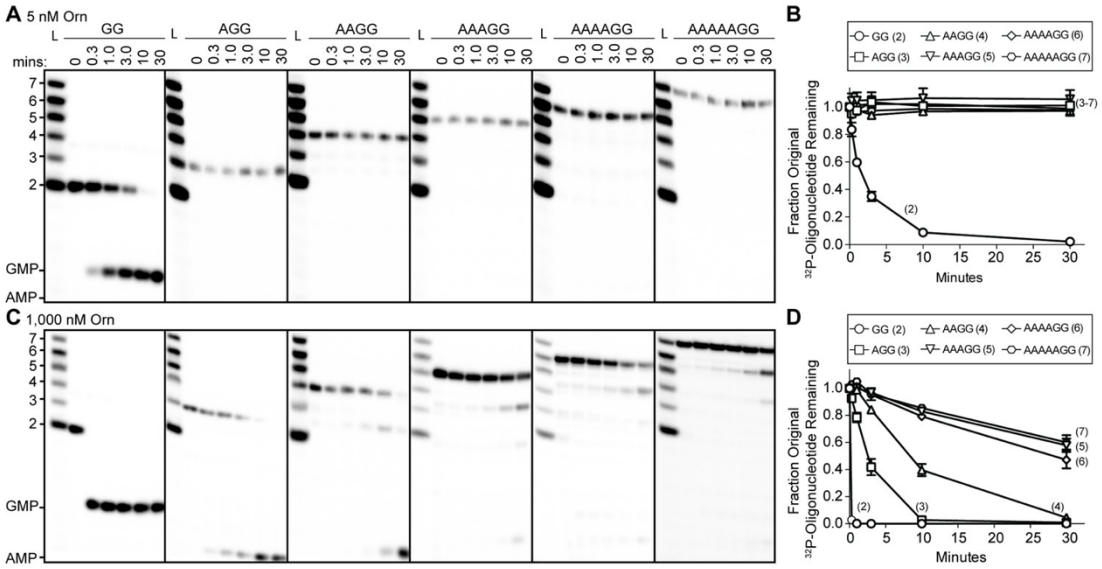

Figure 12. Orn has a stark preference for diribonucleotide cleavage *in vitro*. RNA nucleotides two to seven residues in length (1 μM, containing the corresponding ^{32}P-labeled RNA tracer) were each subjected to cleavage over time with 5 nM (A, B) or 1000 nM Orn$_{Vc}$ (C, D). Aliquots of each reaction were stopped at indicated times (min), and assessed by denaturing 20% PAGE (A, C). Quantification of the intensities of bands corresponding to the amount of uncleaved initial oligonucleotide over time are plotted as the average and SD of three independent experiments (B, D).

To determine if Orn can indeed cleave substrates longer than a diribonucleotide, the enzyme was incubated with RNA substrates at a 1:1 molar ratio. Under these conditions, the diribonucleotide substrate was completely processed to nucleoside monophosphates by the earliest time point, 20 seconds (Figure 12C, D). Orn_{Vc} also facilitated the degradation of the longer RNA substrates, but only after significantly longer incubation times. For example, it required 10 minutes and 30 minutes to fully degrade 3-mer and 4-mer RNAs, respectively (Figure 12C, D). Cleavage was reduced further for longer RNAs; only 40–53% of the 5-mer, 6-mer and 7-mer RNAs were processed to nucleoside monophosphates at 30 minutes (Figure 12C, D). Of note, a non-uniform distribution of degradation products for the longer RNA substrates was observed. Specifically, the diribonucleotide intermediate was never observed as a reaction intermediate for the longer RNAs. This reaction pattern indicates that RNAs of more than two residues could accumulate, but that diribonucleotide RNAs were always rapidly processed to nucleoside monophosphates. Together, these results indicate that Orn exhibits a strong substrate preference for diribonucleotides over longer oligoribonucleotides – far greater than reported previously.

The relative substrate affinities of Orn to 5'-radiolabeled oligoribonucleotides that ranged from two to seven nucleotides in length was also determined (Table 2). For this, the Lee laboratory (University of Maryland) used an established ligand-binding assay, Differential radial capillary action of ligand assay (DRaCALA) (226). Briefly, protein and substrate are incubated and spotted on nitrocellulose membranes. At the point of application, nitrocellulose can then sequester protein-ligand complexes, and

Table 2. Quantitative measurement of length-dependent oligoribonucleotide affinities.

Substrate	Dissociation constant (K_d)
GG	90 -/+ 9 nM
AGG	630 -/+ 80 nM
AAGG	890 -/+ 90 nM
AAAGG	2.56 -/+ 170 μM
AAAAGG	3.83 -/+ 370 μM
AAAAAGG	3.75 -/+ 530 μM

(Performed by Dr. Soo-kyoung Kim, Lee Laboratory, University of Maryland)

allow unbound ligands to diffuse due to capillary action. By this assay, quantification of the diffusion zone reveals that Orn_{Vc} exhibits the highest affinity for diribonucleotides (K_d pGpG = 90 -/+9 nM), as compared to oligoribonucleotides of greater lengths (Table 2). Increase in the length to three or four residues reduced the affinity 7- or 10-fold, respectively. Substrates with five or more bases showed a greater than 28-fold reduction in affinity compared to diribonucleotides. The weak affinities determined for these substrates correlates with the weak nucleolytic activity observed by Orn_{Vc}. These results confirm that Orn has a strong preference for diribonucleotides over longer oligonucleotides.

3.3.3 Orn cleaves all diribonucleotides

The ability to cleave pGpG suggests that Orn may also be able to cleave all other 15 diribonucleotide combinations. To test this, Orn_{Vc} was incubated with each 5'-^{32}P-radiolabeled diribonucleotide at a 200:1 substrate:enzyme molar ratio for 10 minutes in the presence of divalent cations that support catalysis. The products of these reactions throughout the time course were resolved by urea-denaturing 20% PAGE (Figure 13). In 10 minutes Orn_{Vc} hydrolyzed di-purine substrates most efficiently, with 90-95% of each substrate cleaved (Figure 13, pRpR). When provided with a mixed diribonucleotide in which a purine or pyrimidine base occupied either position, Orn_{Vc} cleaved 64-95% of these substrates. Diribonucleotides with a 5' purine were 77-95% cleaved (pRpY). However, diribonucleotides with a 5' pyrimidine exhibited moderately reduced levels of cleavage (64-80%) (pYpR).

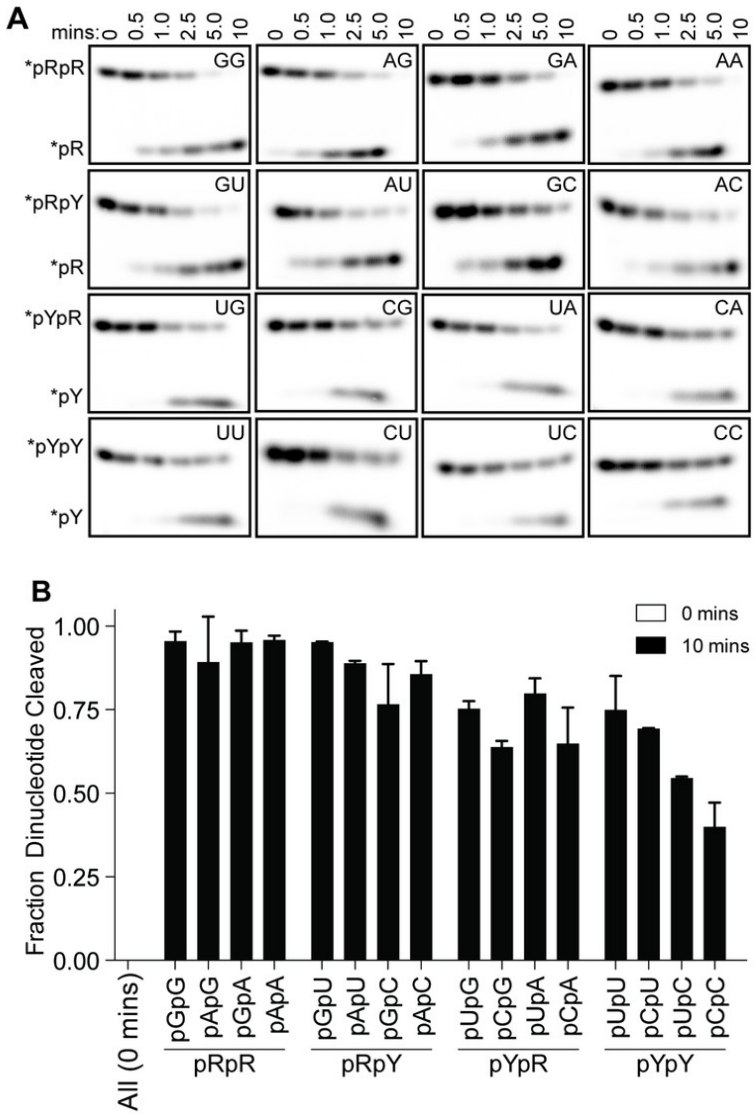

Figure 13. Orn$_{Vc}$ cleaves all diribonucleotides. (A) Orn$_{Vc}$ (5 nM) was incubated with di-purine (pRpR), purine-pyrimidine (pRpY or pYpR), or di-pyrimidine (pYpY) diribonucleotides (1 μM) containing the corresponding ^{32}P-labeled RNA tracer. Aliquots of each reaction were stopped at the indicated times (min) and assessed by denaturing 20% PAGE. (B) Quantification of the intensities of bands corresponding to the amount of diribonucleotide cleaved at the 10 min time point. Results are the average and SD of duplicate independent experiments. Orn cleaves all diribonucleotides to nucleoside monosphosphates, albeit to varying extents.

In contrast, di-pyrimidine substrates showed the slowest turnover from the substrates tested, with only 40-75% of each di-pyrimidine substrate cleaved in the given time (pYpY). In particular, Orn$_{Vc}$ cleaved 55% of pUpC and 40% of pCpC in 10 minutes. These aggregate data suggest that Orn$_{Vc}$ cleaves all diribonucleotides to nucleoside monophosphates, albeit to varying extents. Furthermore, Orn$_{Vc}$ exhibits a small but detectable preference for purine-containing substrates, in which a purine occupies the 5' position or both positions.

3.3.4 The structure of pGpG-bound Orn reveals a unique active site

To elucidate the molecular basis for Orn's substrate specificity, the Sondermann laboratory (Cornell University) determined Orn/substrate co-crystal structures. Two representative homologs, Orn$_{Vc}$ (227) and the human REXO2 (also known as small fragment nuclease or Sfn) (228), were each crystallized bound to the diribonucleotide pGpG (Figure 14A, B). Superimposing the two structures indicates their identical fold. The pGpG-bound structures reveal a narrow active site that is lined by the conserved acidic residues of the signature DEDD motif (D12, E14, and D112 of Orn$_{Vc}$; D15, E17, and D115 of REXO2) and the general base H158 or H162 in Orn$_{Vc}$ or REXO2, respectively (Figure 14A, B). In Orn$_{Vc}$, the bases of the diribonucleotide buttress against aromatic residues W61 and Y129, the latter being contributed from the second half-side of the dimeric enzyme. The corresponding residues, W64 and Y132, are conserved in REXO2. Residue L18 in Orn$_{Vc}$ (L21 in REXO2) wedges in between the two bases. Most notably, residues S108, R130, S135 and the hydroxyl group on Y129 (S111, R133, S138, and Y132 in REXO2) form hydrogen bonds with the 5'

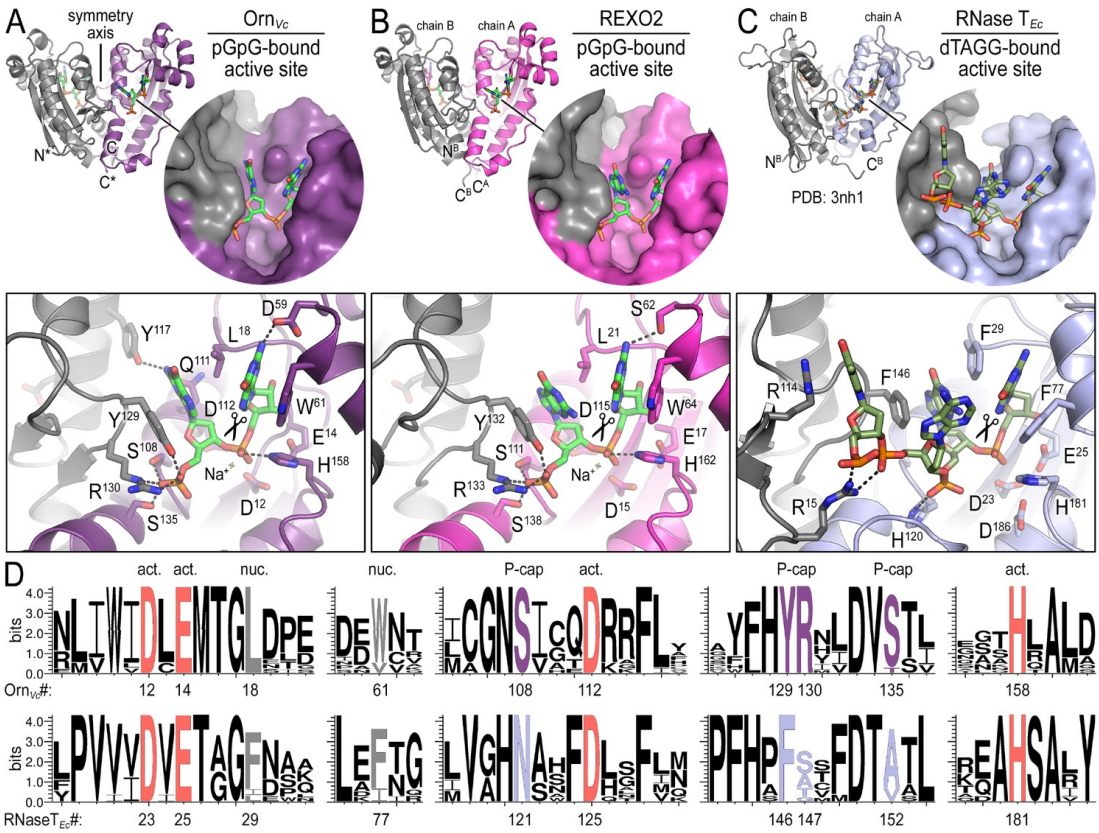

Figure 14. Structures reveal Orn's conserved substrate preference for diribonucleotides. Crystal structures of pGpG-bound *V. cholerae* Orn (A) and human REXO2 (B) are shown in comparison to *E. coli* RNase T bound to substrate (PDB 3nh1) (C), another DnaQ-fold 3'−5' exoribonuclease with a DEDD(h) active site motif. The top panels show ribbon representations of the dimeric enzymes. The insets are surface representations of the enzymes' active sites shown in similar orientations. The bottom panel describes the active site residues involved in RNA binding and catalysis. Residue numbering for REXO2 refers to its cytosolic isoform lacking the mitochondria-targeting pre-sequence. The sequence logos in (D) were constructed based on multi-sequence alignments of Orn and RNase T orthologs. Sequence logos were plotted using WebLogo. Conserved residues of the active site's DEDD motif ('act.'; red), for ribonucleotide base binding ('nuc.'; gray), and of the phosphate cap ('P-cap'; purple) are highlighted. *Performed by Sondermann Laboratory, Cornell University. Figure provided by Sondermann Laboratory, Cornell University.*

phosphate of pGpG, capping the substrate. This phosphate cap creates a major constriction of the active site, which is not observed in structurally related 3'-5' exoribonucleases such as RNase T or ExoI (Figure 14C) (229–231). RNase T and ExoI accommodate longer RNA substrates, facilitated by an expansive active site. The structural analysis correlates closely with sequence conservation of the phosphate cap motif, which is strict in Orn homologs but divergent in RNase T proteins (Figure 14D). The structural analysis also suggests that modifications at the bases may be tolerated. This is consistent with the observation that Orn$_{Vc}$ can cleave all diribonucleotides. Together, the structural analysis uncovered Orn's mode of substrate binding, which is conserved from bacteria to humans and indicates a unique selection for linear diribonucleotides with a 5' phosphate.

3.3.5 The phosphate cap and active site are required for Orn's function

The structural analysis of pGpG-bound Orn$_{Vc}$ allowed us to identify specific residues that might directly interact with the nucleotide. These residues were then individually mutagenized to assess the impact on catalysis of the phosphate cap or other interacting residues, in comparison to other active site residues (Table 3). Consequently, the Lee laboratory (University of Maryland) evaluated purified protein variants for pGpG degradation. As expected, mutations in the DEDD active site motif, such as D12A and H158A, led to complete loss of catalytic activity (Figure 15A, B). Mutations of the central phosphate cap residues Y129 and R130 to alanine also led to complete loss of catalytic activity, comparable to the DEDD active site mutants. Complete loss of activity was also observed for L18A (wedge) and W61A (aromatic

Table 3. **Mutations Constructed in Orn$_{Vc}$ and Phenotypic Consequences.**

Orn$_{Vc}$ Residue	**Proposed interaction**	**Mutation Made**	**Phenotypic Consequence**
D12	Catalytic residue	D→A	complete loss of activity (pGpG degradation) auto-aggregation
L18	Separates bases, wedge	L→A	complete loss of activity (pGpG degradation) auto-aggregation
D59	Interaction with 3' bases	D→A	complete loss of activity (pGpG degradation) moderate auto-aggregation
W61	Interaction with 3' base, pi stacking	W→A	complete loss of activity (pGpG degradation) auto-aggregation
W61	Interaction with 3' base, pi stacking	W→Y	turbid like wild-type
H66	Interaction with 3' phosphate	H→A	mildly cleaves pGpG turbid like wild-type
Q111	Interaction with 5' base	Q→A	moderately cleaves pGpG turbid like wild-type
Y129	Interaction with 5' phosphate, pi stacking	Y→A	complete loss of activity (pGpG degradation) auto-aggregation
Y129	Interaction with 5' phosphate, pi stacking	Y→W	turbid like wild-type
R130	Interaction with 5' phosphate	R→A	complete loss of activity (pGpG degradation) auto-aggregation
H158	Catalytic residue	H→A	complete loss of activity (pGpG degradation) auto-aggregation

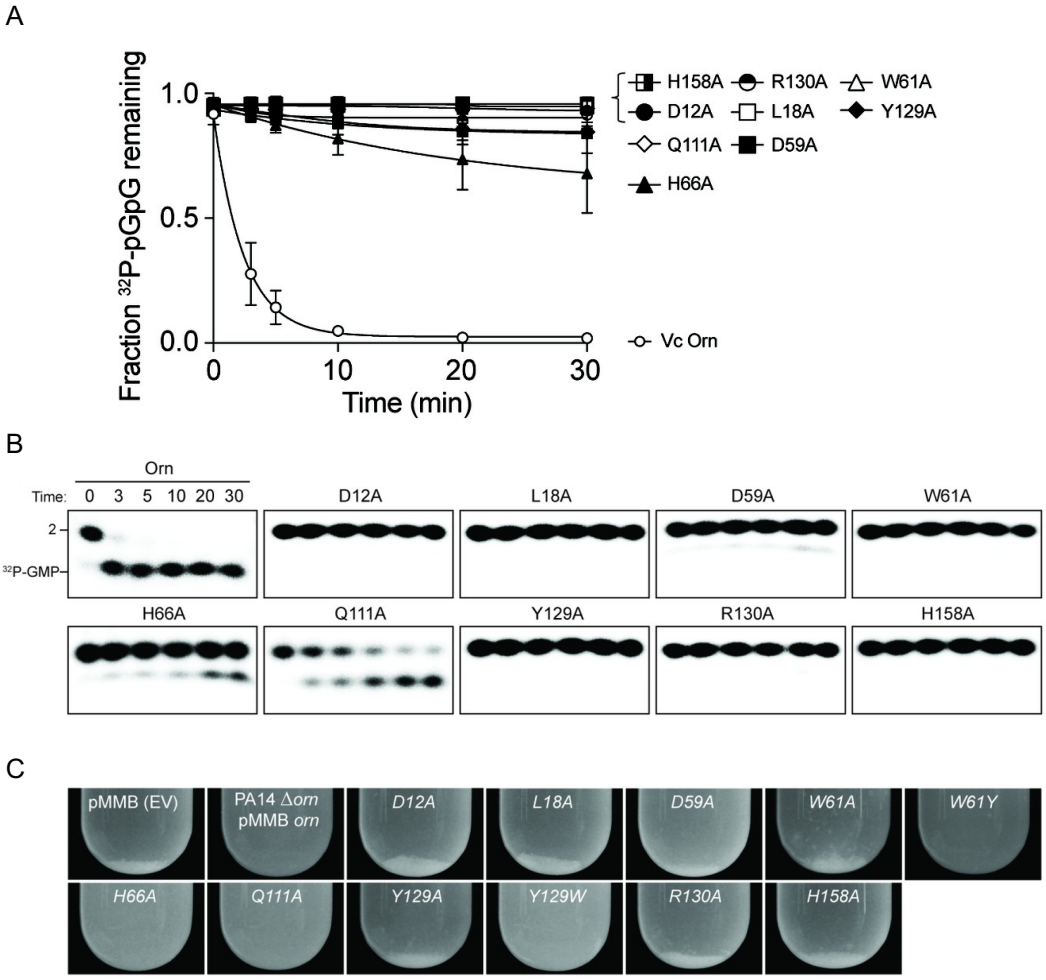

Figure 15. pGpG degradation by purified wild-type Orn$_{Vc}$ or Orn$_{Vc}$ variants. Functional importance of active-site and phosphate-cap residues for Orn function. 1 μM pGpG was treated with 5 nM of the indicated Orn protein and sampled at indicated time points to assess *in vitro* enzyme activity. Samples were stopped at the indicated times (min) and analyzed by denaturing 20% PAGE. (A) Quantification of the means and SD of three independent experiments, of which (B) representative gel images are shown with the indicated RNA size. (C) Overnight cultures of the indicated strains were allowed to stand for 10 min without agitation to allow bacterial aggregates to sediment. Representative images of the cultures of triplicated assays are shown. *Performed by Dr. Soo-kyoung Kim, Asan Turdiev, and Husan Turdiev, Lee Laboratory, University of Maryland. Figure provided by Lee Laboratory.*

buttress). We next asked whether the Orn_{Vc} mutants could complement the deletion of *orn* in *P. aeruginosa*. *P. aeruginosa* Δ*orn* accumulates pGpG that in turn inhibits c-di-GMP-specific phosphodiesterases (113, 118). As a net result, c-di-GMP accumulates in these cells, an effect that is associated with a hyper-biofilm and cell aggregation phenotype. While expression of wild-type Orn_{Vc} complements the *P. aeruginosa* Δ*orn* resulting in a dispersed culture, complementation with variants that carry mutations in either the active site (D12A) or phosphate cap residues (Y129A, R130A) results in cell aggregation indistinguishable from the Δ*orn* phenotype (Figure 15C). The Δ*orn* phenotype was also observed for L18A and W61A. When Y129 and W61 were mutagenized to the converse aromatic residues, however, activity of Orn was restored, suggesting that the pi-stacking between the aromatic residues and each substrate base is critical (Figure 15C). Together, these experiments demonstrate that an intact phosphate cap, as well as other key interactions, are required for enzyme function.

3.3.6 Orn is the only diribonucleotidase in *P. aeruginosa*

To determine Orn's *in vivo* function as a general 3'-5' exoribonuclease capable of degrading short oligoribonucleotides or as a diribonucleotidase, the Lee laboratory (University of Maryland) developed experimental conditions to measure Orn's activity in cellular extracts. The *orn* gene is essential in most γ-proteobacteria; however, it is not essential for growth of *P. aeruginosa* under most conditions (69, 70). Therefore, lysates were generated from *P. aeruginosa* strains, including parental PA14, Δ*orn*, and Δ*orn* complemented with orn_{Vc}. 5'-^{32}P-radiolabeled 2-mer or 7-mer RNA was then added to each of these lysates (Figure 16). Aliquots of the mixtures were removed

throughout the time course and analyzed by urea denaturing 20% PAGE. Extracts from parental PA14 digested the entire radiolabeled diribonucleotide in less than 5 minutes (Figure 16A). In contrast, lysates from strains lacking Orn failed to show any signs of diribonucleotidase activity even at longer time points. Similarly, complementation with a catalytically inactive allele of *orn*, *orn D12A*, also failed to clear the diribonucleotide (Figure 16A). Diribonucleotidase activity in the lysates could be restored by ectopic expression of *orn* from a self-replicating plasmid or by addition of purified Orn (Figure 16A). When the ^{32}P-7-mer RNA substrate was incubated in extracts from parental PA14 it was digested to a ladder of degradative intermediates including 6-mer, 5-mer, 4-mer and 3-mer RNAs (Figure 16B). Of note, while these intermediates and the final mononucleotide product accumulated over time, the 2-mer intermediate was never observed over the time course. In contrast, lysates from the Δ*orn* mutant specifically accrued the diribonucleotide intermediate with no apparent production of its mononucleotide products. Ectopic expression of plasmid-borne *orn*, but not *orn D12A*, restored the degradation of the 7-mer to mononucleotides and the diribonucleotide intermediate could no longer be observed. Furthermore, the diribonucleotide intermediate that accumulated in the Δ*orn* lysate was fully processed upon addition of purified Orn protein (Figure 16B). Together, these results show that *P. aeruginosa* accumulates diribonucleotide intermediates in a Δ*orn* background, which is only resolved upon addition of Orn. Degradation of RNA fragments with three or more residues by Orn was not observed in a cellular context, considering that Δ*orn* lysates preserve nuclease activities for the processing of RNAs down to diribonucleotides. These data confirm that Orn is required for degrading diribonucleotides and no other

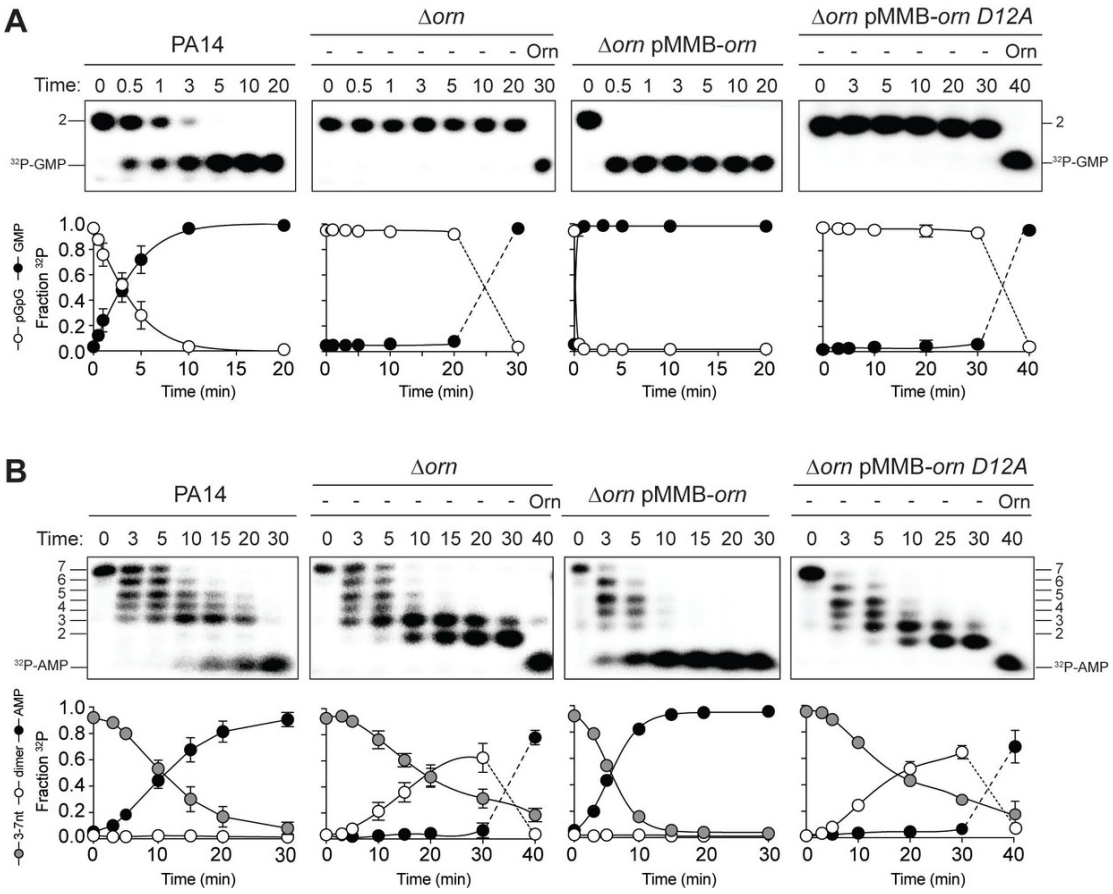

Figure 16. Orn acts as a diribonucleotidase in cell lysates. Degradation of ^{32}P-GG (A) and ^{32}P-AAAAAGG (B) by whole cell lysates of wild-type, *orn* mutant, *orn* mutant complemented with orn_{Vc}, or orn_{Vc} $D^{12}A$. For Δ*orn* and Δ*orn* complemented with orn_{Vc} $D^{12}A$,100 nM of purified $Orn_{Vc}$was added at 30 min time point and incubated for an additional 10 min. Samples were stopped at the indicated time and analyzed by 20% denaturing PAGE. Representative gel images of triplicated assays are shown with the indicated RNA size. Graphs show quantitation of triplicate data for indicated RNA species over time. *Performed by Dr. Soo-kyoung Kim, Lee Laboratory, University of Maryland. Figure provided by Lee Laboratory.*

cellular RNase of *P. aeruginosa* can substitute for Orn activity under these laboratory growth conditions.

3.4 Discussion

Bacteria use a variety of different RNases to carry out mRNA turnover (232). Furthermore, the individual mechanisms that bacteria use to accomplish this have profound effects on gene expression, environmental adaptation, and indeed, cellular viability. The action of individual RNases is transcript specific, and triggered by sequence specificity and structure, among other things. The data provided above proposes a general model of RNA degradation, wherein following endonucleolytic cleavage of RNA, a combination of exoribonucleases process RNA down to diribonucleotides and Orn completes RNA recycling by cleaving diribonucleotides to nucleoside monophosphates. The presented study shows that the substrate specificity for diribonucleotides appears to be driven by an active site that is enclosed by a "cap" that has multiple interactions with the 5' phosphate of diribonucleotide substrates. The constricted active site prevents longer substrates from binding with high affinity, rendering them poor substrates for catalytic cleavage.

Orn is unique amongst exoribonucleases because it is essential in some γ -proteobacteria and is required to degrade the pGpG intermediate in c-di-GMP signaling. Yet, c-di-GMP signaling is not essential for viability. While the molecular mechanism underlying this essentiality has yet to be explored, the mechanism for essentiality should not be c-di-GMP. Rather, it is likely that the accumulation of diribonucleotides in the absence of Orn does not permit viability. Prior studies have

shown that *orn* depletion can lead to accumulation of diribonucleotides and longer oligoribonucleotides in some cellular backgrounds (119, 233). In our own studies, both di- and tri-ribonucleotides accumulated in RNA cleavage assays of the *P. aeruginosa orn* mutant. The increase in oligoribonucleotides longer than dimers in cells could occur through feedback inhibition of other RNases, analogous to the feedback inhibition of c-di-GMP linearization by PDE-As, thereby preventing cleavage. Alternatively, accumulation of pGpG might lead to specific off-target interactions with essential proteins. For example, c-di-GMP has been implicated in the regulation of ribosome modification. In *Pseudomonas* species, RimK is a glutamate ligase that modifies ribosomal protein S6 (RpsF) by the addition of glutamate residues to the C-terminus (234). RimK has also shown to be a c-di-GMP receptor that interacts with two additional proteins: a poly-glutamate protease RimB, and the c-di-GMP PDE-A RimA. The modification of RpsF has been shown to result in altered Hfq abundance, although the mechanisms by which this takes place is not yet clear. Hfq is an RNA chaperone that is crucial to mRNA/sRNA stability, translation, and post-transcriptional regulation. Indeed, a deletion of *rimK* resulted in significantly lower abundance of ribosomal proteins, reduction in Hfq and an increased stress response (234, 235). If pGpG inhibits c-di-GMP linearization by PDE-A RimA in a similar fashion to other *Pseudomonas* PDE-A's, accumulation of pGpG may have detrimental consequences to ribosomal function, leading to an altered proteome profile. Therefore, the extent to which c-di-GMP, and by extension pGpG, fine-tune ribosome function and control Hfq levels remains an important open question. Another possibility is that the accumulation of pGpG may directly lead to altered transcription profiles. Recent studies have provided

evidence that 2- to 4-nucleotide long RNAs prime transcription initiation in *E. coli.* Transcription initiation due to elevated levels of these short RNAs resulted in global alterations in gene expression due to shifting of transcription start sites (233). Therefore, alterations in transcription initiation could result in cellular toxicity (236, 237). Our studies reveal a discrete step in RNA degradation—the enzymatic cleavage of diribonucleotides into mononucleotides—and require further investigation into how, mechanistically, diribonucleotide accumulation is detrimental to cell survival. While our evidence on the true molecular function of Orn is important, it is only the beginning.

3.5 Materials and Methods

3.5.1 Bacterial strains, plasmids, and growth conditions

P. aeruginosa is routinely grown in LB supplemented with the appropriate antibiotic (50 mg/mL carbenicillin or 75 mg/mL gentamicin) at 37°C. To create the point mutants of orn_{Vc}, mutations were generated by using the Q5 Site-Directed Mutagenesis Kit (New England Biolabs). All mutations were verified by sequencing.

3.5.2 Protein expression and purification for protein crystallography

orn genes from *V.cholerae* O1 El Tor VC0341 (residues 1–181) and Homo sapiens REXO2 (residues 33–237) were synthesized by Geneart (Life Technologies). Genes were cloned by ligation between BamHI and NotI sites of a modified pET28a vector (Novagen) yielding N-terminally His6-tagged small ubiquitin-like modifier (SUMO) fusion proteins cleavable by recombinant Ulp-1 protease. Orn proteins were

overexpressed in *E. coli* BL21 T7 Express cells (New England Biolabs). Fresh transformants were grown in Terrific Broth (TB) supplemented with 50 ug/mL kanamycin at 37°C to an OD_{600} ~1.0, at which point the temperature was reduced to 18°C and expression was induced by addition of 0.5 mM IPTG. Cells were harvested after 16 hours of expression by centrifugation and resuspended in a minimal volume of Ni-NTA binding buffer (25 mM Tris-Cl, 500 mM NaCl, 20 mM imidazole, pH 8.5) followed by flash freezing in liquid nitrogen. Cells were thawed and lysed by sonication. Cell debris was removed by centrifugation and clarified soluble lysate was incubated with Ni-NTA resin (Qiagen) pre-equilibrated with Ni-NTA binding buffer. Following one hour of binding, the resin was washed three times with 10 column volumes of Ni-NTA binding buffer, and then eluted with six column volumes of Ni-NTA elution buffer (25 mM Tris-Cl, 500 mM NaCl, 350 mM imidazole, pH 8.5). Eluates were buffer exchanged into gel filtration buffer (25 mM Tris-Cl, 150 mM NaCl, pH 7.5) via a HiPrep 26/10 desalting column (GE Healthcare), followed by overnight incubation with Ulp-1 to cleave off the His6-tagged SUMO moiety. Untagged Orn proteins were recovered in the flow-through of a HisTrap Ni-NTA column (GE Healthcare), separated from His6-SUMO, uncleaved proteins and His6-tagged Ulp-1. Orn was concentrated via Amicon Ultra 10K concentrator prior to loading onto a HiLoad 16/60 Superdex 200 gel filtration column GE Healthcare) equilibrated in gel filtration buffer. Fractions containing Orn were pooled and concentrated to 100 mg/mL, frozen in liquid nitrogen, and stored at -80°C.

3.5.3 Protein crystallography and data deposition

REXO2-RNA and OrnVc-RNA complexes (pGpG and pApA from BioLog Life Science Institute, other nucleotides from GE Healthcare Dharmacon) were formed prior to crystallization by mixing a 1:2 molar ratio of Orn:RNA in gel filtration buffer, followed by incubation for 30 minutes at the crystallization temperature. Orn-RNA complexes (10–30 mg/ml) were crystallized via hanging-drop vapor diffusion by mixing equal volumes (0.8 mL) of sample with reservoir solution. OrnVc crystals grew at 20°C over a reservoir solution that was composed of 0.1 M BisTris (pH 5.5), 17% polyethylene glycol 3350, and 20% xylitol. Crystals were flash-frozen in liquid nitrogen. REXO2 crystals grew at 4°C, using a reservoir comprised of 0.2 M sodium malonate (pH 5.5) and 15–20% polyethylene glycol 3350. REXO2 crystals were soaked in cryoprotectant of reservoir solution supplemented with 25% glycerol prior to flash freezing with liquid nitrogen. All crystals were stored in liquid nitrogen. Data were collected by synchrotron radiation at 0.977 A° on frozen crystals at 100 K at beamline F1 of the Cornell High Energy Synchrotron Source (CHESS). Diffraction data sets were processed using XDS, Pointless, and Scala. The initial structures were solved by Molecular Replacement using the software package Phenix and the unpublished coordinates of E. coli Orn (PDB: 2igi) as the search model. Manual model building and refinement were carried out with Coot and Phenix, respectively. Illustrations were prepared in Pymol (Version 2.2.0, Schrodinger, LLC). All software packages were accessed through SBGrid. The atomic coordinates and structure factors have been deposited in the Protein Data Bank, www.rcsb.org (PDB ID codes 6N6A, 6N6C, 6N6D, 6N6E, 6N6F, 6N6G, 6N6H, 6N6I, 6N6J, and 6N6K).

3.5.4 Protein expression and purification for biochemical assays

E. coli T7Iq strains harboring expression vector pVL847 expressing an His10-MBP-Orn and His10-MBP-Orn mutants from *V. cholerae* were grown overnight, subcultured in LB M9 fresh media supplemented with 15 mg/ml gentamicin and grown to approximately OD_{600} 0.5 ~ 1.0 at 30°C. Expression was induced with 1 mM IPTG for 4 hours. Induced bacteria were collected by centrifugation and resuspended in 10 mM Tris, pH 8, 100 mM NaCl, and 25 mM imidazole. After addition of 10 mg/mL DNase, 25 mg/mL lysozyme, and 1 mM PMSF, bacteria were lysed by sonication. Insoluble material was removed by centrifugation. The His-fusion protein was purified by separation over a Ni-NTA column. Purified proteins were pooled and dialyzed for 1 hour and overnight against 10 mM Tris, pH 8, 100 mM NaCl. The proteins were dialyzed for 3 hours in 10 mM Tris, pH 8, 100 mM NaCl, and 50% (vol/vol) glycerol, aliquoted, and flash frozen with liquid nitrogen and stored at -80°C.

3.5.5 Labeling of RNAs

5’ un-phosphorylated RNAs were purchased from TriLink Biotechnologies or Sigma. Each RNA was subjected to radioactive end-labeling or non-radioactive phosphorylation by T4 Polynucleotide Kinase (New England Biolabs). Each RNA was subjected to phosphorylation with equimolar concentrations of either 32P-gammaATP or ATP, T4 PNK, and 1X T4 PNK Reaction Buffer. Reactions comprising a final concentration of either 0.5 μM radiolabeled RNA or 2.0 μM phosphorylated RNA were incubated at 37°C for 40 minutes, followed by heat inactivation of T4 PNK at 65°C for 20 minutes.

3.5.6 Purified Orn cleavage reactions

Phosphorylated RNA (1.0 μM), including trace amounts of radiolabeled substrate, was subjected to cleavage by either 5.0 nM or 1.0 μM purified Orn at room temperature. These reactions were in the presence of 10 mM Tris, pH 8.0, 100 mM NaCl, and 5 mM $MgCl_2$. At the appropriate times, aliquots of the reaction were removed and quenched in the presence of 150 mM EDTA on ice and heat inactivated at 95°C for 5 min. Samples were separated on denaturing 20% PAGE containing 1X TBE and 4 M urea. The gels were imaged using Fujifilm FLA-7000 phosphorimager (GE) and analyzed for the appearance of truncated ^{32}P-labeled products. The intensity of the radiolabeled nucleotides was quantified using Fujifilm Multi Gauge software v3.0.

3.5.7 Whole cell lysate cleavage reactions

Activity of whole cell lysates against ^{32}P-labeled oligoribonucleotide substrates was performed at room temperature in reaction buffer (10 mM Tris, pH 8, 100 mM NaCl, and 5 mM $MgCl_2$). At the indicated times, the reaction was stopped by the addition of 0.2 M EDTA and heated at 98°C for 5 min. Samples were separated on denaturing 20% PAGE containing 1X TBE and 4 M urea. The gels were imaged using Fujifilm FLA-7000 phosphorimager (GE) and analyzed for the appearance of truncated ^{32}P-labeled products. The intensity of the radiolabeled nucleotides was quantified using Fujifilm Multi Gauge software v3.0.

3.5.8 DRaCALA measurement of dissociation constants

To measure K_d, serial dilutions of purified His_{10}-MBP-Orn, His_{10}-MBP Orn mutants, or untagged Orn were mixed with radiolabeled nucleotides in binding buffer 10 mM Tris, pH 8, 100 mM NaCl, 5 mM $CaCl_2$). Aliquots were applied to nitrocellulose sheets, dried, imaged and K_d values were calculated as described previously (226, 238).

3.5.9 Preparation of *P. aeruginosa* whole cell lysates

Overnight cultures of *P. aeruginosa* PA14 WT, Δ*orn*, or complemented strains were sub-cultured into fresh media with antibiotic and 1 mM IPTG, grown at 37°C with shaking to OD_{600} ~ 2.5.All bacterial samples were collected by centrifugation and resuspended in 1/10 volume of buffer comprised of 100 mM Tris, pH 8, 100 mM NaCl. This was further supplemented with 25 mg/mL lysozyme, 10 mg/mL DNase, and 1 mM PMSF and stored at -80°C.

3.5.10 Aggregation assay

A colony of each strain of *P. aeruginosa* grown on LB agar plates supplemented with 50 mg/mL carbenicillin was inoculated into borosilicate glass tubes containing 2.5 mL of LB supplemented with 0.1 mM IPTG. The cultures were placed in a fly-wheel in a 37°C incubator to spin for 18 ~ 22 hours. Culture tubes were allowed to settle at room temperature for 10 min and photographed.

Chapter 4: *Bacillus subtilis* NrnA and NrnB Selectively Target Short RNA Oligonucleotides, But Differ in Their Substrate Preferences

4.1 Copyright Notice

In this chapter, Figure 18 and Table 4 were originally published by *Journal of Bacteriology*: Orr MW, Weiss CA, Severin GB, Turdiev H, Kim SK, Turdiev A, Liu K, Tu BP, Waters CM, Winkler WC, Lee VT. (2018). A Subset of Exoribonucleases Serve as Degradative Enzymes for pGpG in c-di-GMP Signaling. 200: (24). e00300-18.

4.2 Introduction

The goal to identify enzymes in other phyla that could complement a conditional *E. coli orn* mutant and thereby participate in the terminal steps of RNA degradation led to the discovery of two RNases encoded by *B. subtilis*: NrnA and NrnB. The *nrnA* and *nrnB* genes appeared to complement the growth phenotype equally well, suggesting that *B. subtilis* encodes for more than one RNase that can restore the growth defect elicited by the conditional *E. coli orn* mutant (120, 121). From this, it was assumed that NrnA and NrnB are likely to behave in a redundant manner to cleave oligoribonucleotides. While the complementation experiment suggested that NrnA and NrnB are fully redundant, several other studies hinted that NrnA and NrnB may exhibit some noteworthy differences between each other.

NrnA and NrnB both belong to the DHH family of proteins. This superfamily consists of enzymes that exhibit DNA or RNA phosphodiesterase activity and that together encompass a broad range of substrate specificities (239). DHH family proteins can be found in higher organisms, such as the model organisms *Drosophila* and *S. cerevisiae,* as well as many bacteria. Proteins in this family have a conserved N-terminal domain that is largely responsible for their inclusion in the DHH superfamily. The N-terminal domain comprises four distinct sequence motifs, each comprising a conserved aspartate residue (Figure 17). The third motif comprises the conserved residues DHH, for which the family is named (Pfam PF01368). In contrast, sequences of the C-terminal domain have been found to vary among family members. For example, only certain proteins within the DHH superfamily have an associated C-terminal DHHA1 (DHH-associated domain 1, Pfam PF02272) domain. This domain is characterized by a conserved pair of glycine residues (Figure 17). The DHHA1 subfamily of DHH proteins includes proteins of diverse functions, such as NrnA, c-di-AMP phosphodiesterase GdpP, alanyl-tRNA synthetase (AlaRS), and RecJ (240–242). RecJ is a single-strand 5'-3' DNase involved in DNA repair. Sequence alignment (ClustalW) between *B. subtilis* NrnA and NrnB shows that they each comprise the DHH and GG residues characteristic of the DHH/DHHA1 family. Interestingly, homology between NrnA and NrnB does not span the full-length sequences of each protein. Rather, NrnB appears to exhibit a unique C terminus that is absent from NrnA, suggesting it might be more distantly related to NrnB than current literature would indicate. It is therefore possible that the differences in protein sequence between NrnA and NrnB might allude to corresponding differences in their substrate preferences.

Figure 17. Alignment of NrnA$_{Bs}$ and NrnB$_{Bs}$. Protein sequences of *B. subtilis* NrnA and NrnB were aligned by ClustalW. Four motifs with conserved aspartate residues make up the DHH domain. The aspartate residues of each motif are in red. Other residues of NrnA that are putatively involved in catalysis are also in red. The DHH domain is shown in a red box, along with the DHHA1 motif. The DHHA1 motif is characterized by a pair of glycine residues. NrnB comprises a nearly 100 residue long sequence that is absent from NrnA.

It has also been suggested that, in addition to cleaving oligoribonucleotides, NrnA has an additional role in sulfur metabolism. The nucleotide 3'-phosphoadenosine 5'-phosphate (pAp) is generated during sulfur assimilation. NrnA was reported to dephosphorylate pAp to AMP *in vitro,* a function reminiscent of CysQ, the pAp phosphatase in *E. coli* (120). However, direct biochemical evidence to support this claim has not yet been published. Instead, support for an interaction between pAp and NrnA stemmed primarily from a screen for proteins that associated with pAp-agarose-beads, which appeared to enrich NrnA in a pAp-dependent manner. NrnA was also shown to complement an *E. coli cysQ* mutant, which is auxotrophic for cysteine; in this strain, expression of *nrnA* restored cysteine prototrophy. These data together provide compelling evidence that suggests NrnA might act as a pAp phosphatase *in vivo.* Similarly, a *B. subtilis nrnA* mutant exhibited a slower growth rate in the absence of cysteine. However, this reduction in growth rate was mild overall, suggesting that there could be an additional enzyme that functions as a pAp phosphatase in *B. subtilis.* Yet, interestingly, NrnB is not thought to fulfill this role. It has been reported that NrnB was not able to complement the *E. coli cysQ* mutant (although the authors report this observation as data not shown) (121). Therefore, while both *nrnA* and *nrnB* can complement a conditional *E. coli orn* mutant, only NrnA is hypothesized to complement an *E. coli cysQ* mutant, suggesting that only NrnA can dephosphorylate pAp in addition to its presumed role as an exoribonuclease. Overall, these data provide support to the hypothesis that NrnA and NrnB exhibit fundamental differences from one another, even though they both complement the *E. coli orn* defect.

Biochemical analyses of NrnA and NrnB *in vitro* have also produced controversial reports. While published experiments suggested that NrnA and NrnB are both 3'-5' exoribonucleases, they also suggested that these enzymes have different but overlapping substrate specificities. In these experiments, NrnA and NrnB were purified and incubated with different RNA oligos that had been labeled with the Cy5 fluorophore at their 5' terminus (121). Purified recombinant NrnA and NrnB were both able to degrade 5'Cy5-CCCCC into shorter RNAs, as resolved by urea-denaturing 22% polyacrylamide gel electrophoresis. However, 3-mers were never observed as a reaction intermediate in the NrnA cleavage reaction, suggesting that NrnA preferentially cleaves 3-mers. Furthermore, when both 5'Cy5-CCCCC and 5'Cy5-CCC were each subjected to cleavage by NrnA, processing of the 3-mer to 2-mer appeared to be faster than degradation of the 5-mer. In contrast, NrnB did not show a preference for RNAs shorter than 5 nucleotides. It was also observed that NrnB was less active on 3-mers than on 5-mers. From this, it is presumed that NrnA and NrnB both cleave short RNAs up to 5 nucleotides in length, but that NrnA might exhibit a preference for 3-mers while NrnB is more active than NrnA against 5-mers. A 3-mer deoxyribonucleotide was also tested against NrnA and NrnB and, intriguingly, they were both reported to be capable of fully processing it; however, this data was regretfully not actually presented in the publication and was instead referred to as 'data not shown'. In addition to short RNAs, a 5' ^{33}P-labeled 24-mer was also tested for degradation by NrnA and NrnB. It was determined that NrnB had "mild activity" against 24-mers, and that this activity was considerably less than the activity observed for short RNAs. An NrnB catalytic site mutant was constructed and purified and also

tested for cleavage of the 24-mer; cleavage by the mutant protein was not observed (data not shown). It should be noted however, that cleavage of 5'Cy5-CCCCC by this mutant was still detectable but reduced as compared to the wild-type protein. In contrast, degradation of 24-mer by NrnA was not observed in this study. However, more recent studies of NrnA suggested that NrnA is in fact bidirectional, preferentially cleaving longer RNA substrates from the 5' end and shorter RNA substrates from the 3' terminus (243). In potential agreement with this hypothesis, NrnA and the 5'-3' exonuclease RecJ exhibit significant similarity in overall sequence and structural homology. Although 3'-5' activity was confirmed for a 3-mer RNA, cleavage of a 3'-^{32}P-labeled 12-mer RNA, was observed from the 5' direction. It should be noted that this was over the course of four hours, whereas cleavage of 3-mers (from the 3' terminus) could be observed in minutes. Confounding straightforward interpretation of these data, however, was the inclusion of 10-fold excess enzyme in the reactions that targeted longer RNA substrates as compared to the shorter ones. Catalytic site mutant variants of NrnA completely abrogated 3'-5' exonuclease activity, but not the 5'-3' cleavage activity. While the evidence is currently inconclusive, if NrnA is indeed bidirectional, it would represent a rare instance of dual polarity for an RNase enzyme.

Our recent re-evaluation of Orn shows that Orn functions not as an oligoribonuclease, as previously believed, but instead functions as a specialized ribonuclease of diribonucleotide substrates. This re-evaluation was based on considerations of equilibrium binding constants, physiologically relevant concentrations of enzyme, and a combination of *in vivo,* biochemical, and structural analyses. Furthermore, the use of native radiolabeled RNA substrates, as opposed to

RNAs containing fluorophore probes, specifically revealed the true substrate specificity for Orn that had remained hidden from prior studies, where bulky fluorophore moieties were likely to have interfered with the substrate binding pocket. Given that NrnA and NrnB can complement Orn deletion mutants, the simplest hypothesis is that they share exactly overlapping substrate requirements and overall cellular roles. But as summarized above, the available data on NrnA and NrnB paint a more confusing picture of what exactly these proteins are likely to be doing inside cells. Simply put, it is currently unclear whether NrnA and NrnB are 'diribonucleotidases' (akin to Orn), whether they are RNases that specialize in "short" RNA substrates, whether they are RNases that process both "long" and "short" substrates, or whether they are nucleases that process both RNA and DNA substrates. Moreover, it is even unclear whether they act only in one direction, as do most RNase enzymes, or exhibit bidirectional abilities. Therefore, in this analysis, we wanted to conduct a preliminary study to assess NrnA and NrnB catalysis under uniform conditions and using the same rigorous analyses that we applied to Orn. From our analysis, we expect to determine the true substrate specificities and cellular functions of these two seemingly redundant RNases.

4.3 Results

4.3.1 In *B. subtilis*, Δ*nrnAB* leads to elevated levels of c-di-GMP and pGpG

The ability of *B. subtilis nrnA* and *nrnB* to complement the *E. coli* and *P. aeruginosa* Δ*orn* mutants suggests that these enzymes could be responsible for pGpG

cleavage in *B. subtilis* in a manner that is analogous to Orn function. If analogous, not only should intracellular pGpG levels accumulate, but also c-di-GMP levels, due to feedback inhibition of PDE-As by pGpG (113, 118). Thus, we constructed a *B. subtilis* Δ*nrnA* Δ*nrnB* double mutant. This mutant, as well as wild-type were consequently assayed for c-di-GMP levels using the fluorescent c-di-GMP riboswitch reporter previously described in Chapter 2. As a control, a constitutively active *yfp* reporter was used (Figure 18A). As expected, the control reporter showed no differences in fluorescence between the wild-type and the Δ*nrnA* Δ*nrnB* double mutant, with the same histogram distribution of fluorescence intensity in the two strains (Figure 18B, D). As discussed previously, assessment of the c-di-GMP reporter in a wild-type *B. subtilis* population shows a bimodal distribution of fluorescence, indicating that some sub-populations of *B. subtilis* within a multicellular community exhibit higher levels intracellular c-di-GMP relative to other subpopulations. Higher intracellular c-di-GMP levels are expected to bind to the c-di-GMP riboswitch within the *lchAA* leader to promote formation of a transcription terminator, thereby halting expression of *yfp*. The Δ*nrnA* Δ*nrnB* mutant exhibited very low fluorescence compared to the wild-type, indicating that c-di-GMP levels are indeed higher in this strain (Figure 18C, E). Correspondingly, the accumulation of c-di-GMP in the Δ*nrnA* Δ*nrnB* mutant is likely to be due to pGpG accumulation that competitively inhibits the linearization of c-di-GMP. As an independent measure of c-di-GMP, intracellular c-di-GMP and pGpG were quantified by LC-MS/MS in *B. subtilis* wild-type and Δ*nrnA* Δ*nrnB* mutant strains (Table 4). This revealed that pGpG was undetectable in wild-type cells, but could be detected in the Δ*nrnA* Δ*nrnB* double mutant at approximately 1.9 μM.

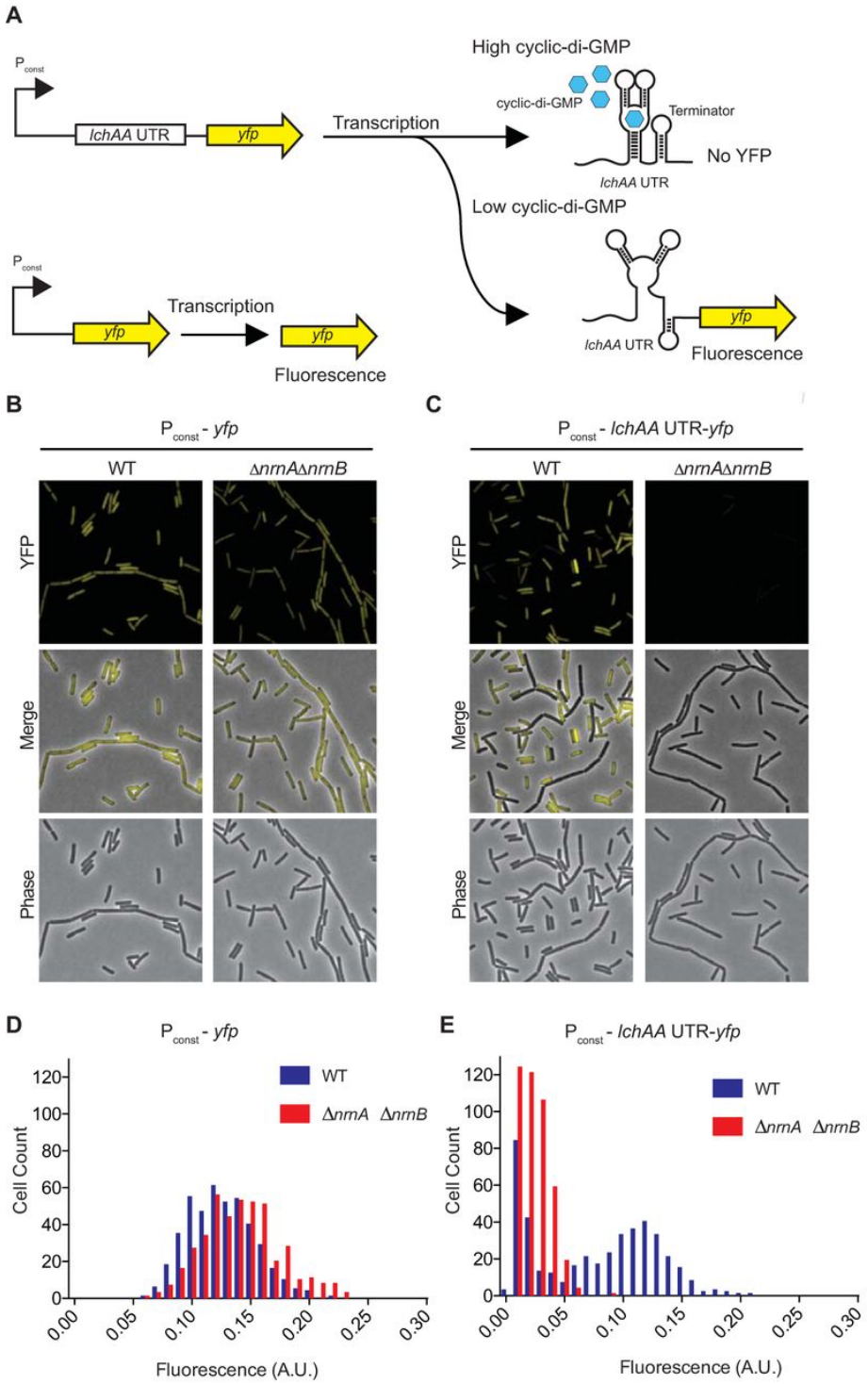

Figure 18. Detection of c-di-GMP levels in *B. subtilis* Δ*nrnA* Δ*nrnB*. (A) Schematic for YFP production by P_{const}-*yfp* and P_{const}-*lchAA* UTR-*yfp* in response to high and low c-di-GMP. Representative images of fluorescence from (B) P_{const}-*yfp* or (C) P_{const}-*lchAA* UTR-*yfp* in either *B. subtilis* 168 wild-type (WT) or *ΔnrnA ΔnrnB*. Histograms of the quantification of average fluorescence intensity of *B. subtilis* 168 wild type and *ΔnrnA ΔnrnB* with (D) P_{const}-*yfp* or (E) P_{const}-*lchAA* UTR-*yfp* cells (n~300).

Table 4. Intracellular concentrations of pGpG and c-di-GMP in *B. subtilis* WT and Δ*nrnA* Δ*nrnB* strains

Substance	Daughter ion	WT 168	Δ*nrnA* Δ*nrnB*	Fold Change (mutant/WT)
pGpG	1	ND	1.8 -/+0.6 μM	NA
pGpG	2	ND	1.8 -/+0.4 μM	NA
c-di-GMP	1	0.8 -/+ 0.2 μM	2.4 -/+0.5 μM	3.0
c-di-GMP	2	0.9 -/+ 0.1 μM	3.0 -/+0.9 μM	3.3

concentrations reported reflect mean -/+ SD
ND-not detectable
NA-not applicable

Furthermore, 1 μM c-di-GMP was measured within wild-type *B. subtilis,* as compared to 3 μM c-di-GMP for the Δ*nrnA* Δ*nrnB* double mutant. From these data we conclude that the Δ*nrnA* Δ*nrnB* mutations cause an increase in both c-di-GMP and pGpG, but that the elevated pGpG levels are still not high enough to trigger the *lchAA* riboswitch. This indicates that product inhibition of c-di-GMP hydrolysis by elevated pGpG occurs in *B. subtilis* as it does in *P. aeruginosa,* suggesting it may be a widespread phenomenon. In summary, these results indicate that NrnA and NrnB are the enzymes primarily responsible for the degradation of pGpG in *B. subtilis*.

4.3.2 Protocol optimization to generate *B. subtilis* lysates for RNA cleavage

In our previous studies, the ability to visualize RNA cleavage patterns in *P. aeruginosa* bacterial lysates by gel electrophoresis allowed us to determine that Orn is the only diribonucleotidase in that organism. Thus, we wanted to use a similar method for the assessment of *B. subtilis* NrnA and NrnB. For these studies we chose to visualize cleavage of 1 μM 7-mer RNA (5'AAAAAGG). 1 μM of 5'-monophosphorylated 7-mer was prepared with trace amounts of ^{32}P end-labeled 7-mer and added to different preparations of lysates from several different *B. subtilis* strains. Reactions were allowed to proceed for up to two hours and aliquots of the cleavage reaction over time were stopped by the addition of 150 mM EDTA and urea. Reaction products were then resolved by urea-denaturing 20% PAGE. All reactions were conducted in the presence of 10 mM Tris pH 8.0 and 100 mM NaCl. 5 mM $MgCl_2$ was added to promote catalysis.

In prior studies of Orn, *P. aeruginosa* cells were lysed with a mixture of lysozyme, DNaseI, and PMSF. Following this treatment, lysates were freeze-thawed

three times (*i.e.,* transferred repeatedly between -80˚C and room temperature). *B. subtilis*, however, is a Gram-positive organism with a thicker peptidoglycan layer. Therefore, *B. subtilis* cells were treated with 10X more lysozyme than is typically used for Gram-negative organisms. However, when wild-type *B. subtilis* 168 was treated with lysozyme, DNaseI, and PMSF alone, the corresponding lysates still showed no detectable cleavage of 7-mer RNA. Consequently, bead-beating methods were used to more rigorously lyse the Gram-positive cells. To determine the ideal amount of cells that would be needed for active lysates (*i.e.,* sufficient to observe RNA cleavage activity), 1 mL, 5 mL, 10 mL, and 25 mL of cultures of *B. subtilis* 168 wild-type or Δ*nrnA* Δ*nrnB* were harvested by centrifugation. These aliquots were pelleted and resuspended in 1 mL buffer, and subjected to bead beating. 1 μM radiolabeled 7-mer RNA was then incubated with aliquots of each resuspension and analyzed by 20% urea-denaturing PAGE; the most optimal activity was observed from lysates prepared from 10 mL of *B. subtilis* culture (Figure 19C). This determination was based on several observations. In reactions generated from 1 mL and 5 mL of culture, no cleavage activity whatsoever was observed, leading us to think that not enough cells were lysed to visualize RNase activity (Figure 19A, B). Furthermore, electrophoresis of the reactions failed to separate residual ^{32}P-γ-ATP from AMP. These two species ran together with the solvent front. In support of this, cleavage of the 7-mer could be observed in the lysates generated from 10 mL and 25 mL *B. subtilis* culture (Figure 19 C, D). Similar to what was observed in the 1-5 mL reactions, however, the 25 mL reactions failed to separate residual ^{32}P-γ-ATP from AMP, for reasons that are not intuitively obvious (Figure 19D). Therefore, we chose to prepare lysates from 10 mL

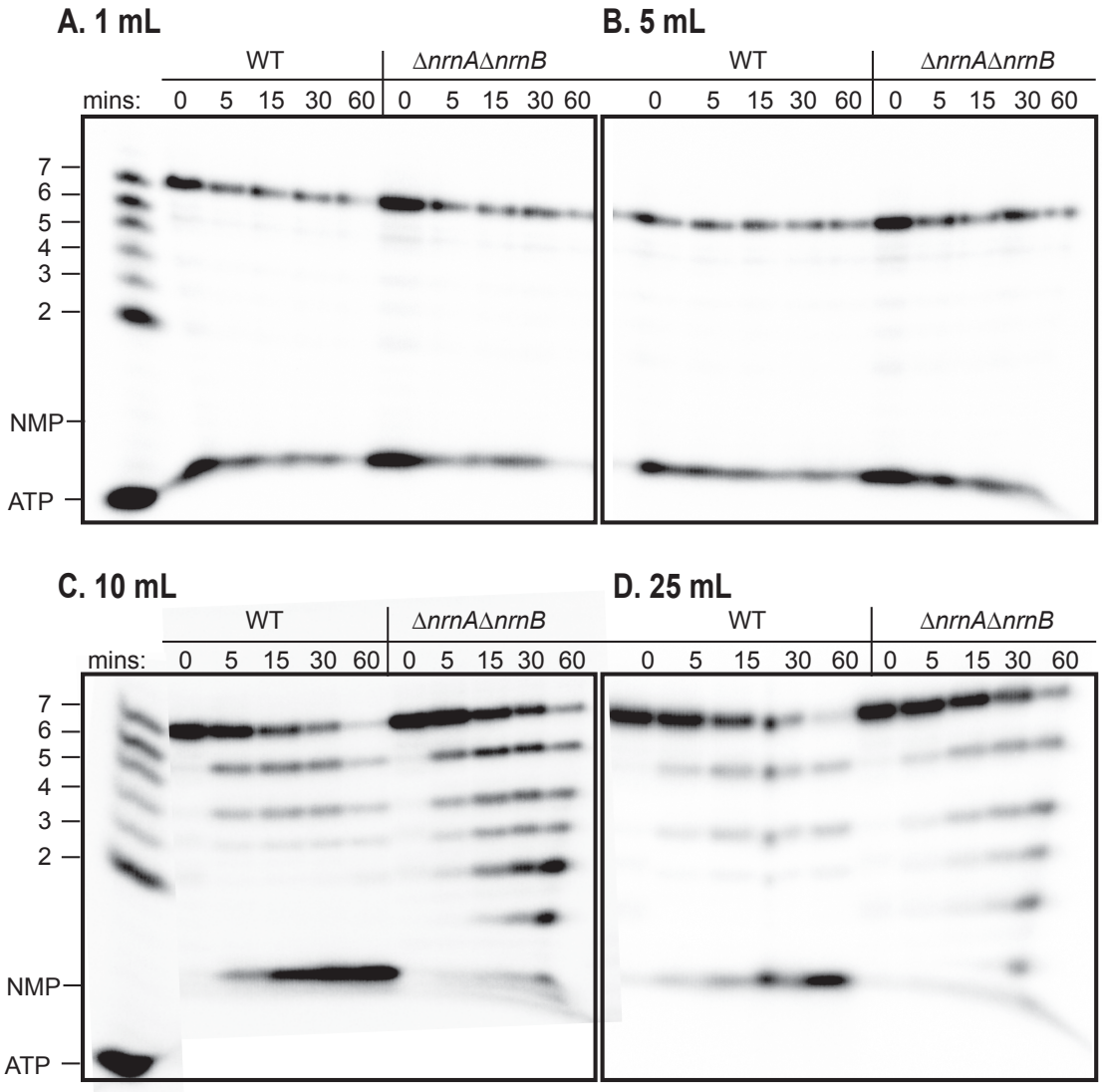

Figure 19. Absence of NrnA and NrnB leads to accumulation of 2-4mers in cell lysates. Degradation of 1μM AAAAAGG (mixed with 5' ^{32}P-labeled tracer) by whole cell lysates of *B. subtilis* wild-type and Δ*nrnA* Δ*nrnB*. Samples were stopped at the indicated time and analyzed by 20% urea-denaturing PAGE.

B. subtilis 168 wild-type or Δ*nrnA* Δ*nrnB* for our analyses of RNA cleavage. As expected, in 1 hour, a 7-mer RNA was cleaved to near completion for lysates prepared from wild-type cells (Figure 19C). In these reactions, intermediates of 6-mer, 5-mer, 4-mer, and nucleoside monophosphate were obversable. Interestingly, 2-mer and 3-mer intermediates were not observed at all, and 4-mer intermediates seemed to be less abundant than 5-mer and 6-mer intermediates. Cleavage of the 7-mer was also possible in the absence of NrnA and NrnB, as determined by incubation of RNA in lysates prepared from Δ*nrnA* Δ*nrnB* cells. Intriguingly, in the Δ*nrnA* Δ*nrnB* lysates there was a distinct accumulation of 2-mer and 3-mer RNAs, and the levels of 4-mer were more abundant than in the wild-type lysates. In summary, analyses of RNA cleavage in lysates of *B. subtilis* suggested that 2-mers, 3-mers, and 4-mers accumulated in the absence of NrnA and NrnB.

4.3.3 NrnA and NrnB have different substrate specificities

Our prior imaging and mass spectrometry studies suggested that pGpG levels accumulated upon depletion of NrnA and NrnB. This was supported by our analysis of RNA cleavage in cell lysates. However, the lysate data also suggested that 3-mers and 4-mers accumulated in the absence of NrnA and NrnB as well. To fully understand the length preferences of NrnA and NrnB, recombinant affinity-tagged *B. subtilis* NrnA ($NrnA_{Bs}$) and NrnB ($NrnB_{Bs}$) were purified to homogeneity and then tested for cleavage of RNA substrates. $NrnA_{Bs}$ and $NrnB_{Bs}$ were incubated with 5'-^{32}P-radiolabeled oligoribonucleotides of varying lengths at substrate concentrations that exceed enzyme concentration (50:1), and in the presence of divalent cations that support catalysis. The

products of these reactions were resolved by urea-denaturing 20% PAGE. Analysis of NrnA$_{Bs}$ showed that, as anticipated, it fully processed the dinucleotide pGpG in 10 minutes (Figure 20A). Importantly, NrnA$_{Bs}$ showed very similar activity against the 3-mer AGG within the same time frame. This provides direct evidence that 2-mers and 3-mers are a preferred substrate of NrnA$_{Bs}$. Similar to our prior studies, a dinucleotide intermediate was not observed. As with our assays on Orn activity, we interpret this observation to suggest that the rate of hydrolysis for 2-mers is faster than the time points that were chosen. Alternatively, these data could also be consistent with the pattern that would be observed if NrnA$_{Bs}$ was able to cleave the 3-mer from the 5' end. In other words, if NrnA$_{Bs}$ removes nucleoside monophosphates from the 5' terminus of a 3-mer oligonucleotide, it would be expected to result in accumulations of NMP and dinucleotide intermediates should be absent. Yet, the same pattern would be expected if dinucleotide substrates were simply processed at a much higher rate than 3-mer RNAs. Our current data cannot differentiate between these two possibilities. While some processing of a 4-mer was observed under these reaction conditions, the observed rate of cleavage appeared to be slower than that of the 3-mer or dinucleotide in the same amount of time (Figure 20B). And, similar to the reaction profile of the 3-mer substrate, intermediate RNA lengths were not observed; the only evidence for RNA cleavage was from a modest increase in nucleoside monophosphate levels. Similarly, NrnA$_{Bs}$ was unable to cleave longer substrates (*i.e.*, from 5-mers to 7-mers. (Figure 20A). These RNA cleavage patterns mirrored what was observed when a 7-mer was treated with lysates of the Δ*nrnA* Δ*nrnB* strain (Figure 19).

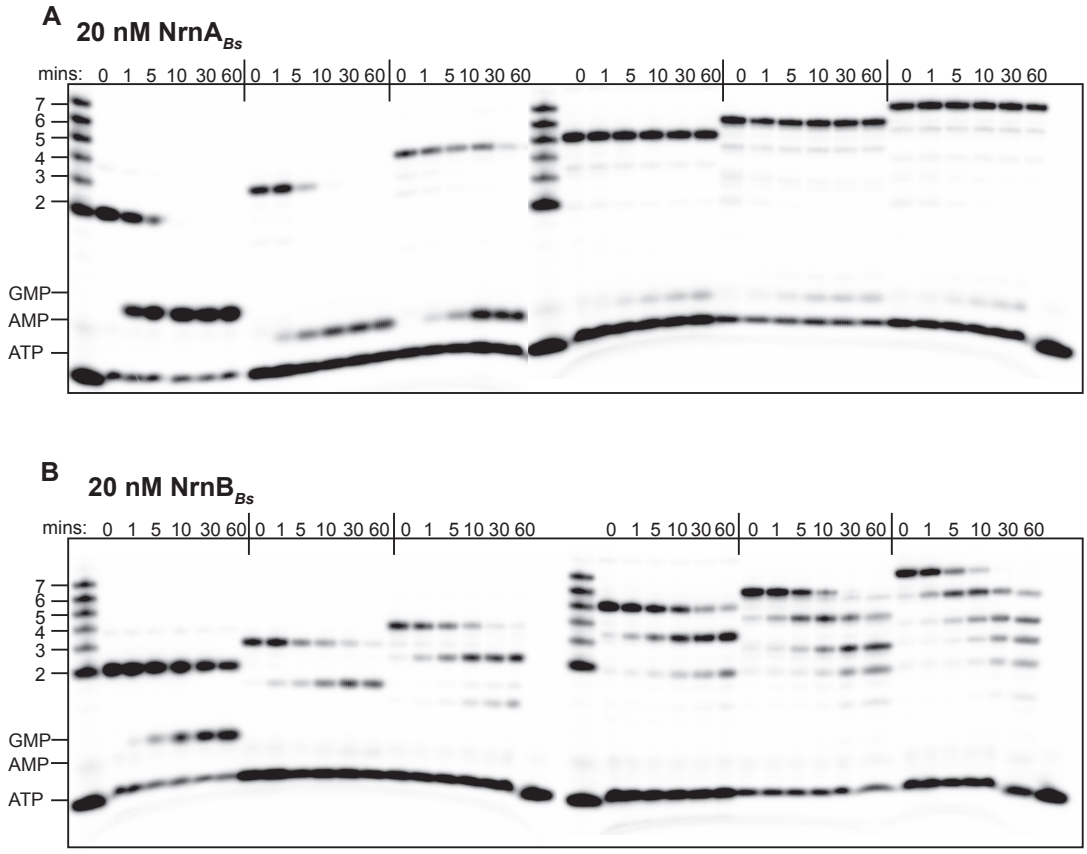

Figure 20. NrnA$_{Bs}$ and NrnB$_{Bs}$ have different substrate preferences in *vitro*. RNA nucleotides two to seven residues in length (1 μM, containing the corresponding ^{32}P-labeled RNA tracer) were each subjected to cleavage over time with 20 nM (A) NrnA$_{Bs}$ or (B) NrnB$_{Bs}$. Aliquots of each reaction were stopped at indicated time (mins), and assessed by denaturing 20% PAGE.

Interestingly, under the same reactions conditions as NrnA$_{Bs}$, which fully processed all pGpG, NrnB$_{Bs}$ cleaved only half (Figure 20B). Moreover, the overall reaction profiles differed dramatically between NrnA$_{Bs}$ and NrnB$_{Bs}$. RNAs that were 3-7 nucleotides in length were all fully processed within the same time frame when incubated with NrnB$_{Bs}$ (Figure 20B). Cleavage of RNA was inversely correlated to the size of RNA substrate, where NrnB$_{Bs}$ cleaved the 7-mer faster than the other substrates. Also, the NrnB$_{Bs}$ cleavage reactions resulted in accumulation of shorter RNA intermediates (Figure 20B). This contrasts strongly with the pattern for NrnA$_{Bs}$, which was active against 2-mer, 3-mer and 4-mer, but in all instances only ever produced an accumulation of nucleoside monophosphates. The production of degradation intermediates provided strong evidence that NrnB$_{Bs}$ acts as a 3'-5' exonuclease. Additionally, these data suggest that NrnB$_{Bs}$ may prefer longer substrates than NrnA$_{Bs.}$ From these data, we conclude that NrnB$_{Bs}$ is an exoribonuclease that acts from the 3' terminus, and that it is not a dedicated dinucleotidase akin to Orn. Our data on NrnA$_{Bs}$ are less clear. Our data can be interpreted in several ways and cannot differentiate between several different models: (1) NrnA$_{Bs}$ is a dinucleotidase, (2) NrnA$_{Bs}$ removes 5' residue(s) from short (between 2-4) RNAs, or (3) NrnA$_{Bs}$ removes 3' residues from short RNAs but processes intermediates faster than the time points that were used in our pilot assays. While more work will need to be done to resolve the enzymatic preferences of NrnA, our pilot data conclusively show that NrnA and NrnB exhibit significant differences in their functional activities.

4.3.4 NrnA and NrnB are expressed under different conditions

The apparent difference in cleavage activity of $NrnA_{Bs}$ and $NrnB_{Bs}$ for pGpG made us consider what the physiological consequences of this might be *in vivo.* Previous imaging studies of the c-di-GMP-responsive riboswitch reporter showed that in the absence of both $NrnA_{Bs}$ and $NrnB_{Bs,}$ intracellular c-di-GMP and pGpG levels accumulate. This result ultimately suggested that $NrnA_{Bs}$ and $NrnB_{Bs}$ are required for pGpG turnover in *B. subtilis.* However, single deletions of each RNase were not analyzed. To determine the relative contributions of pGpG turnover from each RNase, c-di-GMP levels were assayed using the c-di-GMP-responsive riboswitch-*yfp* reporter in a *B. subtilis* wild-type, Δ*nrnA,* or Δ*nrnB* background, in a manner described in Chapter 2. As expected, the constitutive *yfp* control reporter showed mild to no differences in fluorescence between the wild-type and the single Δ*nrnA* or Δ*nrnB* mutants (Figure 21A, B). This was exemplified by the similar histogram distributions of fluorescence intensity among the three strains (Figure 21A, B). Also, in agreement with our prior observations, assessment of the c-di-GMP reporter in a wild-type *B. subtilis* population showed a bimodal distribution of fluorescence, indicating differences in intracellular c-di-GMP among the subpopulations (Figure 21C, D). In the Δ*nrnA* background, the riboswitch reporter exhibited very low fluorescence compared to the wild-type, indicating that c-di-GMP levels, and, consequently, pGpG levels, are higher in this strain (Figure 21C, D). This observation is consistent with a role in turnover of pGpG for $NrnA_{Bs}$. It should be noted that although diminished fluorescence was observed in the Δ*nrnA* strain, the fluorescence intensity does not exactly copy what was observed in the Δ*nrnA* Δ*nrnB* mutant (Figure 18). However,

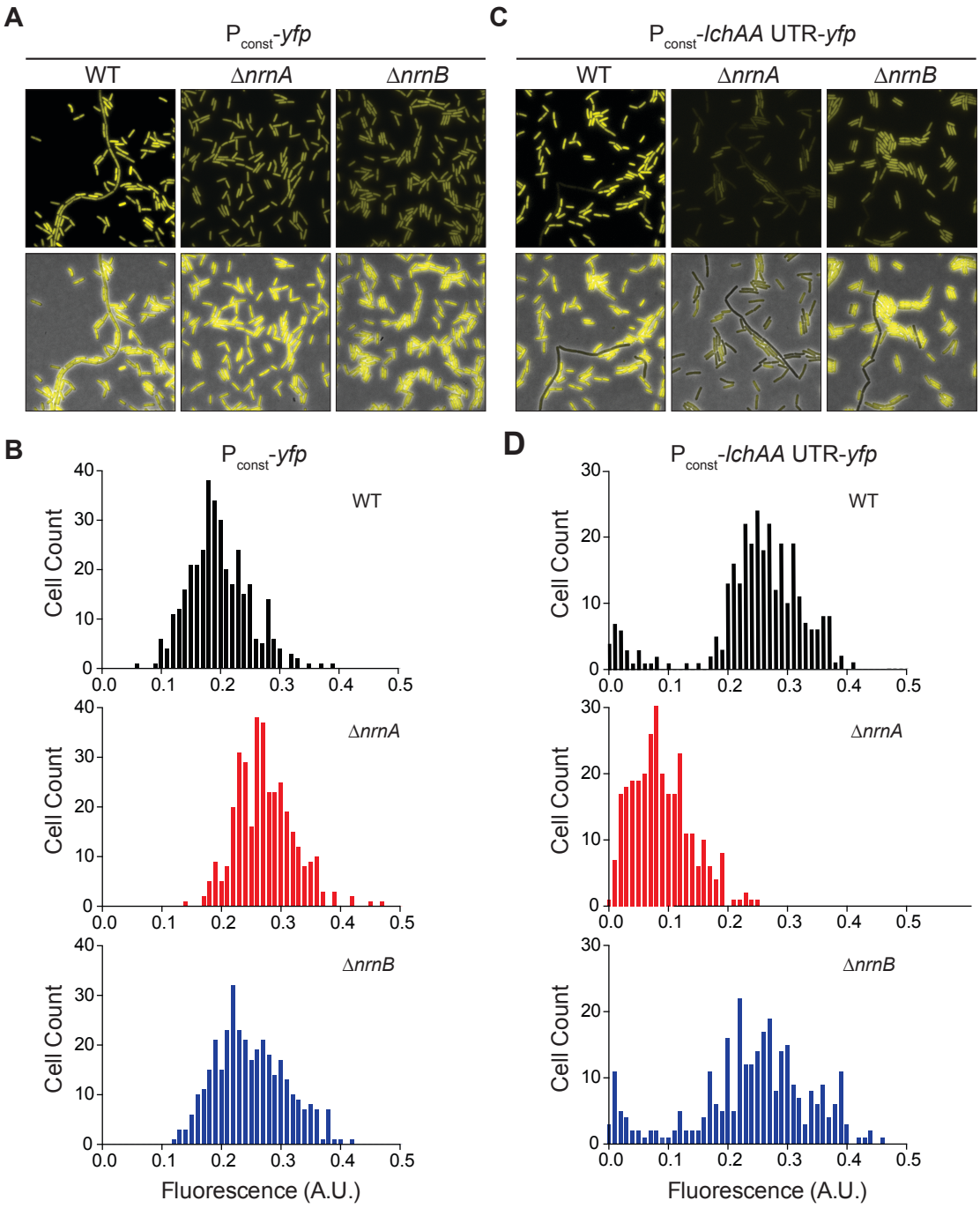

Figure 21. In *B. subtilis* c-di-GMP levels change in response to Δ*nrnA* during vegetative growth. Representative fluorescence microscopy images of YFP production from (A) P_{const}-*yfp* or (C) P_{const}-*lchAA* UTR-*yfp* in *B. subtilis* 168 wild-type (WT), *ΔnrnA,* or *ΔnrnB* strains. Histograms of the quantification of average fluorescence intensity of *B. subtilis* 168 wild type, *ΔnrnA,* and *ΔnrnB* with (B) P_{const}-*yfp* or (D) P_{const}-*lchAA* UTR-*yfp* cells (n~300).

these two experimental conditions cannot be directly compared, as different exposure conditions were used between experiments. Interestingly, a bimodal distribution of fluorescence was observed from the riboswitch-*yfp* reporter in the Δ*nrnB* strain, similar to wild-type (Figure 21C, D). This suggests that if $NrnB_{Bs}$ does cleave pGpG during late exponential phase of growth (OD_{600} ~1.0), accumulation of the dinucleotide in the absence of $NrnB_{Bs}$ is not enough to promote feedback inhibition of enzymes that linearize c-di-GMP. This result was also supported by treatment of pGpG with *B. subtilis* lysates from single Δ*nrnA* or Δ*nrnB* mutants harvested at late exponential phase. 1 μM pGpG was mixed with trace amounts of 5'-^{32}P end-labeled pGpG and subjected to cleavage over the course of two hours in the presence of 5 mM $MgCl_2$. While pGpG was readily degraded by wild-type lysates and Δ*nrnB* lysates in a similar manner, cleavage of pGpG was not observed in the Δ*nrnA* strain (Figure 22). Together these data suggest that $NrnA_{Bs}$ is the primary RNase responsible for cleaving pGpG during late exponential phase.

The observation that $NrnB_{Bs}$ either does not cleave pGpG at all or does not do this during late exponential phase of growth, led us to consider when in *B. subtilis* development *nrnA* and nrnB are expressed. Recently, a large-scale study was undertaken to systematically and quantitatively explore transcriptional changes that occur in *B. subtilis* in response to over 100 nutritional changes and chemical stresses (179). The data generated from this large study is accessible on a freely available database, *B. subtilis Expression Data Browser*, for researchers (http://genome.jouy.inra.fr/cgi-bin/seb/index.py). Expression patterns of all *B. subtilis* open reading frames can be individually assessed on this database.

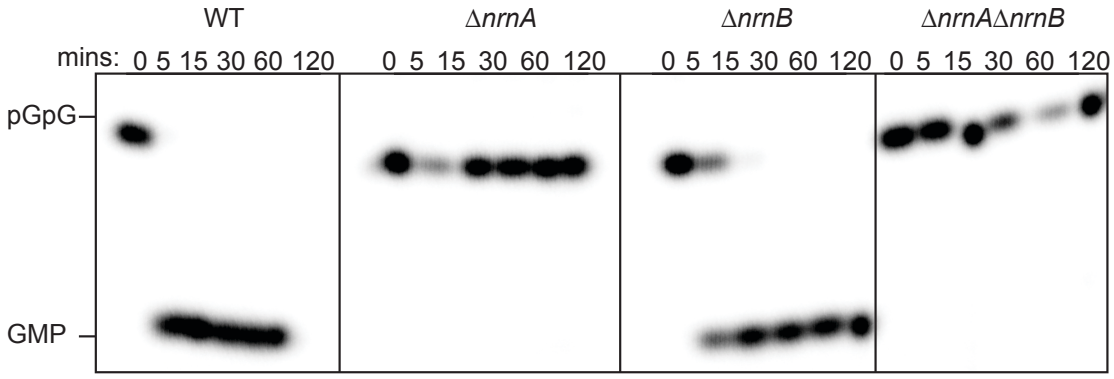

Figure 22. Absence of NrnA alone results in loss of pGpG cleavage activity for *B. subtilis* during vegetative growth. 1 μM pGpG (containing the corresponding 5' ^{32}P-labeled RNA tracer) was subjected to cleavage by lysates of *B. subtilis* 168 wild-type (WT), Δ*nrnA,* Δ*nrnB, or* Δ*nrnAB* that had been grown to late log (OD_{600} ~ 1.0). Reactions were stopped at indicated times and resolved by urea-denaturing 20% PAGE.

Based on this study, there were several different conditions that induced the highest expression of *nrnA* (Figure 23A). These included induction of competence (C90), treatment with the oxidative drug diamide (dia5, dia15), exponential growth in low and high phosphate defined medium (LPh, HPh), during growth in a synthetic minimal medium (Belitsky Minimal Medium) prior to stress (BMM), and finally, during germination from sporulation (G135, G180). The general trends suggests its expression occurs during exponential phase of growth in diverse media. This is consistent with our microscopy data that suggested c-di-GMP and pGpG levels accumulate at OD_{600} ~ 1.0 in MSgg medium when *nrnA* is removed. Intriguingly, however, the expression conditions for *nrnB* were highest throughout development of sporulation (Figure 23B). Cells were grown in CH medium at 37°C and sporulation was induced by resuspension in warm sporulation medium as described by Sterlini and Mandelstam (244). Following induction of sporulation, samples were harvested at hourly intervals, and *nrnB* expression levels were highest 4-8 hours into sporulation (S4-S8). These time points are concurrent with the activation of specific transcription factors in the forespore and mother cell that allow for compartmentalized gene expression. This compartment specific gene expression program directs proper formation of the spore coat and cortex prior to spore release. The highest expression of *nrnB* was also observed during stationary phase (LBGstat), as well as after 24 hours of incubation in MSgg medium to induce biofilm formation (BT). It should be noted that many studies have shown that spores are spatially organized within a *B. subtilis* biofilm community (135, 140). Therefore, the currently available transcriptomic data suggests that *nrnB* is expressed during sporulation. This is also consistent with our microscopy

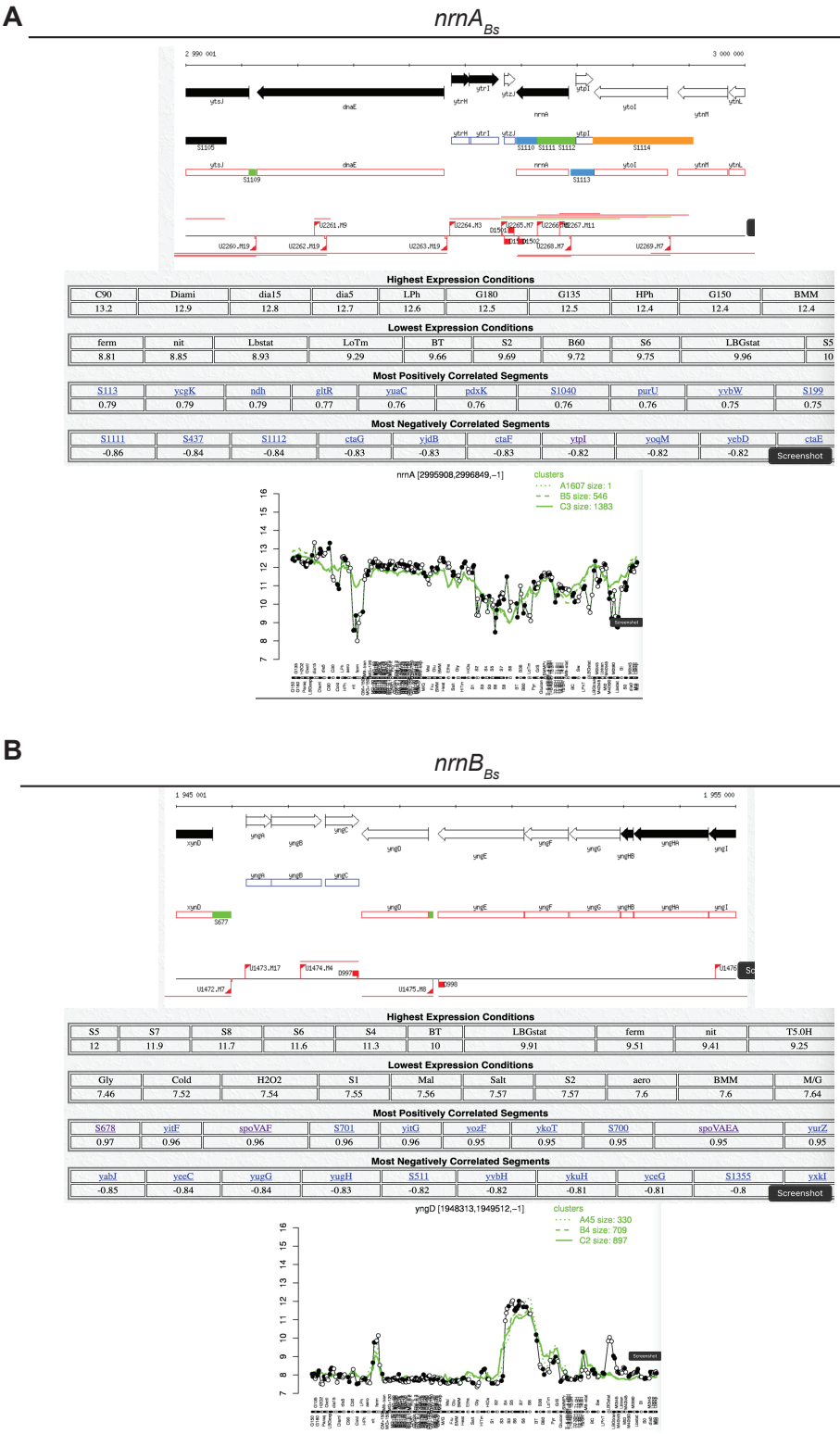

Figure 23. Transcriptomic data reveals when *B. subtilis nrnA* and *nrnB* are expressed. Expresion data of (A) *nrnA* and (B) *nrnB* taken from *B. subtilis Expression Data Browser*, (http://genome.jouy.inra.fr/cgi-bin/seb/index.py).

data. The deletion of *nrnB* had no observed effect on c-di-GMP or pGpG levels in late-exponential phase, as measured by our fluorescent c-di-GMP riboswitch reporter. If *nrnB* is expressed during sporulation, then we would not expect to see activity during the phase of growth that we assessed. Therefore, it is possible that *nrnB* is a sporulation-specific exoribonuclease. If true, this would be the first instance of an RNase that plays a role during the endospore developmental program.

4.4 Discussion

At best, the published literature that is currently available poses a remarkably confusing picture of the functions of NrnA and NrnB. As discussed in the Introduction of this chapter, initial characterization of NrnA and NrnB suggested that they are generally involved in degradation of short RNAs as 3'-5' exonucleases and are fully redundant with one another (120, 121). However, subsequent studies also propose that NrnA might act as a 5'-3' exonuclease as well as a 3'-5' exonuclease (243). Therefore, in this chapter, our goal was to conduct an initial survey using a common set of reaction conditions to determine whether NrnA and NrnB exhibited differences in their substrate preferences. From our data we conclude that NrnA and NrnB clearly exhibit substrate differences and are expressed under entirely different physiological conditions; therefore, they are not redundant proteins, and likely serve different functions in *B. subtilis.*

While the original complementation experiment that identified $NrnA_{Bs}$ and $NrnB_{Bs}$ is important in that it led to identification of the Orn-like functions of NrnA and

NrnB, it also exemplifies the challenges in utilizing a single term (*i.e.,* "nanoRNase") to refer to degradation of short RNAs. The term "nanoRNA" was coined to distinguish extremely short oligoribonucleotides 2-7 nucleotides in length from longer microRNAs, which are presumably around 20-30 nucleotides in length. Subsequently, enzymes such as Orn, NrnA, NrnB, and NrnC are all defined as general "nanoRNases" capable of processing "nanoRNA" of any length shorter than 7 nucleotides. A problem with this term is that it could lead to inaccurate assumptions about the biochemistry and functional roles of these RNase enzymes if they exhibit substrate differences from one another. Indeed, the work described in this dissertation clearly demonstrates, however, that Orn is not a "nanoRNase" at all, but is in fact a dedicated diribonucleotidase in cells. This discovery indicates that, by reducing cellular diribonucleotides, this activity clears a very specific terminal bottleneck in global RNA degradation. This discovery also exemplifies the danger in introducing a term that poorly defines the substrate specificities of multiple enzymes that do not share common evolutionary history. The immediate goal of our preliminary experiments was to identify if under standardized conditions, $NrnA_{Bs}$ and $NrnB_{Bs}$ had different substrate specificities. Our preliminary observations suggest that this may very well be the case. $NrnB_{Bs}$ seemed to cleave 5-7 nucleotide-long RNAs more readily than $NrnA_{Bs.}$ Although $NrnB_{Bs}$ has the biochemical capacity to cleave the dinucleotide pGpG as well as 3-mers and 4-mers, $NrnB_{Bs}$ may not even be expressed during exponential growth. Instead, NrnB may have a specific role in clearing short RNAs during the developmental program of endospore formation, and this should be explored. We believe that NrnA and NrnB are not redundant RNases, but have defined physiological

roles. Therefore, defining NrnA and NrnB as general "nanoRNases" precludes them from having different substrate specificities, and only serves to add confusion in determining true functions of these RNases in the cell. We argue that this term should be removed from future characterizations of RNases.

One of the earliest pieces of evidence that Orn shows substrate specificity for diribonucleotides came from equilibrium binding constants of purified Orn_{Vc} and ^{32}P-5' end labeled RNAs two to seven nucleotides in length. A similar approach should be carried out with purified $NrnA_{Bs}$ and $NrnB_{Bs.}$ This may help identify which RNA substrates $NrnA_{Bs}$ and $NrnB_{Bs}$ are most likely to process. RNA cleavage assays with different concentrations of each enzyme may also determine how the substrate specificity of NrnA and NrnB changes directly in response to altered enzyme concentrations. After all, in our investigations of Orn, RNA substrates were incubated with Orn_{Vc} at different molar ratios to show that while Orn specifically prefers dinucleotides, Orn has the ability to cleave substrates longer than a dinucleotide. These assays demonstrate how biochemical studies alone are susceptible to many variables, such as enzyme concentration, substrate concentration, temperature, and time. Our data begins to address that a systematic analysis, where reaction conditions and products are all uniform in all assays, can reveal unequivocally the substrate preferences of NrnA and NrnB and how they compare to Orn. Finally, further *in vivo* characterization of these enzymes will determine whether or not they are differentially regulated.

Cleavage of RNAs 2-4 nucleotides in length by purified NrnA resulted in visualization of nucleoside monophosphates. However, intermediate species were not observed during cleavage of 3-mers and 4-mers. This would be an expected outcome

if NrnA were removing the terminal phosphate from the 5' direction. Consequently, this remains an important open question that will require more definitive experiments. While our data do not conclusively resolve NrnA's activities, they do demonstrate that NrnA exhibits significant differences from NrnB and should not be considered redundant proteins. Therefore, our work in this chapter establishes the questions that should be asked next in trying to understand the molecular function(s) of the NrnA and NrnB proteins.

4.5 Materials and Methods

4.5.1 Bacterial strains, plasmids, and growth conditions

All *B. subtilis* strains in this study are derived from 168 (unless otherwise noted). Strains were grown at 37˚C on Lysogeny Broth (LB) plates supplemented with 1.5% Bacto Agar and when appropriate, with final concentrations of the following antibiotics: 5 μg/mL chloramphenicol, and 1 μg/mL erythromycin added alongside 25 μg/mL lincomycin (mls). Integration at the *amyE* locus was performed with plasmids derived from pJG019 (GenBank: KX499653.1), To construct pRSL_F4, the *lchAA* leader sequence was synthesized (GenScript) and subcloned into the HindIII restriction site of pJG019. To make markerless deletions of Δ*nrnA* and Δ*nrnB,* strains harboring an erythromycin-resistance cassette inserted in loci BSU29250 (*nrnA*), and BSU18200 (*nrnB*), were obtained from the BKE collection (BGSC). Markerless deletions were created through transformation with pDR244 (BGSC), as previously described (215).

Removal of the erythromycin-resistance cassette was verified by Sanger sequencing. Transformation of 168 was performed using a previously described protocol (216).

.

4.5.2 Fluorescence microscopy and quantification

The *B. subtilis* 168 wild-type (WT) and the Δ*nrnA* Δ*nrnB* and mutant-derived reporter strains were grown at 37˚C on LB plates supplemented with 1.5% Bacto agar and 5 μg/ml chloramphenicol, when appropriate. Single colonies were used to inoculate liquid minimal salts glycerol glutamate (MSgg) medium (40) and were grown at 37˚C with shaking overnight. The following day, cultures of each strain were inoculated 1:50 on fresh medium and grown at 37˚C shaking until reaching an optical density at 600 nm (OD_{600}) of 1.0. Aliquots of these cultures were placed on 1.5% low-melting-point agarose MSgg pads and allowed to dry for 10 min. The agarose pads were inverted onto a glass-bottom dish (Willco Wells). Cells were imaged at room temperature using a Zeiss Axio Observer Z1 inverted fluorescence microscope, equipped with a Rolera EM-C^2 electron-multiplying charge-coupled (EMCC) camera and an environmental chamber. Fluorescence intensity per cell was quantified using the Oufti analysis software (41). Images were analyzed and adjusted with the Fiji software (42)

4.5.3 Metabolite extraction of c-di-GMP and pGpG in *B. subtilis.*

Three independent replicates of *B. subtilis* 168 WT and Δ*nrnA* Δ*nrnB* mutant strains were grown overnight in liquid MSgg medium (40) with shaking at 37˚C. The following day, cultures of each strain were inoculated 1:50 and grown with shaking at 37˚C until reaching an optical density at 600 nm (OD_{600}) of 1.0. Metabolite extraction

was described previously (45). Five-milliliter cultures were passed through 0.2-µm nylon filters (EMD Millipore). Metabolism was quenched, and metabolites were extracted by inverting the filters into petri dishes that contained 1.5 mL prechilled extraction solvent composed of 40:40:20 acetonitrile-methanol-water. Dishes were placed on dry ice for 15 minutes before the wash was collected in microcentrifuge tubes and allowed to spin at maximum speed for 5 minutes at 4˚C. The supernatant was then transferred to new microcentrifuge tubes and placed in a vacuum centrifuge until the metabolite extracts were dry.

4.5.4 Detection and quantification of c-di-GMP and pGpG in *B. subtilis*

The detection of c-di-GMP by LC-MS/MS was described previously (46). Briefly, bacterial extract was resuspended in solvent A (10 mM tributylamine in water [pH 5.0]) and centrifuged twice to remove insoluble particles. Metabolites were then separated on a Synergi Fusion-RP column (4-µm particle size, 80-Å pore size, 150 mm by 2 mm; Phenomenex) using a Shimadzu high-performance liquid chromatography machine and simultaneously analyzed by a triple quadrupole mass spectrometer (3200 QTrap; Ab Sciex). The total run time was 20 min, at a binary flow rate of 0.5 ml·min^{-1}, with 10 mM tributylamine in water (pH 5.0) as solvent A and 100% methanol as solvent B. The following gradient was performed: 0.01 min, 0% B; 4 min, 0% B; 11 min, 50% B; 13 min, 100% B; 15 min, 100% B; 16 min, 0% B; and 20 min, 0% B. c-di-GMP and pGpG were detected by multiple-reaction monitoring (MRM) under negative mode using the ion pairs 689/79 and 689/344 (c-di-GMP) and 707/79 and 707/150 (pGpG). C-di-GMP and pGpG were quantified using the Analyst software

(version 1.6.2) by calculating the total peak area and were normalized by total ion current (TIC). Authentic c-di-GMP and pGpG standards were injected and analyzed alongside the samples.

4.5.5 Labeling of RNAs

5' un-phosphorylated RNAs were purchased from TriLink Biotechnologies or Sigma. Each RNA was subjected to radioactive end-labeling or non-radioactive phosphorylation by T4 Polynucleotide Kinase (New England Biolabs). Each RNA was subjected to phosphorylation with equimolar concentrations of either ^{32}P-gamma ATP or ATP, T4 PNK, and 1X T4 PNK Reaction Buffer. Reactions comprising a final concentration of either 0.5 μM radiolabeled RNA or 2.0 μM phosphorylated RNA were incubated at 37°C for 40 min, followed by heat inactivation of T4 PNK at 65°C for 20 mins.

4.5.6 Protein expression and purification for biochemical assays

E. coli T7Iq strains harboring expression vector pVL847 expressing an His_{10}-MBP-NrnA and His_{10}-MBP-NrnB from *B. subtilis* were grown overnight, subcultured in LB M9 fresh media supplemented with 15 mg/ml gentamicin and grown to approximately OD_{600}~0.5 at 30°C. Expression was induced with 1 mM IPTG for 4 hours. Induced bacteria were collected by centrifugation and resuspended in 10 mM Tris, pH 8, 100 mM NaCl, and 25 mM imidazole. After addition of 10 mg/mL DNase, 25 mg/mL lysozyme, and 1 mM PMSF, bacteria were lysed by sonication. Insoluble material was removed by centrifugation. The His-fusion protein was purified by

separation over a Ni-NTA column. Purified proteins were pooled and dialyzed for 1 hour and overnight against 10 mM Tris, pH 8, 100 mM NaCl, aliquoted, and flash frozen with liquid nitrogen and stored at -80°C.

4.5.7 Purified NrnA$_{Bs}$ and NrnB$_{Bs}$ cleavage reactions

Phosphorylated RNA (1.0 μM), including trace amounts of radiolabeled substrate, was subjected to cleavage by purified 20 nM His$_{10}$-MBP-NrnA$_{Bs}$ or His$_{10}$-MBP-NrnB$_{Bs}$ at room temperature. These reactions were in the presence of 10 mM Tris, pH 8.0, 100 mM NaCl, and 5 mM $MgCl_2$. At the appropriate times, aliquots of the reaction were removed and quenched in the presence of 150 mM EDTA on ice and heat inactivated at 95°C for 5 min. Samples were separated on denaturing 20% PAGE containing 1X TBE and 4 M urea. The gels were imaged using Fujifilm FLA-7000 phosphorimager (GE) and analyzed for the appearance of truncated ^{32}P-labeled products. The intensity of the radiolabeled nucleotides was quantified using Fujifilm Multi Gauge software v3.0.

Chapter 5: Conclusions and Perspectives

5.1 A Broadening Role for c-di-GMP Regulation in Bacteria

The second messenger molecule c-di-GMP is a widely used regulator in the switching of lifestyle choices among bacteria. In general, high levels of c-di-GMP promote biofilm formation and cell cycle control, while low levels are associated with motility and virulence (16). This theme is largely maintained for *B. subtilis,* where a high level of c-di-GMP is correlated with production of an unknown biofilm EPS and reduced motility. An increasing number of studies suggest a broadening role for c-di-GMP signaling in Gram-positive bacteria, however. Studies on *Bacillus cereus* group organisms, *Clostridioides difficile*, and *Streptomyces coelicolor* have revealed a link between c-di-GMP metabolism and spore formation, which is a developmental program almost exclusive to the three genera (160). As mentioned earlier in this dissertation, there is an ortholog of *B. subtilis* YkuI in the *B. cereus* bacterial group, named CdgJ, that has been implicated in the regulation of biofilm formation and sporulation (181). The high similarity in protein sequences between YkuI and CdgJ allows for the possibility that YkuI might also exhibit a similar role in *B. subtilis*, although it has yet to be explored. Sporulation is also affected by c-di-GMP in *S. coelicolor*. Overexpression of DGCs *cdgA* or *cdgB*, or deletion of PDEs *rmdA* or *rmdB* led to an increase in intracellular c-di-GMP and inhibition of sporulation (245, 246). Studies on *S. coelicolor* have also revealed the only c-di-GMP-sensing, transcriptional regulator to date among Gram-positive organisms (BldD) (247, 248). When bound by

c-di-GMP, BldD represses sporulation genes during vegetative growth. Correspondingly, deletion of BldD leads to accelerated sporulation. These phenotypes were inhibited through overexpression of the diguanylate cyclases *cdgA* and *cdgB*, which are also direct targets of BldD (245, 246). C-di-GMP was also shown to repress expression of antibiotic synthesis genes via BldD. The presence of a c-di-GMP riboswitch upstream of the *B. licheniformis lchAA* secondary metabolite biosynthesis gene cluster suggests that secondary metabolites might be under direct regulatory influence by c-di-GMP in some *Bacillus* species and other Gram-positive organisms. If confirmed, this would represent a new functional category of genes regulated by c-di-GMP in bacteria. In summary, while *B. subtilis* has served as a general model organism for many Gram-positive bacteria, emerging studies in *B. subtilis* and other organisms have revealed an unambiguous role for c-di-GMP signaling during differentiation pathways such as motility and biofilm formation (160, 174, 181, 249–255). However, a theme is emerging that c-di-GMP signaling may affect secondary metabolite production, competence, and sporulation. Our own work discussed in Chapter 2 suggests that c-di-GMP levels are markedly different between competent and sporulating cells. Therefore, *B. subtilis* and other Gram-positive organisms utilize c-di-GMP signaling to regulate unique cell development pathways.

The creation of a fluorescent reporter based on a c-di-GMP-responsive riboswitch provides an accessible tool for elucidating the outcomes of c-di-GMP regulation in specific sub-populations of bacteria. For example, our reporter provided data on tricellular c-di-GMP levels during competence and sporulation. These populations represent two cell types that have not been previously tested for c-di-GMP

regulation in this organism. Moreover, many different riboswitches can be used as fluorescent tools for measuring intracellular metabolite dynamics.

The molecular details of c-di-GMP targets in *B. subtilis* also require further exploration. Additional c-di-GMP effectors and their targets likely have yet to be identified. Several high-throughput methods have been recently developed for assessing c-di-GMP-binding partners (226, 256–259). It is possible that the use of one of these methods to target *B. subtilis* c-di-GMP interactions could potentially reveal new c-di-GMP binding partners in the future. Analysis of transcriptomic changes that occur in response to changes in c-di-GMP should also reveal yet undiscovered regulatory targets of c-di-GMP under different physiological conditions.

5.2 Differences in RNA Recycling Mechanisms Among Bacteria

C-di-GMP signaling is terminated when phosphodiesterases (PDE-As) cleave c-di-GMP into the linear diribonucleotide pGpG (70, 73). Different classes of phosphodiesterases have been shown to also linearize c-di-AMP into pApA (124). While the phosphodiesterases involved in cGAMP and cyclic UMP-AMP signaling have yet to be discovered, these cyclic nucleotides are expected to be linearized into their respective dinucleotide constituents in a similar fashion. Cyclic dinucleotide signaling, therefore, represents one pathway in which diribonucleotides are generated in bacteria. Diribonucleotides are expected to be produced from other cellular mechanisms as well. For example, short RNAs 2-15 nucleotides in length are also generated from multiple rounds of abortive transcription initiation by RNA Polymerase (260). Lastly, diribonucleotide products are generated as products of mRNA processing

and degradation (232). It is likely that the accumulation of diribonucleotides in the absence of Orn does not permit viability, but the mechanistic details of how diribonucleotides specifically cause toxicity remains to be elucidated. If diribonucleotides target specific proteins, their identity could be resolved by performing additional screens for proteins that bind diribonucleotides. Alternatively, identification of suppressors that promote growth in the absence of Orn might also reveal proteins involved in diribonucleotide regulation.

While the data in this dissertation reveal the mechanism of diribonucleotide processing by Orn in *P. aeruginosa*, they raise additional questions. How do organisms that lack Orn process diribonucleotides and other short RNAs? Are there multiple classes of enzymes that specifically process short RNAs? Do any of them specialize in other short RNA lengths, other than dinucleotides? Currently, NrnA and NrnB are presumed to terminate RNA degradation in a manner functionally redundant to Orn. Yet, our preliminary investigations argue against this. Our data suggests that NrnA and NrnB have unique substrate preferences, as well as broader substrate preferences compared to Orn; therefore, they are not redundant proteins. Future studies will need to explore the turnover rate of these enzymes with different substrates, to elucidate the enzymology of these proteins and their catalytic strategies. Furthermore, NrnA and NrnB may not be co-expressed. NrnB may have a specific role in clearing short RNAs during the developmental program of endospore formation, and this should be explored. If NrnB is regulated during endospore formation, one would expect to see defects in aspects of sporulation as a result of loss of NrnB.

Moreover, our data continues to raise questions about 5' cleavage. Our data demonstrate that NrnA may act on the 5' terminus. An experiment that assesses NrnA activity against radiolabeled modified RNAs with nonhydrolyzable linkages will help determine the direction of NrnA processivity. Comparing cleavage assays for RNA substrates containing radiolabeled phosphates at either the 5' or 3' termini will also help reveal the directionality of NrnA. If these experiments show that NrnA recognizes the 5' end of short RNAs and, moreover, show that it is relevant *in vivo*, it would be a remarkable discovery. The only known 5'-3' exoribonuclease in bacteria is RNase J (261). Our data showing removal of the 5' residues by NrnA raise an interesting hypothesis; the enzyme may act as a 5'-3' exoribonuclease that specializes in the degradation of short RNAs.

Interestingly, *B. subtilis* RNase J (*rnjA)* was previously tested for *orn* complementation (121). Partial complementation of an *E. coli* conditional *orn* mutant was observed at low levels of *rnjA* expression; overexpression of *rnjA* in the *orn* mutant was lethal. While RNase J showed differing extents of activity against oligoribonucleotides *in vitro,* it was determined that short RNA oligomers were likely to be physiologically relevant substrates. Interestingly, a triple deletion mutant of *nrnA, nrnB,* and *yhaM* was shown to have a negligible effect on exponential growth in *B. subtilis.* This suggests that either RNase J can cleave oligoribonucleotides in the absence of the three genes or that additional RNases exist that perform this function. Alternatively, the accumulation of dinucleotides is not toxic in this organism, while it is for bacteria that encode Orn. Together, these data contribute to the fundamental

understanding of how RNAs are degraded in bacteria. Briefly, differences in mechanisms of mRNA degradation between *E. coli* and *B. subtilis* are addressed below

5.2.1 mRNA Degradation Mechanisms in *E. coli*

In *E. coli* and other bacteria, RNases cooperate with various interacting partners in the form of a large, stable complex called the degradosome (262, 263). The degradosome, which localizes to the membrane, is organized around the C-terminal half of RNase E. RNase E is responsible for the initiation of mRNA degradation, which begins with endonucleolytic cleavage of single-stranded AU-rich regions. RNase E has little sequence specificity, and therefore impacts bulk mRNA turnover (264). Following endonucleolytic cleavage, distinct sets of exoribonucleases continue to degrade mRNA transcripts (232, 265). In *E. coli,* exonucleolytic cleavage is performed exclusively by 3'-5' exoribonucleases. These include polynucleotide phosphorylase (PNPase), RNase II, and R. Despite the fact that the exoribonucleases all act on the 3' end of mRNAs and have been shown to widely overlap with one another, each RNase may still have particular substrate specificities. For example, while RNase II has been shown to stall upon encounter of a stem-loop, RNase R performs this function readily. Furthermore, when a structured region of RNA is encountered, PNPase works in conjunction with the helicase RhlB, which assists PNPase in unwinding stem-loops. PNPase has also been shown to have both degradative and synthetic capabilities, and can add single-stranded adenine-rich tails to the 3' end of an mRNA transcript. Other 3'-5' exoribonucleases, such as RNase D, T, Z (BN), and PH have been implicated in

tRNA and rRNA maturation (232). Finally, while all available literature leading up to this study characterized Orn as an additional 3'-5' exoribonuclease of short RNAs, our data reveals that Orn specifically cleaves diribonucleotide substrates, to complete the terminal step of RNA degradation.

5.2.2 mRNA Degradation Mechanisms in *B. subtilis*

Organisms that lack RNase E use RNase Y instead. RNase Y also initiates global mRNA degradation via endonucleolytic cleavage and has been proposed to form a complex akin to the *E. coli* degradosome (266, 267). Like RNase E, RNase Y also recognizes single-stranded AU-rich sequences of RNA. *B. subtilis* not only lacks RNase E, but also the 3'-5' exoribonuclease RNase II. Instead, PNPase, RNase R, and YhaM are considered the main 3'-5' exoribonucleases (268, 269). Like *E. coli, B. subtilis* also encodes RNase PH, which has a primary role in tRNA maturation, but also a minor role in mRNA degradation. *B. subtilis* also features the only known 5'-3' exoribonuclease, RNase J, which cleaves monophosphorylate mRNA transcripts (261). Most low-GC Gram-positive bacteria encode two orthologs of RNase J, RNase J1 and RNase J2. It has also been argued that RNase J has endonucleolytic activity *in vitro* (270), but the physiological relevance of this activity is still under debate. This theme is also addressed in our work—multiple approaches are critical for the assessment of enzyme activity, as biochemical experiments alone can produce varied results. Interestingly, RNase J is essential in some organisms, but not others (269, 271). While essential in *Streptococcus pyogenes,* the deletion of RNase J in *B. subtilis, S. aureus, or Streptococcus mutans* results in a severe growth defect. Furthermore, the relative

dependence on RNase J1 or J2 is variable across organisms. The deletion of RNase J1 has a more pronounced effect in some organisms, while others rely more heavily on RNase J2.

5.3 Concluding Remarks

While the general principles of RNA processing and degradation are conserved among bacteria, there is no universally conserved set of ribonucleolytic enzymes that all bacteria rely upon for mRNA turnover. Our own work highlights aspects of this; fluorescent tools described in Chapter 2 reveals which enzymes are able to cleave diribonucleotides *in vivo.* Work discussed in Chapter 3 reveals that in some bacteria, Orn is singularly responsible for 'diribonucleotidase' activity, and that this is a discrete step in RNA degradation. Orn is not encoded in all bacterial genomes, however, and is generally encoded in genomes belonging to Betaproteobacteria, Gammaproteobacteria, and Actinobacteria. Work discussed in Chapter 4 extends our new knowledge of Orn to NrnA and NrnB. NrnA and NrnB have been described as redundant proteins generally responsible for cleaving 'short RNAs.' Yet our preliminary data suggests that NrnA and NrnB are not redundant. NrnA and NrnB exhibit different substrate preferences and may have unique cellular functions in Firmicutes, Deltaproteobacteria, Actinobacteria, and other phyla. Moreover, while RNase J is currently the only known 5'-3' exoribonuclease in bacteria, our work also provides the possibility that a different enzyme, NrnA, also acts at the 5' terminus. RNA degradation is an essential process in all domains of life and ends with the recycling of short oligonucleotides. This work

provides evidence that short oligonucleotides may be processed by unique enzymes in discrete steps. However, the mechanisms by which diribonucleotide clearance feeds back to cyclic dinucleotide signaling still remains an open area of investigation.

Appendix

A. DNA Sequence of P_{T7}-*lchAA* aptamer-Spinach2 used for fluorescence activation assays

5'-
TAATACGACTCACTATAGGGCCCGGATAGCTCAGTCGGTAGAGCAGCGGCCG**G**
ATGTAACTGAATGAAATGGTGAAGGACGGGTCCAAT*GATAAAGGCAAACCTGC*
GGAAACGCAGGGACGCAAAGCCATGGCCTAAGGTGCTGACGGTGCTACGGTTGACAG
*GTTGCC*AT**TTGTTGAGTAGAGTGTGAGCTCCGTAACTAGTTACATC**CGGCCGC
GGGTCCAGGGTTCAAGTCCCTGTTCGGGCGCCA

B. DNA template sequence of P_{const}-*lchAA* leader used for *in vitro* transcription termination assays

5'-
CTACATCCAGAACAACCTCTGCTAAAATTCCTGAAAAATTTTCGAAAAAGTTGTT
GACTTTATCTACAAGGTGTGGCATAATGTGTGTGCA*GCAGAAAATGAATTTATATCA*
AGAAAAGCAGATAAAGGCAAACCTGCGGAAACGCAGGGACGCAAAGCCATGGCCTAA
GGTGCTGACGGTGCTACGGTTGACAGGTTGCCGAATAAACAGGGAGTTCGCCCGTTTT
TATTCGGGCGGGCTCTTTTCTTTTTATTTCCAATATAATGTTTTATTGGAAACGACAAATC
TGTGACAGCGTTTTTCG

C. DNA sequence of P_{const}-*lchAA* leader-*yfp* reporter used for fluorescence microscopy

5'-
GTAGCCCTTGCCTACCTAGCTTCCAAGAAAGATATCCTTACAGCACAAGAGCGG
AAAGATGTTTTGTTCTACATCCAGAACAACCTCTGCTAAAATTCCTGAAAAATTT
TCGAAAAAGTTGTTGACTTTATCTACAAGGTGTGGCATAATGTGTGTGCA*GCAGA*
AAATGAATTTATATCAAGAAAAGCAGATAAAGGCAAACCTGCGGAAACGCAGGGACGC
AAAGCCATGGCCTAAGGTGCTGACGGTGCTACGGTTGACAGGTTGCCGAATAAACAGG
GAGTTCGCCCGTTTTTATTCGGGCGGGCTCTTTTCTTTTTATTTCCAATATAATGTTTTAT
TGGAAACGACAAATCTGTGACAGCGTTTTTCGCTCATCGCAAAACCGCAACATTGCATT
*GCGGCTTGGCTGTTCGCATCGTCATACATAACAAGAGAT*AAGCTTAAGGAGGAAAGT
CACATT**ATGAGCAAAGGTGAAGAACTGTTCACCGGCGTTGTGCCAATTCTGG**
TTGAGCTGGATGGTGACGTGAATGGCCACAAATTTTCCGTGTCTGGTGAAG
GCGAGGGTGATGCTACTTATGGCAAACTGACTCTGAAACTGATCTGTACCAC
CGGCAAACTGCCTGTTCCGTGGCCAACTCTGGTCACTACTCTGGGTTACGGC
CTGATGTGTTTTGCGCGTTACCCGGATCACATGAAACAGCATGACTTCTTCA
AATCTGCCATGCCGGAAGGCTATGTCCAAGAACGTACGATCTTTTTCAAGGA
CGACGGCAACTATAAAACCCGTGCCGAAGTTAAATTCGAGGGTGACACCCT
GGTCAACCGCATCGAACTGAAAGGCATTGACTTCAAAGAGGACGGCAACAT
TCTGGGTCACAAGCTGGAATACAACTACAACTCCCACAACGTTTACATTACT
GCTGACAAGCAGAAAAACGGCATCAAAGCAAACTTCAAGATCCGTCACAAC
ATTGAAGATGGTGGCGTACAGCTGGCAGATCACTACCAGCAGAACACTCCA
ATCGGTGATGGCCCAGTACTGCTGCCAGATAACCATTACCTGTCCTACCAGA
GCAAACTGTCTAAAGACCCGAACGAAAAACGTGACCACATGGTACTGCTGG
AATTTGTTACCGCGGCAGGCATTACCCACGGTATGGACGAACTGTATAAATA
AGCTAGCAAAAACCCCGCCCCTGACAGGGCGGGGTTTTTTTT-3'

Bibliography

1. Galperin MY. 2004. Bacterial signal transduction network in a genomic perspective†. Environmental Microbiology 6:552–567.

2. Cashin P, Goldsack L, Hall D, O'Toole R. 2006. Contrasting signal transduction mechanisms in bacterial and eukaryotic gene transcription. FEMS Microbiology Letters 261:155–164.

3. Hengge R, Gründling A, Jenal U, Ryan R, Yildiz F. 2016. Bacterial Signal Transduction by Cyclic Di-GMP and Other Nucleotide Second Messengers. Journal of Bacteriology 198:15–26.

4. Hengge R, Häussler S, Pruteanu M, Stülke J, Tschowri N, Turgay K. 2019. Recent Advances and Current Trends in Nucleotide Second Messenger Signaling in Bacteria. Journal of Molecular Biology.

5. Kalia D, Merey G, Nakayama S, Zheng Y, Zhou J, Luo Y, Guo M, Roembke BT, Sintim HO. 2012. Nucleotide, c-di-GMP, c-di-AMP, cGMP, cAMP, (p)ppGpp signaling in bacteria and implications in pathogenesis. Chem Soc Rev 42:305–341.

6. Pesavento C, Hengge R. 2009. Bacterial nucleotide-based second messengers. Current Opinion in Microbiology 12:170–176.

7. Krasteva PV, Sondermann H. 2017. Versatile modes of cellular regulation via cyclic dinucleotides. Nature Chemical Biology 13:350–359.

8. Makman RS, Sutherland EW. 1965. Adenosine 3',5'-Phosphate in Escherichia coli. J Biol Chem 240:1309–1314.

9. Ullmann A, Monod J. 1968. Cyclic AMP as an antagonist of catabolite repression in Escherichia coli. FEBS Letters 2:57–60.

10. Cashel M, Gallant J. 1969. Two Compounds implicated in the Function of the RC Gene of Escherichia coli. Nature 221:838–841.

11. Gaca AO, Colomer-Winter C, Lemos JA. 2015. Many Means to a Common End: the Intricacies of (p)ppGpp Metabolism and Its Control of Bacterial Homeostasis. J Bacteriol 197:1146–1156.

12. Liu K, Bittner AN, Wang JD. 2015. Diversity in (p)ppGpp metabolism and effectors. Curr Opin Microbiol 24:72–79.

13. Dalebroux ZD, Swanson MS. 2012. ppGpp: magic beyond RNA polymerase. Nat Rev Micro 10:203–212.

14. Ross P, Weinhouse H, Aloni Y, Michaeli D, Weinberger-Ohana P, Mayer R, Braun S, de Vroom E, van der Marel GA, van Boom JH, Benziman M. 1987. Regulation of cellulose synthesis in Acetobacter xylinum by cyclic diguanylic acid. Nature 325:279–281.

15. Romling U, Galperin MY, Gomelsky M. 2013. Cyclic di-GMP: the First 25 Years of a Universal Bacterial Second Messenger. Microbiology and Molecular Biology Reviews 77:1–52.

16. Jenal U, Reinders A, Lori C. 2017. Cyclic di-GMP: second messenger extraordinaire. Nature Reviews Microbiology 15:nrmicro.2016.190.

17. Hall CL, Lee VT. Cyclic-di-GMP regulation of virulence in bacterial pathogens. WIREs RNA n/a-n/a.

18. Witte G, Hartung S, Büttner K, Hopfner K-P. 2008. Structural Biochemistry of a Bacterial Checkpoint Protein Reveals Diadenylate Cyclase Activity Regulated by DNA Recombination Intermediates. Molecular Cell 30:167–178.

19. Commichau FM, Dickmanns A, Gundlach J, Ficner R, Stülke J. 2015. A jack of all trades: the multiple roles of the unique essential second messenger cyclic di-AMP. Molecular Microbiology 97:189–204.

20. Corrigan RM, Gründling A. 2013. Cyclic di-AMP: another second messenger enters the fray. Nature Reviews Microbiology 11:513–524.

21. Commichau FM, Gibhardt J, Halbedel S, Gundlach J, Stülke J. 2017. A Delicate Connection: c-di-AMP Affects Cell Integrity by Controlling Osmolyte Transport. Trends Microbiol.

22. Gundlach J, Rath H, Herzberg C, Mäder U, Stülke J. 2016. Second Messenger Signaling in Bacillus subtilis: Accumulation of Cyclic di-AMP Inhibits Biofilm Formation. Front Microbiol 7.

23. Corrigan RM, Abbott JC, Burhenne H, Kaever V, Gründling A. 2011. c-di-AMP Is a New Second Messenger in Staphylococcus aureus with a Role in Controlling Cell Size and Envelope Stress. PLOS Pathogens 7:e1002217.

24. Witte CE, Whiteley AT, Burke TP, Sauer J-D, Portnoy DA, Woodward JJ. 2013. Cyclic di-AMP Is Critical for Listeria monocytogenes Growth, Cell Wall Homeostasis, and Establishment of Infection. mBio 4:e00282-13.

25. Huynh TN, Choi PH, Sureka K, Ledvina HE, Campillo J, Tong L, Woodward JJ. 2016. Cyclic di-AMP targets the cystathionine beta-synthase domain of the osmolyte transporter OpuC. Molecular Microbiology 102:233–243.

26. Gundlach J, Herzberg C, Kaever V, Gunka K, Hoffmann T, Wei\s s M, Gibhardt J, Thürmer A, Hertel D, Daniel R, others. 2017. Control of potassium homeostasis is an essential function of the second messenger cyclic di-AMP in Bacillus subtilis. Sci Signal 10:eaal3011.

27. Sureka K, Choi PH, Precit M, Delince M, Pensinger DA, Huynh TN, Jurado AR, Goo YA, Sadilek M, Iavarone AT, Sauer J-D, Tong L, Woodward JJ. 2014. The Cyclic Dinucleotide c-di-AMP Is an Allosteric Regulator of Metabolic Enzyme Function. Cell 158:1389–1401.

28. Gándara C, Alonso JC. 2015. DisA and c-di-AMP act at the intersection between DNA-damage response and stress homeostasis in exponentially growing Bacillus subtilis cells. DNA Repair 27:1–8.

29. Bejerano-Sagie M, Oppenheimer-Shaanan Y, Berlatzky I, Rouvinski A, Meyerovich M, Ben-Yehuda S. 2006. A Checkpoint Protein That Scans the Chromosome for Damage at the Start of Sporulation in Bacillus subtilis. Cell 125:679–690.

30. Oppenheimer-Shaanan Y, Wexselblatt E, Katzhendler J, Yavin E, Ben-Yehuda S. 2011. c-di-AMP reports DNA integrity during sporulation in Bacillus subtilis. EMBO Rep 12:594–601.

31. Mehne FMP, Schröder-Tittmann K, Eijlander RT, Herzberg C, Hewitt L, Kaever V, Lewis RJ, Kuipers OP, Tittmann K, Stülke J. 2014. Control of the Diadenylate Cyclase CdaS in Bacillus subtilis AN AUTOINHIBITORY DOMAIN LIMITS CYCLIC DI-AMP PRODUCTION. J Biol Chem 289:21098–21107.

32. Gundlach J, Mehne FMP, Herzberg C, Kampf J, Valerius O, Kaever V, Stülke J. 2015. An Essential Poison: Synthesis and Degradation of Cyclic Di-AMP in Bacillus subtilis. Journal of Bacteriology 197:3265–3274.

33. Mehne FMP, Gunka K, Eilers H, Herzberg C, Kaever V, Stülke J. 2013. Cyclic Di-AMP Homeostasis in Bacillus subtilis BOTH LACK AND HIGH LEVEL ACCUMULATION OF THE NUCLEOTIDE ARE DETRIMENTAL FOR CELL GROWTH. J Biol Chem 288:2004–2017.

34. Kamegaya T, Kuroda K, Hayakawa Y. 2011. Identification of a Streptococcus pyogenes SF370 gene involved in production of c-di-AMP. Nagoya J Med Sci 73:49–57.

35. Blötz C, Treffon K, Kaever V, Schwede F, Hammer E, Stülke J. 2017. Identification of the Components Involved in Cyclic Di-AMP Signaling in Mycoplasma pneumoniae. Front Microbiol 8.

36. Danilchanka O, Mekalanos JJ. 2013. Cyclic Dinucleotides and the Innate Immune Response. Cell 154:962–970.

37. Woodward JJ, Iavarone AT, Portnoy DA. 2010. c-di-AMP Secreted by Intracellular Listeria monocytogenes Activates a Host Type I Interferon Response. Science 328:1703–1705.

38. McWhirter SM, Barbalat R, Monroe KM, Fontana MF, Hyodo M, Joncker NT, Ishii KJ, Akira S, Colonna M, Chen ZJ, Fitzgerald KA, Hayakawa Y, Vance RE. 2009. A host type I interferon response is induced by cytosolic sensing of the bacterial second messenger cyclic-di-GMP. Journal of Experimental Medicine 206:1899–1911.

39. Davies BW, Bogard RW, Young TS, Mekalanos JJ. 2012. Coordinated Regulation of Accessory Genetic Elements Produces Cyclic Di-Nucleotides for V. cholerae Virulence. Cell 149:358–370.

40. Sun L, Wu J, Du F, Chen X, Chen ZJ. 2013. Cyclic GMP-AMP synthase is a cytosolic DNA sensor that activates the type I interferon pathway. Science 339:786–791.

41. Wu J, Sun L, Chen X, Du F, Shi H, Chen C, Chen ZJ. 2013. Cyclic GMP-AMP is an endogenous second messenger in innate immune signaling by cytosolic DNA. Science 339:826–830.

42. Chen Q, Sun L, Chen ZJ. 2016. Regulation and function of the cGAS-STING pathway of cytosolic DNA sensing. Nat Immunol 17:1142–1149.

43. Burdette DL, Monroe KM, Sotelo-Troha K, Iwig JS, Eckert B, Hyodo M, Hayakawa Y, Vance RE. 2011. STING is a direct innate immune sensor of cyclic di-GMP. Nature 478:515–518.

44. Sauer J-D, Sotelo-Troha K, von Moltke J, Monroe KM, Rae CS, Brubaker SW, Hyodo M, Hayakawa Y, Woodward JJ, Portnoy DA, Vance RE. 2011. The N-ethyl-N-nitrosourea-induced Goldenticket mouse mutant reveals an essential function of Sting in the in vivo interferon response to Listeria monocytogenes and cyclic dinucleotides. Infect Immun 79:688–694.

45. Andrade WA, Firon A, Schmidt T, Hornung V, Fitzgerald KA, Kurt-Jones EA, Trieu-Cuot P, Golenbock DT, Kaminski P-A. 2016. Group B Streptococcus Degrades Cyclic-di-AMP to Modulate STING-Dependent Type I Interferon Production. Cell Host & Microbe 20:49–59.

46. Firon A, Dinis M, Raynal B, Poyart C, Trieu-Cuot P, Kaminski PA. 2014. Extracellular Nucleotide Catabolism by the Group B Streptococcus Ectonucleotidase NudP Increases Bacterial Survival in Blood. J Biol Chem 289:5479–5489.

47. Parvatiyar K, Zhang Z, Teles RM, Ouyang S, Jiang Y, Iyer SS, Zaver SA, Schenk M, Zeng S, Zhong W, Liu Z-J, Modlin RL, Liu Y, Cheng G. 2012. The helicase DDX41 recognizes the bacterial secondary messengers cyclic di-GMP and cyclic di-AMP to activate a type I interferon immune response. Nature Immunology 13:1155–1161.

48. McFarland AP, Luo S, Ahmed-Qadri F, Zuck M, Thayer EF, Goo YA, Hybiske K, Tong L, Woodward JJ. 2017. Sensing of bacterial cyclic dinucleotides by the oxidoreductase RECON promotes NF-κB activation and shapes a proinflammatory antibacterial state. Immunity 46:433–445.

49. McFarland AP, Burke TP, Carletti AA, Glover RC, Tabakh H, Welch MD, Woodward JJ. 2018. RECON-Dependent Inflammation in Hepatocytes Enhances Listeria monocytogenes Cell-to-Cell Spread. MBio 9.

50. Whiteley AT, Eaglesham JB, Mann CC de O, Morehouse BR, Lowey B, Nieminen EA, Danilchanka O, King DS, Lee ASY, Mekalanos JJ, Kranzusch PJ. 2019. Bacterial cGAS-like enzymes synthesize diverse nucleotide signals. Nature 567:194–199.

51. Mills E, Pultz IS, Kulasekara HD, Miller SI. 2011. The bacterial second messenger c-di-GMP: mechanisms of signalling. Cellular Microbiology 13:1122–1129.

52. Schild S, Tamayo R, Nelson EJ, Qadri F, Calderwood SB, Camilli A. 2007. Genes induced late in infection increase fitness of Vibrio cholerae after release into the environment. Cell Host Microbe 2:264–277.

53. Matilla MA, Travieso ML, Ramos JL, Ramos-González MI. 2011. Cyclic diguanylate turnover mediated by the sole GGDEF/EAL response regulator in Pseudomonas putida: its role in the rhizosphere and an analysis of its target processes. Environ Microbiol 13:1745–1766.

54. Bedrunka P, Graumann PL. 2017. Subcellular clustering of a putative c-di-GMP-dependent exopolysaccharide machinery affecting macro colony architecture in Bacillus subtilis. Environmental Microbiology Reports 9:211–222.

55. García B, Latasa C, Solano C, Portillo FG, Gamazo C, Lasa I. 2004. Role of the GGDEF protein family in Salmonella cellulose biosynthesis and biofilm formation. Molecular Microbiology 54:264–277.

56. Krasteva PV, Bernal-Bayard J, Travier L, Martin FA, Kaminski P-A, Karimova G, Fronzes R, Ghigo J-M. 2017. Insights into the structure and assembly of a bacterial cellulose secretion system. Nat Commun 8:2065.

57. Thongsomboon W, Serra DO, Possling A, Hadjineophytou C, Hengge R, Cegelski L. 2018. Phosphoethanolamine cellulose: A naturally produced chemically modified cellulose. Science 359:334–338.

58. Bedrunka P, Graumann PL. 2017. New Functions and Subcellular Localization Patterns of c-di-GMP Components (GGDEF Domain Proteins) in B. subtilis. Front Microbiol 8.

59. Pultz IS, Christen M, Don Kulasekara H, Kennard A, Kulasekara B, Miller SI. 2012. The response threshold of Salmonella PilZ domain proteins is determined by their binding affinities for c-di-GMP. Mol Microbiol 86:1424–1440.

60. Fong JCN, Yildiz FH. 2008. Interplay between cyclic AMP-cyclic AMP receptor protein and cyclic di-GMP signaling in Vibrio cholerae biofilm formation. J Bacteriol 190:6646–6659.

61. Boehm A, Steiner S, Zaehringer F, Casanova A, Hamburger F, Ritz D, Keck W, Ackermann M, Schirmer T, Jenal U. 2009. Second messenger signalling governs Escherichia coli biofilm induction upon ribosomal stress. Molecular Microbiology 72:1500–1516.

62. Corrigan RM, Bowman L, Willis AR, Kaever V, Gründling A. 2015. Cross-talk between Two Nucleotide-signaling Pathways in *Staphylococcus aureus*. J Biol Chem 290:5826–5839.

63. Rao F, See RY, Zhang D, Toh DC, Ji Q, Liang Z-X. 2010. YybT is a signaling protein that contains a cyclic dinucleotide phosphodiesterase domain and a GGDEF domain with ATPase activity. J Biol Chem 285:473–482.

64. Ryjenkov DA, Tarutina M, Moskvin OV, Gomelsky M. 2005. Cyclic Diguanylate Is a Ubiquitous Signaling Molecule in Bacteria: Insights into Biochemistry of the GGDEF Protein Domain. J Bacteriol 187:1792–1798.

65. Ausmees N, Mayer R, Weinhouse H, Volman G, Amikam D, Benziman M, Lindberg M. 2001. Genetic data indicate that proteins containing the GGDEF domain possess diguanylate cyclase activity. FEMS Microbiology Letters 204:163–167.

66. Paul R, Weiser S, Amiot NC, Chan C, Schirmer T, Giese B, Jenal U. 2004. Cell cycle-dependent dynamic localization of a bacterial response regulator with a novel di-guanylate cyclase output domain. Genes Dev 18:715–727.

67. Hickman JW, Tifrea DF, Harwood CS. 2005. A chemosensory system that regulates biofilm formation through modulation of cyclic diguanylate levels. PNAS 102:14422–14427.

68. Malone JG, Williams R, Christen M, Jenal U, Spiers AJ, Rainey PB. 2007. The structure–function relationship of WspR, a Pseudomonas fluorescens response regulator with a GGDEF output domain. Microbiology 153:980–994.

69. Chou S-H, Galperin MY. 2015. Diversity of Cyclic Di-GMP-Binding Proteins and Mechanisms. J Bacteriol 198:32–46.

70. Tal R, Wong HC, Calhoon R, Gelfand D, Fear AL, Volman G, Mayer R, Ross P, Amikam D, Weinhouse H, Cohen A, Sapir S, Ohana P, Benziman M. 1998. Three cdg Operons Control Cellular Turnover of Cyclic Di-GMP in Acetobacter xylinum: Genetic Organization and Occurrence of Conserved Domains in Isoenzymes. J Bacteriol 180:4416–4425.

71. Tischler AD, Camilli A. 2004. Cyclic diguanylate (c-di-GMP) regulates Vibrio cholerae biofilm formation. Mol Microbiol 53:857–869.

72. Tamayo R, Tischler AD, Camilli A. 2005. The EAL Domain Protein VieA Is a Cyclic Diguanylate Phosphodiesterase. J Biol Chem 280:33324–33330.

73. Galperin MY, Natale DA, Aravind L, Koonin EV. 1999. A specialized version of the HD hydrolase domain implicated in signal transduction. Journal of molecular microbiology and biotechnology 1:303–305.

74. Miner KD, Kurtz DM. 2016. Active Site Metal Occupancy and Cyclic Di-GMP Phosphodiesterase Activity of Thermotoga maritima HD-GYP. Biochemistry 55:970–979.

75. Taylor BL, Zhulin IB. 1999. PAS domains: internal sensors of oxygen, redox potential, and light. Microbiol Mol Biol Rev 63:479–506.

76. Hurley JH. 2003. GAF domains: cyclic nucleotides come full circle. Sci STKE 2003:PE1.

77. Gomelsky M, Klug G. 2002. BLUF: a novel FAD-binding domain involved in sensory transduction in microorganisms. Trends Biochem Sci 27:497–500.

78. Tschowri N, Busse S, Hengge R. 2009. The BLUF-EAL protein YcgF acts as a direct anti-repressor in a blue-light response of Escherichia coli. Genes Dev 23:522–534.

79. Galperin MY, Nikolskaya AN, Koonin EV. 2001. Novel domains of the prokaryotic two-component signal transduction systems. FEMS Microbiology Letters 203:11–21.

80. Schmidt AJ, Ryjenkov DA, Gomelsky M. 2005. The Ubiquitous Protein Domain EAL Is a Cyclic Diguanylate-Specific Phosphodiesterase: Enzymatically Active and Inactive EAL Domains. J Bacteriol 187:4774–4781.

81. Christen M, Christen B, Folcher M, Schauerte A, Jenal U. 2005. Identification and Characterization of a Cyclic di-GMP-specific Phosphodiesterase and Its Allosteric Control by GTP. J Biol Chem 280:30829–30837.

82. Amikam D, Galperin MY. 2006. PilZ domain is part of the bacterial c-di-GMP binding protein. Bioinformatics 22:3–6.

83. Benach J, Swaminathan SS, Tamayo R, Handelman SK, Folta-Stogniew E, Ramos JE, Forouhar F, Neely H, Seetharaman J, Camilli A, Hunt JF. 2007. The structural basis of cyclic diguanylate signal transduction by PilZ domains. EMBO J 26:5153–5166.

84. Ryjenkov DA, Simm R, Römling U, Gomelsky M. 2006. The PilZ Domain Is a Receptor for the Second Messenger c-di-GMP THE PilZ DOMAIN PROTEIN YcgR CONTROLS MOTILITY IN ENTEROBACTERIA. J Biol Chem 281:30310–30314.

85. Christen M, Christen B, Allan MG, Folcher M, Jenö P, Grzesiek S, Jenal U. 2007. DgrA is a member of a new family of cyclic diguanosine monophosphate receptors and controls flagellar motor function in Caulobacter crescentus. Proc Natl Acad Sci U S A 104:4112–4117.

86. Pratt JT, Tamayo R, Tischler AD, Camilli A. 2007. PilZ Domain Proteins Bind Cyclic Diguanylate and Regulate Diverse Processes in Vibrio cholerae. J Biol Chem 282:12860–12870.

87. Simm R, Morr M, Kader A, Nimtz M, Römling U. 2004. GGDEF and EAL domains inversely regulate cyclic di-GMP levels and transition from sessility to motility: Cyclic di-GMP turnover by GGDEF and EAL domains. Molecular Microbiology 53:1123–1134.

88. Kazmierczak BI, Lebron MB, Murray TS. 2006. Analysis of FimX, a phosphodiesterase that governs twitching motility in Pseudomonas aeruginosa. Mol Microbiol 60:1026–1043.

89. Newell PD, Monds RD, O'Toole GA. 2009. LapD is a bis-(3′,5′)-cyclic dimeric GMP-binding protein that regulates surface attachment by Pseudomonas fluorescens Pf0–1. PNAS 106:3461–3466.

90. Petters T, Zhang X, Nesper J, Treuner-Lange A, Gomez-Santos N, Hoppert M, Jenal U, Søgaard-Andersen L. 2012. The orphan histidine protein kinase SgmT is a c-di-GMP receptor and regulates composition of the extracellular matrix together with the orphan DNA binding response regulator DigR in Myxococcus xanthus. Mol Microbiol 84:147–165.

91. Duerig A, Abel S, Folcher M, Nicollier M, Schwede T, Amiot N, Giese B, Jenal U. 2009. Second messenger-mediated spatiotemporal control of protein degradation regulates bacterial cell cycle progression. Genes Dev 23:93–104.

92. Lee VT, Matewish JM, Kessler JL, Hyodo M, Hayakawa Y, Lory S. 2007. A cyclic-di-GMP receptor required for bacterial exopolysaccharide production. Mol Microbiol 65:1474–1484.

93. Chan C, Paul R, Samoray D, Amiot NC, Giese B, Jenal U, Schirmer T. 2004. Structural basis of activity and allosteric control of diguanylate cyclase. Proc Natl Acad Sci U S A 101:17084–17089.

94. Christen B, Christen M, Paul R, Schmid F, Folcher M, Jenoe P, Meuwly M, Jenal U. 2006. Allosteric Control of Cyclic di-GMP Signaling. J Biol Chem 281:32015–32024.

95. Gomelsky M. 2010. The Core Pathway: Diguanylate Cyclases, Cyclic Di-GMP-Specific Phosphodiesterases, and Cyclic Di-GMP-Binding Proteins. The Second Messenger Cyclic Di-GMP 37–56.

96. Hickman JW, Harwood CS. 2008. Identification of FleQ from Pseudomonas aeruginosa as a c-di-GMP-responsive transcription factor. Mol Microbiol 69:376–389.

97. Krasteva PV, Fong JCN, Shikuma NJ, Beyhan S, Navarro MVAS, Yildiz FH, Sondermann H. 2010. Vibrio cholerae VpsT Regulates Matrix Production and Motility by Directly Sensing Cyclic di-GMP. Science 327:866–868.

98. Li W, He Z-G. 2012. LtmA, a novel cyclic di-GMP-responsive activator, broadly regulates the expression of lipid transport and metabolism genes in Mycobacterium smegmatis. Nucleic Acids Res 40:11292–11307.

99. Tao F, He Y-W, Wu D-H, Swarup S, Zhang L-H. 2010. The Cyclic Nucleotide Monophosphate Domain of Xanthomonas campestris Global Regulator Clp Defines a New Class of Cyclic Di-GMP Effectors. Journal of Bacteriology 192:1020–1029.

100. Srivastava D, Hsieh M-L, Khataokar A, Neiditch MB, Waters CM. 2013. Cyclic di-GMP inhibits Vibrio cholerae motility by repressing induction of transcription and inducing extracellular polysaccharide production. Mol Microbiol 90:1262–1276.

101. Srivastava D, Harris RC, Waters CM. 2011. Integration of cyclic di-GMP and quorum sensing in the control of vpsT and aphA in Vibrio cholerae. J Bacteriol 193:6331–6341.

102. Roelofs KG, Jones CJ, Helman SR, Shang X, Orr MW, Goodson JR, Galperin MY, Yildiz FH, Lee VT. 2015. Systematic Identification of Cyclic-di-GMP Binding Proteins in Vibrio cholerae Reveals a Novel Class of Cyclic-di-GMP-Binding ATPases Associated with Type II Secretion Systems. PLoS Pathog 11.

103. Winkler WC, Breaker RR. 2005. Regulation of Bacterial Gene Expression by Riboswitches. Annual Review of Microbiology 59:487–517.

104. Sudarsan N, Lee ER, Weinberg Z, Moy RH, Kim JN, Link KH, Breaker RR. 2008. Riboswitches in Eubacteria Sense the Second Messenger Cyclic Di-GMP. Science 321:411–413.

105. Lee ER, Baker JL, Weinberg Z, Sudarsan N, Breaker RR. 2010. An Allosteric Self-Splicing Ribozyme Triggered by a Bacterial Second Messenger. Science 329:845–848.

106. Lee ER, Sudarsan N, Breaker RR. 2010. Riboswitches That Sense Cyclic Di-GMP. The Second Messenger Cyclic Di-GMP 215–229.

107. Bordeleau E, Burrus V. 2015. Cyclic-di-GMP signaling in the Gram-positive pathogen Clostridium difficile. Curr Genet 61:497–502.

108. Kellenberger CA, Wilson SC, Hickey SF, Gonzalez TL, Su Y, Hallberg ZF, Brewer TF, Iavarone AT, Carlson HK, Hsieh Y-F, Hammond MC. 2015. GEMM-I riboswitches from *Geobacter* sense the bacterial second messenger cyclic AMP-GMP. Proc Natl Acad Sci USA 112:5383–5388.

109. Winkler WC. 2005. Riboswitches and the role of noncoding RNAs in bacterial metabolic control. Current Opinion in Chemical Biology 9:594–602.

110. Pursley BR, Fernandez NL, Severin GB, Waters CM. 2019. The Vc2 Cyclic di-GMP-Dependent Riboswitch of Vibrio cholerae Regulates Expression of an Upstream Putative Small RNA by Controlling RNA Stability. Journal of Bacteriology 201:e00293-19.

111. Pursley BR, Maiden MM, Hsieh M-L, Fernandez NL, Severin GB, Waters CM. 2018. Cyclic di-GMP Regulates TfoY in *Vibrio cholerae* To Control Motility by both Transcriptional and Posttranscriptional Mechanisms. J Bacteriol 200:e00578-17, /jb/200/7/e00578-17.atom.

112. Ramesh A. 2015. Second messenger – Sensing riboswitches in bacteria. Seminars in Cell & Developmental Biology 47–48:3–8.

113. Orr MW, Donaldson GP, Severin GB, Wang J, Sintim HO, Waters CM, Lee VT. 2015. Oligoribonuclease is the primary degradative enzyme for pGpG in Pseudomonas aeruginosa that is required for cyclic-di-GMP turnover. Proc Natl Acad Sci USA 112:E5048-5057.

114. Stevens A, Niyogi SK. 1967. Hydrolysis of oligoribonucleotides by an enzyme fraction from Escherichia coli. Biochemical and Biophysical Research Communications 29:550–555.

115. Niyogi SK, Datta AK. 1975. A novel oligoribonuclease of Escherichia coli. I. Isolation and properties. Journal of Biological Chemistry 250:7307–7312.

116. Datta AK, Niyogi K. 1975. A novel oligoribonuclease of Escherichia coli. II. Mechanism of action. Journal of Biological Chemistry 250:7313–7319.

117. Yu D, Deutscher MP. 1995. Oligoribonuclease is distinct from the other known exoribonucleases of Escherichia coli. J Bacteriol 177:4137–4139.

118. Cohen D, Mechold U, Nevenzal H, Yarmiyhu Y, Randall TE, Bay DC, Rich JD, Parsek MR, Kaever V, Harrison JJ, Banin E. 2015. Oligoribonuclease is a central feature of cyclic diguanylate signaling in Pseudomonas aeruginosa. PNAS 112:11359–11364.

119. Ghosh S, Deutscher MP. 1999. Oligoribonuclease is an essential component of the mRNA decay pathway. PNAS 96:4372–4377.

120. Mechold U, Fang G, Ngo S, Ogryzko V, Danchin A. 2007. YtqI from Bacillus subtilis has both oligoribonuclease and pAp-phosphatase activity. Nucleic Acids Res 35:4552–4561.

121. Fang M, Zeisberg W-M, Condon C, Ogryzko V, Danchin A, Mechold U. 2009. Degradation of nanoRNA is performed by multiple redundant RNases in Bacillus subtilis. Nucleic Acids Res 37:5114–5125.

122. Liu MF, Cescau S, Mechold U, Wang J, Cohen D, Danchin A, Boulouis H-J, Biville F. 2012. Identification of a novel nanoRNase in Bartonella. Microbiology, 158:886–895.

123. Orr MW, Weiss CA, Severin GB, Turdiev H, Kim S-K, Turdiev A, Liu K, Tu BP, Waters CM, Winkler WC, Lee VT. 2018. A Subset of Exoribonucleases Serve as Degradative Enzymes for pGpG in c-di-GMP Signaling. Journal of Bacteriology 200.

124. Commichau FM, Heidemann JL, Ficner R, Stülke J. 2019. Making and Breaking of an Essential Poison: the Cyclases and Phosphodiesterases That Produce and Degrade the Essential Second Messenger Cyclic di-AMP in Bacteria. Journal of Bacteriology 201:e00462-18.

125. Drews G. 2000. The roots of microbiology and the influence of Ferdinand Cohn on microbiology of the 19th century. FEMS Microbiol Rev 24:225–249.

126. Aguilar C, Vlamakis H, Losick R, Kolter R. 2007. Thinking about Bacillus subtilis as a multicellular organism. Current Opinion in Microbiology 10:638–643.

127. Piggot PJ, Hilbert DW. 2004. Sporulation of Bacillus subtilis. Current Opinion in Microbiology 7:579–586.

128. Errington J. 2003. Regulation of endospore formation in Bacillus subtilis. Nature Reviews Microbiology 1:117.

129. Kearns DB, Losick R. 2005. Cell population heterogeneity during growth of Bacillus subtilis. Genes Dev 19:3083–3094.

130. Kearns DB. 2010. A field guide to bacterial swarming motility. Nat Rev Microbiol 8:634–644.

131. Kearns DB, Losick R. 2003. Swarming motility in undomesticated Bacillus subtilis. Molecular Microbiology 49:581–590.

132. Leisner M, Stingl K, Frey E, Maier B. 2008. Stochastic switching to competence. Current Opinion in Microbiology 11:553–559.

133. Chen I, Christie PJ, Dubnau D. 2005. The Ins and Outs of DNA Transfer in Bacteria. Science 310:1456–1460.

134. Dubnau D, Losick R. 2006. Bistability in bacteria. Molecular Microbiology 61:564–572.

135. Vlamakis H, Aguilar C, Losick R, Kolter R. 2008. Control of cell fate by the formation of an architecturally complex bacterial community. Genes & Development 22:945–953.

136. Claessen D, Rozen DE, Kuipers OP, Søgaard-Andersen L, van Wezel GP. 2014. Bacterial solutions to multicellularity: a tale of biofilms, filaments and fruiting bodies. Nature Reviews Microbiology 12:115–124.

137. Gestel J van, Vlamakis H, Kolter R. 2015. From Cell Differentiation to Cell Collectives: Bacillus subtilis Uses Division of Labor to Migrate. PLOS Biology 13:e1002141.

138. Veening J-W, Smits WK, Kuipers OP. 2008. Bistability, Epigenetics, and Bet-Hedging in Bacteria. Annu Rev Microbiol 62:193–210.

139. Dragoš A, Kiesewalter H, Martin M, Hsu C-Y, Hartmann R, Wechsler T, Eriksen C, Brix S, Drescher K, Stanley-Wall N, Kümmerli R, Kovács ÁT. 2018. Division of labor during biofilm matrix production. Curr Biol 28:1903-1913.e5.

140. Lopez D, Vlamakis H, Kolter R. 2009. Generation of multiple cell types in Bacillus subtilis. FEMS Microbiology Reviews 33:152–163.

141. Vlamakis H, Chai Y, Beauregard P, Losick R, Kolter R. 2013. Sticking together: building a biofilm the Bacillus subtilis way. Nature Reviews Microbiology 11:157–168.

142. Roux D, Cywes-Bentley C, Zhang Y-F, Pons S, Konkol M, Kearns DB, Little DJ, Howell PL, Skurnik D, Pier GB. 2015. Identification of Poly-N-acetylglucosamine as a Major Polysaccharide Component of the Bacillus subtilis Biofilm Matrix. J Biol Chem 290:19261–19272.

143. Romero D, Aguilar C, Losick R, Kolter R. 2010. Amyloid fibers provide structural integrity to Bacillus subtilis biofilms. PNAS 107:2230–2234.

144. Branda SS, Chu F, Kearns DB, Losick R, Kolter R. 2006. A major protein component of the Bacillus subtilis biofilm matrix. Molecular Microbiology 59:1229–1238.

145. Hobley L, Ostrowski A, Rao FV, Bromley KM, Porter M, Prescott AR, MacPhee CE, Aalten DMF van, Stanley-Wall NR. 2013. BslA is a self-assembling bacterial hydrophobin that coats the Bacillus subtilis biofilm. PNAS 110:13600–13605.

146. Kobayashi K, Iwano M. 2012. BslA(YuaB) forms a hydrophobic layer on the surface of Bacillus subtilis biofilms. Molecular Microbiology 85:51–66.

147. Cairns LS, Hobley L, Stanley-Wall NR. 2014. Biofilm formation by Bacillus subtilis: new insights into regulatory strategies and assembly mechanisms. Mol Microbiol 93:587–598.

148. Ghelardi E, Salvetti S, Ceragioli M, Gueye SA, Celandroni F, Senesi S. 2012. Contribution of Surfactin and SwrA to Flagellin Expression, Swimming, and Surface Motility in Bacillus subtilis. Appl Environ Microbiol 78:6540–6544.

149. Nakano MM, Magnuson R, Myers A, Curry J, Grossman AD, Zuber P. 1991. srfA is an operon required for surfactin production, competence development, and efficient sporulation in Bacillus subtilis. J Bacteriol 173:1770–1778.

150. Lopez D, Vlamakis H, Losick R, Kolter R. 2009. Paracrine signaling in a bacterium. Genes & Development 23:1631–1638.

151. Davidson FA, Seon-Yi C, Stanley-Wall NR. 2012. Selective Heterogeneity in Exoprotease Production by Bacillus subtilis. PLOS ONE 7:e38574.

152. Marlow VL, Cianfanelli FR, Porter M, Cairns LS, Dale JK, Stanley-Wall NR. 2014. The prevalence and origin of exoprotease-producing cells in the Bacillus subtilis biofilm. Microbiology (Reading, Engl) 160:56–66.

153. Hall-Stoodley L, Costerton JW, Stoodley P. 2004. Bacterial biofilms: from the Natural environment to infectious diseases. Nature Reviews Microbiology 2:95–108.

154. Flemming H-C, Wingender J, Szewzyk U, Steinberg P, Rice SA, Kjelleberg S. 2016. Biofilms: an emergent form of bacterial life. Nature Reviews Microbiology 14:563–575.

155. Branda SS, González-Pastor JE, Ben-Yehuda S, Losick R, Kolter R. 2001. Fruiting body formation by Bacillus subtilis. Proceedings of the National Academy of Sciences 98:11621–11626.

156. Marlow VL, Porter M, Hobley L, Kiley TB, Swedlow JR, Davidson FA, Stanley-Wall NR. 2014. Phosphorylated DegU Manipulates Cell Fate Differentiation in the Bacillus subtilis Biofilm. J Bacteriol 196:16–27.

157. Chai Y, Chu F, Kolter R, Losick R. 2008. Bistability and biofilm formation in Bacillus subtilis. Molecular Microbiology 67:254–263.

158. Blair KM, Turner L, Winkelman JT, Berg HC, Kearns DB. 2008. A molecular clutch disables flagella in the Bacillus subtilis biofilm. Science 320:1636–1638.

159. Kearns DB, Chu F, Branda SS, Kolter R, Losick R. 2005. A master regulator for biofilm formation by Bacillus subtilis. Molecular Microbiology 55:739–749.

160. Purcell EB, Tamayo R. 2016. Cyclic diguanylate signaling in Gram-positive bacteria. FEMS Microbiol Rev 40:753–773.

161. Gao X, Mukherjee S, Matthews PM, Hammad LA, Kearns DB, Dann CE. 2013. Functional Characterization of Core Components of the Bacillus subtilis Cyclic-Di-GMP Signaling Pathway. Journal of Bacteriology 195:4782–4792.

162. Chen Y, Chai Y, Guo J -h., Losick R. 2012. Evidence for Cyclic Di-GMP-Mediated Signaling in Bacillus subtilis. Journal of Bacteriology 194:5080–5090.

163. Minasov G, Padavattan S, Shuvalova L, Brunzelle JS, Miller DJ, Baslé A, Massa C, Collart FR, Schirmer T, Anderson WF. 2009. Crystal Structures of YkuI and Its Complex with Second Messenger Cyclic Di-GMP Suggest Catalytic Mechanism of Phosphodiester Bond Cleavage by EAL Domains. J Biol Chem 284:13174–13184.

164. Fang X, Gomelsky M. 2010. A post-translational, c-di-GMP-dependent mechanism regulating flagellar motility. Molecular Microbiology 76:1295–1305.

165. Wolfe AJ, Visick KL. 2008. Get the Message Out: Cyclic-Di-GMP Regulates Multiple Levels of Flagellum-Based Motility. Journal of Bacteriology 190:463–475.

166. Boehm A, Kaiser M, Li H, Spangler C, Kasper CA, Ackermann M, Kaever V, Sourjik V, Roth V, Jenal U. 2010. Second Messenger-Mediated Adjustment of Bacterial Swimming Velocity. Cell 141:107–116.

167. Paul K, Nieto V, Carlquist WC, Blair DF, Harshey RM. 2010. The c-di-GMP Binding Protein YcgR Controls Flagellar Motor Direction and Speed to Affect Chemotaxis by a "Backstop Brake" Mechanism. Mol Cell 38:128–139.

168. Subramanian S, Gao X, Dann CE, Kearns DB. 2017. MotI (DgrA) acts as a molecular clutch on the flagellar stator protein MotA in Bacillus subtilis. PNAS 114:13537–13542.

169. Ko J, Ryu K-S, Kim H, Shin J-S, Lee J-O, Cheong C, Choi B-S. 2010. Structure of PP4397 reveals the molecular basis for different c-di-GMP binding modes by Pilz domain proteins. J Mol Biol 398:97–110.

170. Whitney JC, Whitfield GB, Marmont LS, Yip P, Neculai AM, Lobsanov YD, Robinson H, Ohman DE, Howell PL. 2015. Dimeric c-di-GMP is required for post-translational regulation of alginate production in Pseudomonas aeruginosa. J Biol Chem 290:12451–12462.

171. Karimova G, Pidoux J, Ullmann A, Ladant D. 1998. A bacterial two-hybrid system based on a reconstituted signal transduction pathway. PNAS 95:5752–5756.

172. Liang Z-X. 2015. The expanding roles of c-di-GMP in the biosynthesis of exopolysaccharides and secondary metabolites. Natural Product Reports 32:663–683.

173. Steiner S, Lori C, Boehm A, Jenal U. 2013. Allosteric activation of exopolysaccharide synthesis through cyclic di-GMP-stimulated protein–protein interaction. The EMBO Journal 32:354–368.

174. Chen L-H, Köseoğlu VK, Güvener ZT, Myers-Morales T, Reed JM, D'Orazio SEF, Miller KW, Gomelsky M. 2014. Cyclic di-GMP-dependent Signaling Pathways in the Pathogenic Firmicute Listeria monocytogenes. PLoS Pathog 10.

175. Köseoğlu VK, Heiss C, Azadi P, Topchiy E, Güvener ZT, Lehmann TE, Miller KW, Gomelsky M. 2015. Listeria monocytogenes exopolysaccharide: origin, structure, biosynthetic machinery and c-di-GMP-dependent regulation. Molecular Microbiology 96:728–743.

176. Jones CJ, Wozniak DJ. 2017. Congo Red Stain Identifies Matrix Overproduction and Is an Indirect Measurement for c-di-GMP in Many Species of Bacteria. Methods Mol Biol 1657:147–156.

177. Cimdins A, Simm R, Li F, Lüthje P, Thorell K, Sjöling Å, Brauner A, Römling U. 2017. Alterations of c-di-GMP turnover proteins modulate semi-constitutive rdar biofilm formation in commensal and uropathogenic Escherichia coli. Microbiologyopen 6.

178. Straight PD, Fischbach MA, Walsh CT, Rudner DZ, Kolter R. 2007. A singular enzymatic megacomplex from Bacillus subtilis. PNAS 104:305–310.

179. Nicolas P, Mäder U, Dervyn E, Rochat T, Leduc A, Pigeonneau N, Bidnenko E, Marchadier E, Hoebeke M, Aymerich S, Becher D, Bisicchia P, Botella E, Delumeau O, Doherty G, Denham EL, Fogg MJ, Fromion V, Goelzer A, Hansen A, Härtig E, Harwood CR, Homuth G, Jarmer H, Jules M, Klipp E, Chat LL, Lecointe F, Lewis P, Liebermeister W, March A, Mars RAT, Nannapaneni P, Noone D, Pohl S, Rinn B, Rügheimer F, Sappa PK, Samson F, Schaffer M, Schwikowski B, Steil L, Stülke J, Wiegert T, Devine KM, Wilkinson AJ, Dijl JM van, Hecker M, Völker U, Bessières P, Noirot P. 2012. Condition-Dependent Transcriptome Reveals High-Level Regulatory Architecture in Bacillus subtilis. Science 335:1103–1106.

180. Chandrangsu P, Helmann JD. 2016. Intracellular Zn(II) Intoxication Leads to Dysregulation of the PerR Regulon Resulting in Heme Toxicity in Bacillus subtilis. PLOS Genetics 12:e1006515.

181. Fagerlund A, Smith V, Røhr ÅK, Lindbäck T, Parmer MP, Andersson KK, Reubsaet L, Økstad OA. 2016. Cyclic diguanylate regulation of Bacillus cereus group biofilm formation. Molecular Microbiology 101:471–494.

182. Hengge R. 2009. Principles of c-di-GMP signalling in bacteria. Nat Rev Micro 7:263–273.

183. Serganov A, Nudler E. 2013. A Decade of Riboswitches. Cell 152:17–24.

184. DebRoy S, Gebbie M, Ramesh A, Goodson JR, Cruz MR, Hoof A van, Winkler WC, Garsin DA. 2014. A riboswitch-containing sRNA controls gene expression by sequestration of a response regulator. Science 345:937–940.

185. Collins JA, Irnov I, Baker S, Winkler WC. 2007. Mechanism of mRNA destabilization by the glmS ribozyme. Genes Dev 21:3356–3368.

186. Kellenberger CA, Hammond MC. 2015. In Vitro Analysis of Riboswitch–Spinach Aptamer Fusions as Metabolite-Sensing Fluorescent Biosensors, p. 147–172. *In* Methods in Enzymology. Elsevier.

187. Kellenberger CA, Sales-Lee J, Pan Y, Gassaway MM, Herr AE, Hammond MC. 2015. A minimalist biosensor: Quantitation of cyclic di-GMP using the conformational change of a riboswitch aptamer. RNA Biology 12:1189–1197.

188. Paige JS, Wu KY, Jaffrey SR. 2011. RNA Mimics of Green Fluorescent Protein. Science 333:642–646.

189. You M, Jaffrey SR. 2015. Structure and Mechanism of RNA Mimics of Green Fluorescent Protein. Annu Rev Biophys 44:187–206.

190. You M, Litke JL, Jaffrey SR. 2015. Imaging metabolite dynamics in living cells using a Spinach-based riboswitch. Proc Natl Acad Sci USA 112:E2756-2765.

191. Zhang J, Fei J, Leslie BJ, Han KY, Kuhlman TE, Ha T. 2015. Tandem Spinach Array for mRNA Imaging in Living Bacterial Cells. Sci Rep 5.

192. Ponchon L, Dardel F. 2007. Recombinant RNA technology: the tRNA scaffold. Nat Meth 4:571–576.

193. Christen M, Kulasekara HD, Christen B, Kulasekara BR, Hoffman LR, Miller SI. 2010. Asymmetrical Distribution of the Second Messenger c-di-GMP upon Bacterial Cell Division. Science 328:1295–1297.

194. Kulasekara BR, Kamischke C, Kulasekara HD, Christen M, Wiggins PA, Miller SI. 2013. c-di-GMP heterogeneity is generated by the chemotaxis machinery to regulate flagellar motility. eLife 2.

195. Abel S, Bucher T, Nicollier M, Hug I, Kaever V, Abel zur Wiesch P, Jenal U. 2013. Bi-modal Distribution of the Second Messenger c-di-GMP Controls Cell Fate and Asymmetry during the Caulobacter Cell Cycle. PLoS Genet 9.

196. Süel GM, Kulkarni RP, Dworkin J, Garcia-Ojalvo J, Elowitz MB. 2007. Tunability and Noise Dependence in Differentiation Dynamics. Science 315:1716–1719.

197. Campo N, Rudner DZ. 2007. SpoIVB and CtpB Are Both Forespore Signals in the Activation of the Sporulation Transcription Factor K in Bacillus subtilis. Journal of Bacteriology 189:6021–6027.

198. Grangemard I, Wallach J, Maget-Dana R, Peypoux F. 2001. Lichenysin. Appl Biochem Biotechnol 90:199–210.

199. Sen R. 2010. Surfactin: biosynthesis, genetics and potential applications. Adv Exp Med Biol 672:316–323.

200. Veith B, Herzberg C, Steckel S, Feesche J, Maurer KH, Ehrenreich P, Bäumer S, Henne A, Liesegang H, Merkl R, Ehrenreich A, Gottschalk G. 2004. The Complete Genome Sequence of Bacillus licheniformis DSM13, an Organism with Great Industrial Potential. MMB 7:204–211.

201. Wickiser JK. 2009. Kinetics of Riboswitch Regulation Studied By In Vitro Transcription, p. 53–63. *In* Serganov, A (ed.), Riboswitches. Humana Press, Totowa, NJ.

202. Wickiser JK, Winkler WC, Breaker RR, Crothers DM. 2005. The speed of RNA transcription and metabolite binding kinetics operate an FMN riboswitch. Mol Cell 18:49–60.

203. Smith KD, Lipchock SV, Strobel SA. 2012. Structural and biochemical characterization of linear dinucleotide analogues bound to the c-di-GMP-I aptamer. Biochemistry 51:425–432.

204. Molle V, Fujita M, Jensen ST, Eichenberger P, González-Pastor JE, Liu JS, Losick R. 2003. The Spo0A regulon of Bacillus subtilis. Molecular Microbiology 50:1683–1701.

205. D'Souza C, Nakano MM, Zuber P. 1994. Identification of comS, a gene of the srfA operon that regulates the establishment of genetic competence in Bacillus subtilis. Proc Natl Acad Sci U S A 91:9397–9401.

206. Nakano MM, Zuber P. 1989. Cloning and characterization of srfB, a regulatory gene involved in surfactin production and competence in Bacillus subtilis. J Bacteriol 171:5347–5353.

207. Hamoen LW, Venema G, Kuipers OP. 2003. Controlling competence in Bacillus subtilis: shared use of regulators. Microbiology 149:9–17.

208. Dubnau D. 1991. Genetic competence in Bacillus subtilis. Microbiology and Molecular Biology Reviews 55:395–424.

209. Yakimov MM, Golyshin PN. 1997. ComA-Dependent Transcriptional Activation of Lichenysin A Synthetase Promoter in Bacillus subtilis cells. Biotechnology Progress 13:757–761.

210. Jakobs M, Hoffmann K, Liesegang H, Volland S, Meinhardt F. 2015. The two putative comS homologs of the biotechnologically important Bacillus licheniformis do not contribute to competence development. Appl Microbiol Biotechnol 99:2255–2266.

211. Dann CE, Wakeman CA, Sieling CL, Baker SC, Irnov I, Winkler WC. 2007. Structure and Mechanism of a Metal-Sensing Regulatory RNA. Cell 130:878–892.

212. Gibson DG, Young L, Chuang R-Y, Venter JC, Hutchison Iii CA, Smith HO. 2009. Enzymatic assembly of DNA molecules up to several hundred kilobases. Nature Methods 6:343–345.

213. Veening J-W, Smits WK, Hamoen LW, Kuipers OP. 2006. Single cell analysis of gene expression patterns of competence development and initiation of sporulation in Bacillus subtilis grown on chemically defined media. Journal of Applied Microbiology 101:531–541.

214. Smits WK, Eschevins CC, Susanna KA, Bron S, Kuipers OP, Hamoen LW. 2005. Stripping Bacillus: ComK auto-stimulation is responsible for the bistable response in competence development. Molecular Microbiology 56:604–614.

215. Koo B-M, Kritikos G, Farelli JD, Todor H, Tong K, Kimsey H, Wapinski I, Galardini M, Cabal A, Peters JM, Hachmann A-B, Rudner DZ, Allen KN, Typas A, Gross CA. 2017. Construction and Analysis of Two Genome-scale Deletion Libraries for Bacillus subtilis. Cell Syst 4:291-305.e7.

216. Jarmer H, Berka R, Knudsen S, Saxild HH. 2002. Transcriptome analysis documents induced competence of Bacillus subtilis during nitrogen limiting conditions. FEMS Microbiol Lett 206:197–200.

217. Paintdakhi A, Parry B, Campos M, Irnov I, Elf J, Surovtsev I, Jacobs-Wagner C. 2016. Oufti: an integrated software package for high-accuracy, high-throughput quantitative microscopy analysis. Molecular microbiology 99:767–777.

218. Schindelin J, Arganda-Carreras I, Frise E, Kaynig V, Longair M, Pietzsch T, Preibisch S, Rueden C, Saalfeld S, Schmid B, Tinevez J-Y, White DJ, Hartenstein V, Eliceiri K, Tomancak P, Cardona A. 2012. Fiji - an Open Source platform for biological image analysis. Nat Methods 9.

219. Liu K, Myers AR, Pisithkul T, Claas KR, Satyshur KA, Amador-Noguez D, Keck JL, Wang JD. 2015. Molecular mechanism and evolution of guanylate kinase regulation by (p)ppGpp. Mol Cell 57:735–749.

220. Tu BP, Mohler RE, Liu JC, Dombek KM, Young ET, Synovec RE, McKnight SL. 2007. Cyclic changes in metabolic state during the life of a yeast cell. PNAS 104:16886–16891.

221. Stelitano V, Giardina G, Paiardini A, Castiglione N, Cutruzzolà F, Rinaldo S. 2013. C-di-GMP Hydrolysis by Pseudomonas aeruginosa HD-GYP Phosphodiesterases: Analysis of the Reaction Mechanism and Novel Roles for pGpG. PLoS One 8.

222. Niyogi SK, Stevens A. 1965. Studies of the Ribonucleic Acid Polymerase from Escherichia coli IV. EFFECT OF OLIGONUCLEOTIDES ON THE

RIBONUCLEIC ACID POLYMERASE REACTION WITH SYNTHETIC POLYRIBONUCLEOTIDES AS TEMPLATES. J Biol Chem 240:2593–2598.

223. Hurwitz J. 2005. The Discovery of RNA Polymerase. J Biol Chem 280:42477–42485.

224. Mechold U, Ogryzko V, Ngo S, Danchin A. 2006. Oligoribonuclease is a common downstream target of lithium-induced pAp accumulation in Escherichia coli and human cells. Nucleic Acids Res 34:2364–2373.

225. Kwok CK, Merrick CJ. 2017. G-Quadruplexes: Prediction, Characterization, and Biological Application. Trends Biotechnol 35:997–1013.

226. Roelofs KG, Wang J, Sintim HO, Lee VT. 2011. Differential radial capillary action of ligand assay for high-throughput detection of protein-metabolite interactions. Proc Natl Acad Sci U S A 108:15528–15533.

227. Kamp HD, Patimalla-Dipali B, Lazinski DW, Wallace-Gadsden F, Camilli A. 2013. Gene Fitness Landscapes of Vibrio cholerae at Important Stages of Its Life Cycle. PLOS Pathogens 9:e1003800.

228. Bruni F, Gramegna P, Oliveira JMA, Lightowlers RN, Chrzanowska-Lightowlers ZMA. 2013. REXO2 Is an Oligoribonuclease Active in Human Mitochondria. PLOS ONE 8:e64670.

229. Hsiao Y-Y, Duh Y, Chen Y-P, Wang Y-T, Yuan HS. 2012. How an exonuclease decides where to stop in trimming of nucleic acids: crystal structures of RNase T–product complexes. Nucleic Acids Res 40:8144–8154.

230. Korada SKC, Johns TD, Smith CE, Jones ND, McCabe KA, Bell CE. 2013. Crystal structures of Escherichia coli exonuclease I in complex with single-stranded DNA provide insights into the mechanism of processive digestion. Nucleic Acids Res 41:5887–5897.

231. Hsiao Y-Y, Yang C-C, Lin CL, Lin JLJ, Duh Y, Yuan HS. 2011. Structural basis for RNA trimming by RNase T in stable RNA 3′-end maturation. Nat Chem Biol 7:236–243.

232. Hui MP, Foley PL, Belasco JG. 2014. Messenger RNA Degradation in Bacterial Cells. Annu Rev Genet 48:537–559.

233. Goldman SR, Sharp JS, Vvedenskaya IO, Livny J, Dove SL, Nickels BE. 2011. NanoRNAs Prime Transcription Initiation In Vivo. Molecular Cell 42:817–825.

234. Grenga L, Little RH, Malone JG. 2017. Quick change: post-transcriptional regulation in Pseudomonas. FEMS Microbiol Lett 364.

235. Little RH, Grenga L, Saalbach G, Howat AM, Pfeilmeier S, Trampari E, Malone JG. 2016. Adaptive Remodeling of the Bacterial Proteome by Specific Ribosomal Modification Regulates Pseudomonas Infection and Niche Colonisation. PLOS Genetics 12:e1005837.

236. Druzhinin SY, Tran NT, Skalenko KS, Goldman SR, Knoblauch JG, Dove SL, Nickels BE. 2015. A Conserved Pattern of Primer-Dependent Transcription Initiation in Escherichia coli and Vibrio cholerae Revealed by 5' RNA-seq. PLoS Genet 11:e1005348.

237. Vvedenskaya IO, Sharp JS, Goldman SR, Kanabar PN, Livny J, Dove SL, Nickels BE. 2012. Growth phase-dependent control of transcription start site selection and gene expression by nanoRNAs. Genes Dev 26:1498–1507.

238. Patel DK, Gebbie MP, Lee VT. 2014. Assessing RNA Interactions with Proteins by DRaCALA, p. 489–512. *In* Methods in Enzymology. Elsevier.

239. Aravind L, Koonin EV. 1998. A novel family of predicted phosphoesterases includes Drosophila prune protein and bacterial RecJ exonuclease. Trends Biochem Sci 23:17–19.

240. Bowman L, Zeden MS, Schuster CF, Kaever V, Gründling A. 2016. New Insights into the Cyclic Di-adenosine Monophosphate (c-di-AMP) Degradation Pathway and the Requirement of the Cyclic Dinucleotide for Acid Stress Resistance in Staphylococcus aureus. J Biol Chem 291:26970–26986.

241. Guo M, Chong YE, Beebe K, Shapiro R, Yang X-L, Schimmel P. 2009. The C-Ala Domain Brings Together Editing and Aminoacylation Functions on One tRNA. Science 325:744–747.

242. Wakamatsu T, Kitamura Y, Kotera Y, Nakagawa N, Kuramitsu S, Masui R. 2010. Structure of RecJ Exonuclease Defines Its Specificity for Single-stranded DNA. J Biol Chem 285:9762–9769.

243. Schmier BJ, Nelersa CM, Malhotra A. 2017. Structural Basis for the Bidirectional Activity of Bacillus nanoRNase NrnA. Scientific Reports 7:11085.

244. Sterlini JM, Mandelstam J. 1969. Commitment to sporulation in Bacillus subtilis and its relationship to development of actinomycin resistance. Biochem J 113:29–37.

245. Tran NT, Hengst CDD, Gomez-Escribano JP, Buttner MJ. 2011. Identification and Characterization of CdgB, a Diguanylate Cyclase Involved in Developmental Processes in Streptomyces coelicolor. Journal of Bacteriology 193:3100–3108.

246. Den Hengst CD, Tran NT, Bibb MJ, Chandra G, Leskiw BK, Buttner MJ. 2010. Genes essential for morphological development and antibiotic production in Streptomyces coelicolor are targets of BldD during vegetative growth. Molecular Microbiology 78:361–379.

247. Tschowri N, Schumacher MA, Schlimpert S, Chinnam NB, Findlay KC, Brennan RG, Buttner MJ. 2014. Tetrameric c-di-GMP mediates effective transcription factor dimerization to control Streptomyces development. Cell 158:1136–1147.

248. Schumacher MA, Zeng W, Findlay KC, Buttner MJ, Brennan RG, Tschowri N. 2017. The Streptomyces master regulator BldD binds c-di-GMP sequentially to create a functional BldD2-(c-di-GMP)4 complex. Nucleic Acids Res 45:6923–6933.

249. Bordeleau E, Fortier L-C, Malouin F, Burrus V. 2011. c-di-GMP Turn-Over in Clostridium difficile Is Controlled by a Plethora of Diguanylate Cyclases and Phosphodiesterases. PLOS Genetics 7:e1002039.

250. Bordeleau E, Purcell EB, Lafontaine DA, Fortier L-C, Tamayo R, Burrus V. 2015. Cyclic Di-GMP Riboswitch-Regulated Type IV Pili Contribute to Aggregation of Clostridium difficile. J Bacteriol 197:819–832.

251. Purcell EB, McKee RW, McBride SM, Waters CM, Tamayo R. 2012. Cyclic Diguanylate Inversely Regulates Motility and Aggregation in Clostridium difficile. J Bacteriol 194:3307–3316.

252. Purcell EB, McKee RW, Courson DS, Garrett EM, McBride SM, Cheney RE, Tamayo R. 2017. A Nutrient-Regulated Cyclic Diguanylate Phosphodiesterase Controls Clostridium difficile Biofilm and Toxin Production during Stationary Phase. Infect Immun 85.

253. Tang Q, Yin K, Qian H, Zhao Y, Wang W, Chou S-H, Fu Y, He J. 2016. Cyclic di-GMP contributes to adaption and virulence of Bacillus thuringiensis through a riboswitch-regulated collagen adhesion protein. Sci Rep 6.

254. Fu Y, Yu Z, Liu S, Chen B, Zhu L, Li Z, Chou S-H, He J. 2018. c-di-GMP Regulates Various Phenotypes and Insecticidal Activity of Gram-Positive Bacillus thuringiensis. Front Microbiol 9.

255. Yang Y, Li Y, Gao T, Zhang Y, Wang Q. 2018. C-di-GMP turnover influences motility and biofilm formation in Bacillus amyloliquefaciens PG12. Research in Microbiology 169:205–213.

256. Düvel J, Bertinetti D, Möller S, Schwede F, Morr M, Wissing J, Radamm L, Zimmermann B, Genieser H-G, Jänsch L, Herberg FW, Häussler S. 2012. A chemical proteomics approach to identify c-di-GMP binding proteins in Pseudomonas aeruginosa. Journal of Microbiological Methods 88:229–236.

257. Nesper J, Reinders A, Glatter T, Schmidt A, Jenal U. 2012. A novel capture compound for the identification and analysis of cyclic di-GMP binding proteins. Journal of Proteomics 75:4874–4878.

258. Düvel J, Bense S, Möller S, Bertinetti D, Schwede F, Morr M, Eckweiler D, Genieser H-G, Jänsch L, Herberg FW, Frank R, Häussler S. 2016. Application of Synthetic Peptide Arrays To Uncover Cyclic Di-GMP Binding Motifs. J Bacteriol 198:138–146.

259. Srivastava D, Waters CM. 2015. A Filter Binding Assay to Quantify the Association of Cyclic di-GMP to Proteins. Bio Protoc 5.

260. Goldman SR, Ebright RH, Nickels BE. 2009. Direct Detection of Abortive RNA Transcripts in Vivo. Science 324:927–928.

261. Mathy N, Bénard L, Pellegrini O, Daou R, Wen T, Condon C. 2007. 5′-to-3′ Exoribonuclease Activity in Bacteria: Role of RNase J1 in rRNA Maturation and 5′ Stability of mRNA. Cell 129:681–692.

262. Bandyra KJ, Luisi BF. 2013. Licensing and due process in the turnover of bacterial RNA. RNA Biol 10:627–635.

263. Bruce HA, Du D, Matak-Vinkovic D, Bandyra KJ, Broadhurst RW, Martin E, Sobott F, Shkumatov AV, Luisi BF. 2018. Analysis of the natively unstructured RNA/protein-recognition core in the Escherichia coli RNA degradosome and its interactions with regulatory RNA/Hfq complexes. Nucleic Acids Res 46:387–402.

264. Babitzke P, Kushner SR. 1991. The Ams (altered mRNA stability) protein and ribonuclease E are encoded by the same structural gene of Escherichia coli. Proc Natl Acad Sci U S A 88:1–5.

265. Condon C. 2007. Maturation and degradation of RNA in bacteria. Current Opinion in Microbiology 10:271–278.

266. Shahbabian K, Jamalli A, Zig L, Putzer H. 2009. RNase Y, a novel endoribonuclease, initiates riboswitch turnover in Bacillus subtilis. EMBO J 28:3523–3533.

267. Lehnik-Habrink M, Schaffer M, Mäder U, Diethmaier C, Herzberg C, Stülke J. 2011. RNA processing in Bacillus subtilis: identification of targets of the essential RNase Y. Molecular Microbiology 81:1459–1473.

268. Condon C. 2003. RNA Processing and Degradation in Bacillus subtilis. Microbiol Mol Biol Rev 67:157–174.

269. Lehnik-Habrink M, Lewis RJ, Mäder U, Stülke J. 2012. RNA degradation in Bacillus subtilis: an interplay of essential endo- and exoribonucleases. Molecular Microbiology 84:1005–1017.

270. Even S, Pellegrini O, Zig L, Labas V, Vinh J, Bréchemmier-Baey D, Putzer H. 2005. Ribonucleases J1 and J2: two novel endoribonucleases in B.subtilis with functional homology to E.coli RNase E. Nucleic Acids Res 33:2141–2152.

271. Durand S, Condon C. 2018. RNases and Helicases in Gram-Positive Bacteria. Microbiology Spectrum 6.